UNIVERSITÀ DEGLI STUDI DI NAPOLI "FEDERICO II"

TESI DI DOTTORATO DI RICERCA IN BIOLOGIA APPLICATA

XXV CICLO

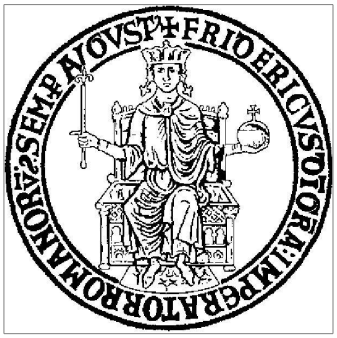

Microbial life and metabolism in Mediterranean Sea extreme environments

PhD in Applied Biology

Curriculum in Ecology and Microbiology

Coordinators:

Chiar.mo Prof. Ezio Ricca

Tutor: *Candidate*:

Chiar.mo Prof. Marco Moracci Donato Giovannelli

Co-Tutor:

Dr. Elena Manini

2010/2013

”..e il mare porterà ad ogni uomo nuove speranze,
come il sonno porta i sogni.”
Cristoforo Colombo

This thesis is dedicated to all the people that never stopped believing in me, that helped me trough those years of works, and pushed me to pass by some though periods and some difficulties.

My first thought goes to my father and my mother, whose passion, moral coherence and dedication had a great influence on the person I am today. To my brother. To my wife and life companion. To my tutor Elena Manini for the faith she had in me despite it all. To my tutor Prof. Moracci for the trust. To Costa for help and mentorship. To all close friends, too many to mention one by one. I feel I am a very lucky person, I will never forget it.

Open-source statement

The work presented in this thesis was realized with open-source software, in a convinced effort to push the open-source philosophy forward. Where possible all scientific software used was open-source. The entire work has been carried out on **Ubuntu** operative system, with **LibreOffice** as office suite and **Inkscape** and **Gimp** for graphics and charts.

This PhD and thesis is one of the many example that working entirely with open-source software is possible and should be done to support informatics and cultural freedom.

Abstract

The Mediterranean Sea is one of the most intensively investigated areas of the world. Despite this, it lags other regions of the world in studies of its deep sea and extreme environments. The contribution of Mediterranean extreme environments to global and regional diversity and biogeochemical cycles is poorly understood. Prokaryotes are the major component of Earth biodiversity, they outnumber any other living form and posses the greatest metabolic plasticity. This is especially true in extreme environments, where prokaryotes often constitute the only life form and play a key role in the functioning of those systems. Aim of this thesis is to investigate the diversity and role of prokaryotes in Mediterranean Sea extreme environment. The samples analyzed in this work were obtained in different oceanographic cruises and field trip around the Mediterranean Sea and are representatives of low- and high-energy environments. The used approach is a mix of traditional microbiology and ecology techniques combined with cutting-the-edge molecular tools, integrating laboratory and field survey. I started investigating the community structure in shallow-water sub-surface sediments evidencing a shift in the prokaryotic community composition. Despite the high biopolymeric organic C amount, results showed the major importance of the environmental factors influencing the availability of inorganic electron donors/acceptors, suggesting that lithotrophy could be an important metabolic pathway in shallow sub-surface sediments. In deep sea surface sediments across the Mediterranean Sea, community structure was instead dominated by *Bacteria*, and major driving force were trophic variables and geographic position within the basin, suggesting that overlaying water masses play a critical role in shaping deep-sea benthic prokaryotic communities. Different factors controlled prokaryotes distribution in shallow-water hydrothermal vents and seeps. In shallow-water vents prokaryotes distribution was controlled by temperature gradients rather than trophic resources. In cold-seeps environments the major drivers were both the presence of hydrocarbons and organic matter. In both areas the diversity was high, with a community evenly dominated by chemoautotrophic and heterotrophic metabolic strategies. Finally, the results obtained in different environments are brought together and emerging trends are analyzed.

In the future, to gain a deeper understand of the diversity and functioning of extreme environments, we will need to integrate ecology, microbiology, geochemistry, oceanography and molecular biology and shift our scale of measuring, reasoning and interpreting the microbial world from “human” to “microbial”.

Table of Contents

Chapter 1

Introduction: prokaryotes and extreme environments

"Universe is not controlled by easy laws, rather by simple laws."

Albert Einstein

Origin of life and prokaryotes as oldest lifeforms

Life originated on Earth about 3.9 billion years ago (Schopf, 1993; Pflug, 2001; Van Kranendonk, 2006; Payne et al., 2009), during the Eoarchean Era when sufficient crust had solidified. Evidence of life during this periods comes from carbon dating of fossil stromatolites (Figure 1.1) and sedimentary rock formation in the Akilia Island, Greenland, the oldest known rocks on Earth. This deposits are known as banded iron formation and may represent 3.85 billion years old hydrothermal deposits and contains carbon with low level of ^{13}C typical of living matter (Mojzsis et al., 1996).

Figure 1.1. Precambrian stromatolites in the Siyeh Formation, Glacier National Park, Montana USA, 3.5 billion years old.

Different theories have been proposed during the years to explain the origin of life on earth. Among others the three main views are:

- Panspermia – According to this theory life did not originated on Earth, but was brought here from elsewhere in space by meteorites, asteroids or comets (Morbidelli et al., 2010; Callahan et al., 2011; Jørgensen et al., 2012). This theory was popular in the early 19th century and is still popular today among those who believe that life could have been brought on Earth from Mars or other extrasolar planets. Whichever the origin of the "life sperm", this theory only moves the question further, on how life began elsewhere in space;
- Genetic first – This theory foreseen the origin of genetic material as first biological molecule. Both DNA and RNA contain the genetic informations necessary needed to support life, however DNA needs proteins in order to replicate and translate. RNA, otherwise, contains genetic information and can serve as enzymes, like in ribosomes (Joyce, 2002; Ma et al., 2007). RNA thus may have preceded DNA and proteins in the first place (the so called RNA world theory). One of the main critics to this theory was the difficulty in abiogenic synthesis of genetic material (Levy and Miller, 1998), however recently researcher demonstrated the ability of clay to catalyze abiotic RNA precursors formation (Huang and Ferris, 2006), giving new credits to this theory (Saladino et al., 2012);
- Metabolism first – Instead of developing from complex molecules such as RNA, life might have begun with smaller molecules interacting with each other in cycles of reactions (Wächtershäuser, 1990; Smith and Morowitz, 2004). Auto catalytic cycles may have formed from simple precursor in a primordial broth. Electric sparks can generate amino acids and sugars from an atmosphere loaded with water, methane, ammonia and hydrogen, as was shown in the famous Miller-Urey experiment reported in 1953 (Miller, 1953). Although research since then has revealed the early atmosphere of Earth was actually hydrogen-poor (Chyba, 2005), this theory still find strong support in the scientific community (Cleaves et al., 2008). These might have been contained in simple capsules akin to cell membranes called proto-cells. Several recent studies point in this directions (Smith and Morowitz, 2004; Braakman and Smith, 2012; Arndt and Nisbet, 2012).

Recent publication identified hydrothermal vents chimney as possible site of life origins (Wächtershäuser, 2000; Lane and Martin, 2012). This theory is consistent with indication that early life form may have been hyperthermophylic (Schwartzman and Lineweaver, 2004), the origin of the genetic code (Schwartzman and Lineweaver, 2004), and with geological evidence of hydrothermal activity and ocean temperatures about 4 billion years ago (Mojzsis et al., 1996; Arndt and Nisbet, 2012). In this regards other extreme geothermal environments, including shallow-water hot spring and hydrothermal vents may have played a primary role in life origins,

coupling reduced atmosphere (Chyba, 2005), presence of geothermal redox gradients and the role of ultraviolet in catalysis (Michaelian, 2011).

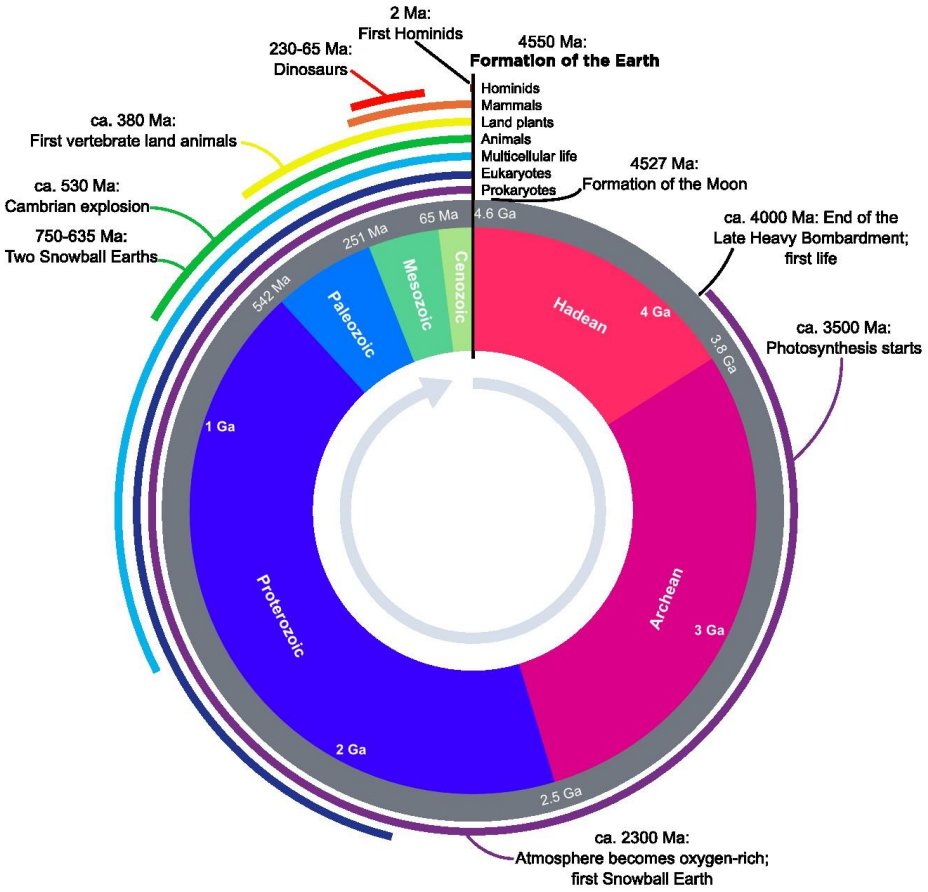

Figure 1.2. Geological time clock and the appearance of life (ca. 4 billion years ago), photosynthesis (ca. 3.5 billion years ago), *Eukaryotes* (ca. 2.2 billion years ago), multicellular life forms (ca. 1.5 billion years ago) and hominids (2 million years ago). *Adapted from* Des Marais (2000).

Despite its origins, prokaryotic life on earth originated long before the appearance of eukaryotic cells, and since then adapted to occupy virtually all ecological niches on Earth (Figure 1.2). The diversity of prokaryotic life on Earth today is a result of the dynamic interplay between genetic opportunity, metabolic capability, and environmental change.

The prokaryotes are a group of organisms whose cells lack a cell nucleus. They are unicellular organisms, although a few such as myxobacteria have multicellular stages in their life cycles or create large colonies like cyanobacteria. They lack a defined nucleus, mitochondria, or any other membrane-bound organelles. In other words, all their intracellular water-soluble components (proteins, DNA and metabolites) are located together in the same area enclosed by cell membrane, rather than separated in different cellular compartments like in Eukaryotes (Figure 1.3). Prokaryotes include two major classification domains: the *Bacteria* and the *Archaea*, formerly

recognized in 1990, with the recognition of the *Archaea* as a domain of life (Woes and Fox, 1977). This arrangement of *Eukarya*, *Bacteria*, and *Archaea* is called the three-domain system, replacing the traditional two-empire system.

There are typically a million prokaryotic cells in a milliliter of water and a billion in a gram of marine sediment; in all it has been estimated that there are 5×10^{30} prokaryotes on Earth, accounting for more than half of total biomass (Whitman et al., 1998). They are vital in many steps of nutrient cycles, such as the fixation of nitrogen from the atmosphere, denitrification, organic matter cycling, methanogenesis and metanotrophy, sulfur oxidation and reduction.

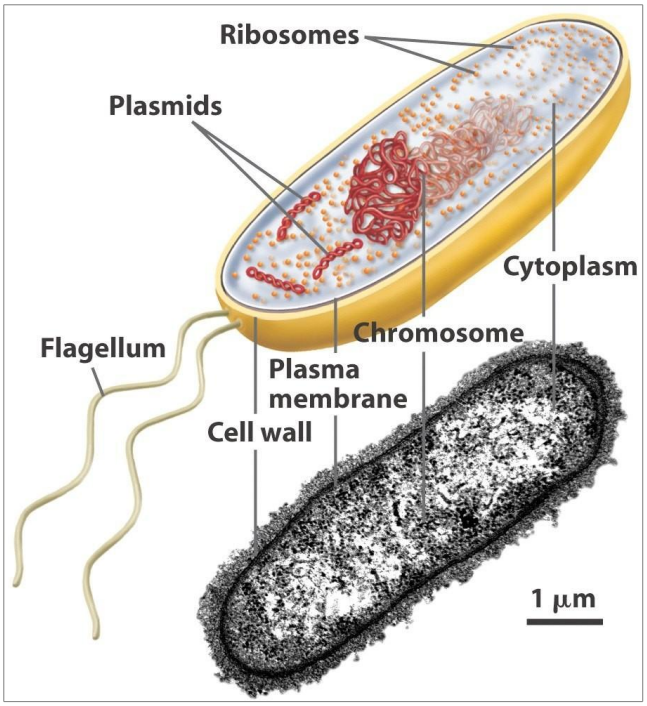

Figure 1.3. Prokaryotic cell organization and structures.

Bacteria and *Archaea* share molecular and morphological structures such as the absence of nucleus and organels, circular genomes, genes grouped in operons, absence of introns among others (Willey et al., Microbiology, 2008). Besides those, *Archaea* appears to share similarities with *Eukarya* in the presence of histones in the DNA, in the RNA polymerase and transcriptional machinery and in the DNA replication and repair mechanisms (Zillig, 1991; Kelman and Kelman, 2003; Sandman and Reeve, 2006; Talbert and Henikoff, 2010).

A "sea" of prokaryotes

The prokaryotes found in ocean and coastal sediments count for approximately the 76% (ca. 3.8 x 10^{30}) of all global prokaryotes (ca. 5 x 10^{30}) with the 13% (ca. 6.6 x 10^{29}) of the total global

population being found in the upper 10 cm of deep-sea sediments (Deming and Yager, 1992; Whitman et al., 1998). Prokaryotes play a key role in all major biogeochemical cycling processes in deep-sea sediments, where they count for the 90% of the benthic biomass (Pfannkuche, 1992). Despite this, our comprehension of the functioning of deep-sea benthic ecosystems is constrained by a poor knowledge on the controlling factors of the prokaryotic distribution, community composition and metabolism. Despite years of investigation carried out by independent research groups using a variety of approaches, the environmental determinants of bacterial abundance in marine sediments are only coarsely resolved in the literature (Deming and Carpenter, 2008).

The idea to break open the "black box" of marine prokaryotic biodiversity, by the application of different molecular tools (cloning and sequencing, *in-situ* hybridization, DNA fingerprinting, 16S rRNA pyrotag sequencing and metagenomic methods), has been the basis of ecological studies on ocean ecosystems in the last 20 years. Very often these studies were focused on bacterioplankton to describe phylogenetic diversity, global distribution (Giovannoni and Stingl, 2005; Ciccarelli et al., 2006; Pommier et al., 2006), community structure and its patterns of distribution (Karner at al., 2001; Herndl et al., 2005; Teira et al., 2006; Varela et al., 2007; Kirchman et al., 2007; Tamburini et al., 2008). In this regard, available studies on deep-sea prokaryotic assemblages have mainly addressed phylogenetic rather than ecological issues, and are spatially and temporally scattered (Moyer et al., 1995, 1998; Takai and Horikoshi, 1999; Lopez-Garcia et al*.,* 2003; Parkes et al., 1994; Inagaki et al., 2004; Biddle et al., 2006; Vetriani et al., 1999).

Recently it has been demonstrated that marine prokaryotes play central role in fixation of CO_2 into organic compounds not only at the ocean's surface but also in the aphotic bathypelagic and abyssal realms of the ocean (Herndl et al., 2005; DeLong, 2006; Wuchter et al., 2006). The chemolitoautotrophs are thought to be among the first organisms that appeared on early Earth (Russell and Hall, 1997; Campbell et al., 2006; Wächtershäuser 1990, 2000). It is suggested that early prokaryotes, inhabiting an Earth marked by "prohibitive" conditions when compared to present ones, were chemoautotrophs satisfying their energetic needs through chemosynthetic processes at the expenses of hydrogen sulphide, methane and other compounds in absence of sunlight. Photosynthesis is thought to have emerged later. Both chemosynthetic and photosynthetic microbial organisms set the pace for life on Earth for a prolonged period of time (Figure 1.2).

Chemosynthetic organisms couple CO_2 fixation with a wide array of metabolic reactions, essential in closing biogeochemical cycles. This metabolic potential is actively shaping our environment but we remain blind to the full array of biogeochemical transformations. This is especially true in extreme environments, where prokaryotes often constitute the only life form (Nealson et al., 1999). In those systems, prokaryotes play a central role in biogeochemical cycles (Nealson et al., 1999), and their influence on surrounding areas and global cycles has not yet been understood (Hedges, 1992). For example, the activity of methanogens and methanotrophs could

influence the presence of methane gas in the atmosphere, a gas with known greenhouse effects. In this context extreme environments may have a strong impact on the functioning of our ecosystems, positively or negatively reinforcing global warming and climate change.

Extreme environment exhibits extreme conditions which are challenging to most eukaryotic life forms. These may be extremely high or low ranges of temperature, radiation, pressure, acidity, alkalinity, salt, sugar, carbon dioxide, sulphur, petroleum and many others compared to the narrow human optimum for life (Taviani, 2011). Despite this human-centric definition of extreme environments prokaryotes thrive successfully in those systems. Taken all together the role of prokaryotes in those systems is key to the functioning of our biosphere (Torsvik et al., 2002).

Ecological surveys, metagenomic and comparative genomic studies, will provide a fuller understanding of microbial biodiversity within communities that control biogeochemical cycles, such as those involving the use of carbon, sulfur, iron, and nitrogen compounds (Des Marais, 2008). This presents novel opportunities for scientists and biotechnologists. The results of those studies will allow scientist in the future to draw conclusion on how life emerged on Earth, which are its limits and the potential presence of life in extraterrestrial planets (Des Marais, 2008).

Why the Mediterranean Sea?

The Mediterranean Sea is one of the most intensively investigated areas of the world in both terrestrial and marine environments. This is due to the extreme urbanization of its coastal area and the presence of historical research centers and universities. Observation on the flora and fauna of the Mediterranean Sea started in the ancient Greek world, with detailed account of the species encountered (Aristotle, from 384-322 BC). Despite this long track of studies and observations, it lags other regions of the world in studies of its extreme environments. Such differences are striking in term of number of publication concerning its deep-sea hydrothermal vents and cold-seeps, its bathyal planes and peculiar environments.

The Mediterranean Sea is divided into western and central-eastern basins separated by the Strait of Sicily. The western basin, with an average depth of about 1,600 m is shallower compared to the central-eastern Mediterranean, with an average depth of about 2,200 m. The deepest point in the Mediterranean, 5,121 m, is found at the North Matapan-Vavilov Trench, Ionian Sea (Vanney and Gennesseaux, 1985; Figure 1.4a), although there is some debate on Calypso Trench being the deepest point.

The Mediterranean Sea is characterized by intense tectonic activities with several faults interacting with the African and Eurasian plates (Figure 1.4b). The eastern basins are the tectonically more active with an active area of crust accretion (the Mediterranean Ridge), a subduction area that forms the Hellenic Trenches and a volcanic back-arc (the Hellenic volcanic

arc). This complex structure creates an extremely active area with sub-regions characterized by complex structural feature: (a) bathyal plains and trenches, (b) deep hypersaline anoxic basins, residuals of the Messinian salinity crisis, (c) cold seepage areas and associated mud volcanoes and pockmarks, (d) volcanism and associated shallow and deep-sea hydrothermal areas (Figure 1.5).

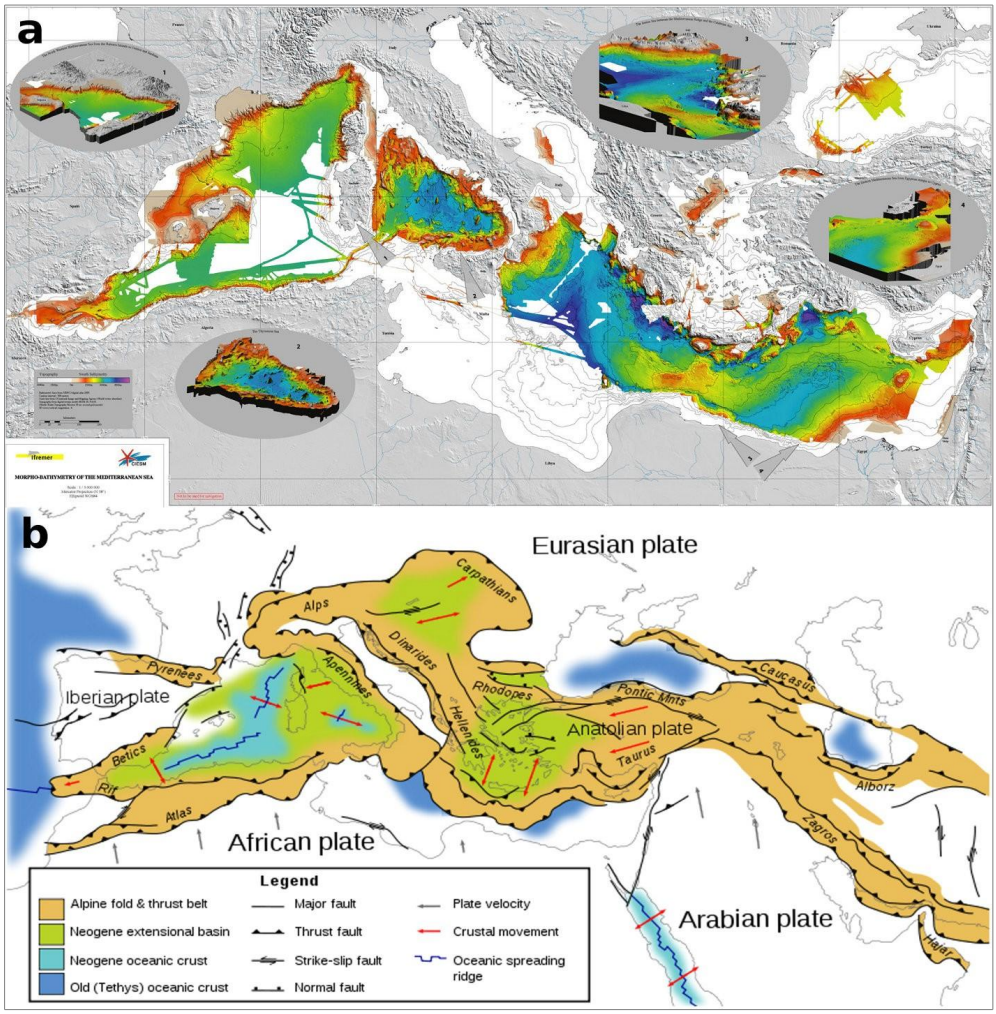

Figure 1.4: Composite image of the Mediterranean Sea. a-Morpho-Bathymetry; b-Geological map of the Mediterranean and main fault systems.

Being nearly landlocked affects conditions in the Mediterranean Sea. Tides are very limited as a result of the narrow connection with the Atlantic Ocean and evaporation greatly exceeds precipitation and river runoff. Evaporation is especially high in its eastern half, causing the water level to decrease and salinity to increase eastward. Oligotrophy is marked in the eastern basin, with average surface primary production being 15–80 time lower than the western basin. Cold low-salinity water from the Atlantic enters the Mediterranean Sea trough the Strait of Gibraltar and travels eastward on the surface of the basin.

The water warms and becomes saltier as it travels eastward, then sinks in the region of the

Levant and circulates westward, to spill over the Strait of Gibraltar. The main features of the Mediterranean Sea are (a) high deep-sea homeothermy from roughly 300–500 m to the bottom, and bottom temperatures of about 12.8 °C to 13.5 °C in the western basin and 13.5 °C to 15.5 °C in the eastern basin, (b) high salinity (from 38 to 39.5 PSU), (c) negative water balance, (d) a micro-tidal regime, (e) high oxygen concentrations, and (f) oligotrophic conditions, marked in the eastern basin (Danovaro et al., 2010). The eastern basin is considered to be one of the most oligotrophic areas of the world. Due to this characteristic the Mediterranean Sea has been considered a "miniature ocean" that can be used as a model to predict effects of anthropogenic and climate induced pressures (Danovaro et al., 2010).

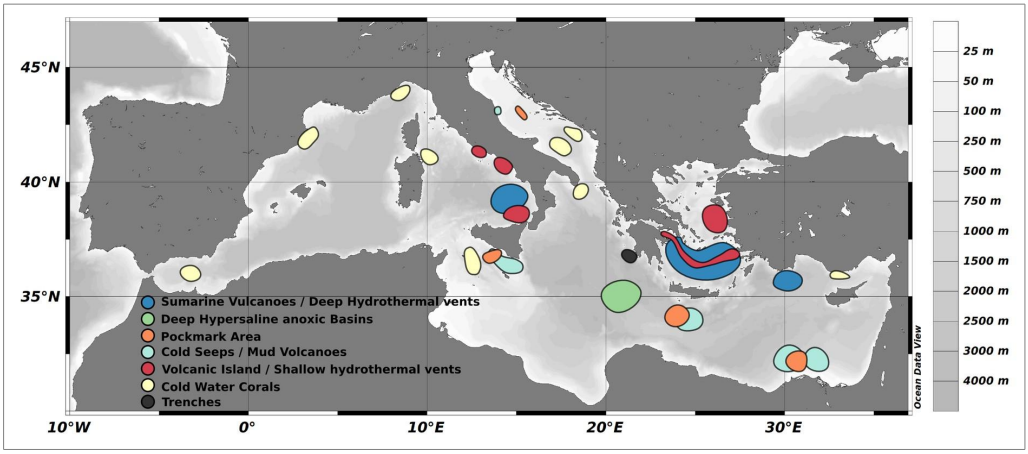

Figure 1.5: Map of known extreme environments in the Mediterranean Sea.

In the past decade numerous studies have attempted to estimate the CO_2 balance in the basin and to estimate Mediterranean geochemical cycles. All this studies failed to include in their calculation the contribution of the numerous Mediterranean extreme habitats. According to Dando et al. (2000) the Hellenic Hydrothermal systems can account for CO_2 emission comparable to those of the oceanic ridges (Figure 1.6). Currently the contribution of Mediterranean extreme environments to regional biogeochemical cycles is poorly understood, and so their contribution to global and regional diversity.

Despite its small dimensions (0.82% of the ocean surface), the Mediterranean basin hosts more than 7.5% of global biodiversity (Myers et al., 2000). However the diversity associated with extreme Mediterranean ecosystems has been investigated only in the last two decades and many location are awaiting further explorations. While the main geological feature of most Mediterranean extreme environments have been characterized, a description of the diversity of micro, meio, macro and megafauna in those environments is still largely lacking.

Figure 1.6. Strong degassing activities in the shallow-water hydrothermal vents of Milos island, Greece. Photo courtesy C. Vetriani.

Chapter 2

Aims and Objectives

> "Any intelligent fool can make things bigger, more complex, and more violent. It takes a touch of genius – and a lot of courage – to move in the opposite direction."
>
> *Albert Einstein*

Prokaryotes are the major component of Earth biodiversity, they outnumber any other living form and posses the greatest metabolic plasticity (Pfannkuche, 1992; Whitman et al., 1998; Des Marais, 2000). They appeared on Earth approximately 3.5 billion years ago and colonized every ecological niche, regardless of temperature, pH, salinity, pressure and food availability. They contributed substantially in shaping our ecosystems thought time and still carry out reaction of crucial importance for global cycling of nutrients and biogeochemistry (Staley and Reysenbach, 2002). This is particularly true in extreme environments were prokaryotes often constitute the main life form present (Nealson et al., 1999). Previous studies evidenced that prokaryotic communities living in the deep-sea were dependent upon the flux of particulate and dissolved organic matter coming from the photic zone (Deming and Carpenter, 2008). During the 70's and 80's, following the discovery of deep-sea hydrothermal vents and cold-seeps communities, this paradigm changed. Those ecosystems were entirely supported by geothermal energy trough chemolithoautotrophy (Lonsdale, 1977). In this framework is now possible to define environments based on the energy source available for carbon fixation. Thus environments in which a single source is available (e.g. geothermal or solar energy) could be classified as mid-energy. Environments were none of the above or both are available can be defined as low- or high-energy, respectively. Shallow-water vents and seeps are high-energy environments, in which phototrophy and chemolithoautotrophy occur within the same spatial boundaries, while deep-sea planes and trenches and subsurface are low-energy environments.

This thesis aims at increase our knowledge of Mediterranean Sea extreme environment functioning and diversity with a focus on the prokaryotes. The idea is to break open the "microbial box" in Mediterranean Sea extreme environment with emphasis on prokaryotes diversity, role and factors driving their distribution in high and low-energy ecosystems of the Mediterranean Sea.

Specific questions addressed in this thesis were:

- Is the prokaryotic abundance in different extreme environment comparable?
- Who's dominating community structure in extreme environments? Which is the role of rare species?
- Which are the dominant metabolic strategies? Is there metabolic redundancy between different extreme ecosystems?
- Which are the drivers controlling prokaryotes distribution and community structure in extreme environments?

The entire work presented in this thesis deals with the microbial ecology of different Mediterranean Sea extreme environments, challenging current view and providing new information on previously understudied ecosystems. The used approach is a mix of traditional microbiology and ecology techniques combined with cutting-the-edge molecular tools, integrating laboratory and field survey. Relevant Mediterranean Sea extreme environment were sampled and analyzed, looking at the prokaryotic community present *in situ*, their role and the driving factors shaping their structure and functioning. The samples analyzed in this work were obtained in different oceanographic cruises and field trip around the Mediterranean Sea. During the three BIOFUN expedition in 2009 and 2010, the Arcadia 2010 expedition in the Adriatic Sea, the MAMBA2010 in the Eastern Mediterranean, all conducted with the R/V Urania, and the Azores Extremophiles sampling expedition in September 2010. Analyses where carried out at the CNR-ISMAR of Ancona and during two visiting periods at the Deep-sea Microbiology Lab, Rutgers University, NJ – USA.

I started analyzing the distribution and community structure in the under-investigated sub-surface of coastal environments (Chapter 4), highlighting driving factors along a sediment profile up to 1 m depth. Chapter 5 re-proposes and extends this approach to the drivers controlling prokaryotic community structure across the deep Mediterranean-Sea, and discuss their large scale distribution and influence on organic matter cycling using innovative statistical tools to delineate large-scale trends. Chapter 6 investigates the community structure and diversity of an active shallow-water hydrothermal vent using a mix of cultivation-dependent and independent techniques, giving a snapshot of the functioning of those abundant, yet understudied Mediterranean Sea environments. During the study of this system we isolated numerous prokaryotic species, and one of those resulted to be a new strain, with low similarity to previously isolated species. Chapter 7 describes in details the ecology and physiology of this newly isolated genus and species of chemolithotroph *Gammaproteobacteria*. This bacteria will be submitted this year for full genome sequencing, providing us with a model organism of the Hellenic shallow-water hydrothermal systems. Chapter 8 contains the detailed analysis, using cutting-the-edge

sequencing approaches, of the diversity of the prokaryotic community of a Mediterranean Sea pockmark systems, whose counterparts in the North Sea have been characterized, both from a biological and geological standpoint, in details. Finally, in Chapter 9, the information obtained during the doctorate project are brought together, and a summary of the information collected in different extreme environment of the Mediterranean Sea is presented.

Chapter 3

Materials and Methods

"Somewhere, something incredible is waiting to be known."

Carl Sagan

The idea to break open the "black box" of marine prokaryotic biodiversity, by the application of different molecular tools, has been the basis of the ecological studies on ocean ecosystems in the last 20 years. They play a key role in all ecosystems (Pfannkuche, 1992) and dominate most extreme environments. In the need to connect diversity with ecosystem functioning, the main vision of microbial ecology exploration is now an integrated approach of traditional microbiology and molecular ecology (Sievert and Vetriani, 2012) to give a more in-depth understanding of the dynamics that shape the system (Figure 3.1).

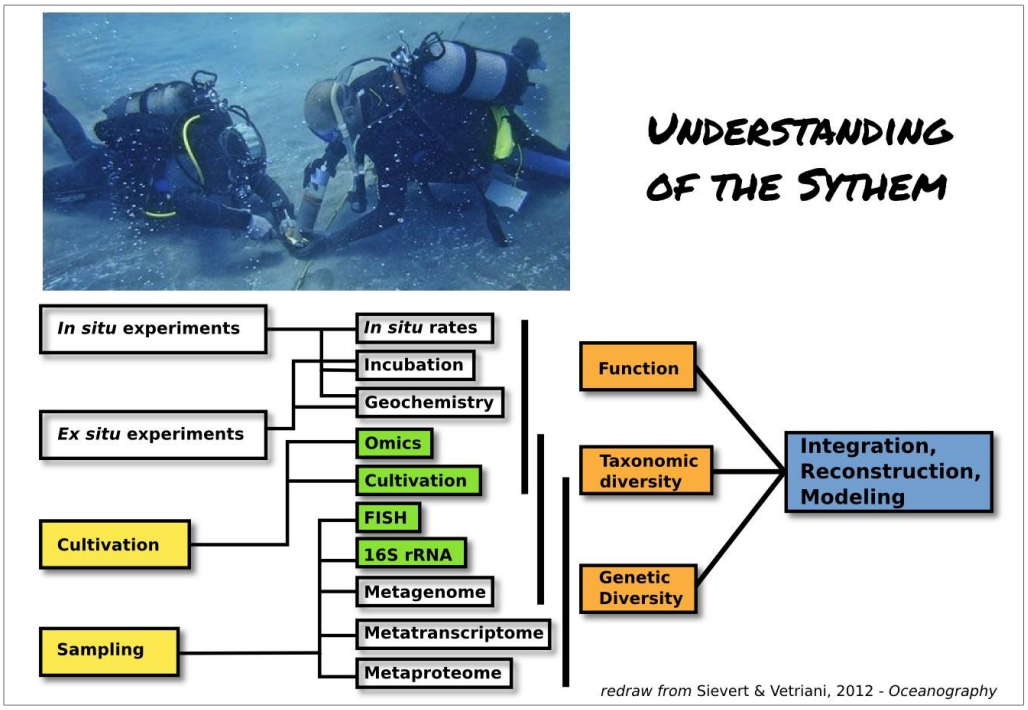

Figure 3.1. Integrated approaches combining traditional microbiological and ecological techniques with molecular and "omics" tools are needed in other to gain a full understanding of the system. In yellow the approaches and in green the techniques used during this thesis. Redrawn from Sievert and Vetriani, 2012.

In the curse of this thesis I tried to combine those approaches to give an in depth view of Mediterranean Sea extreme environments, and contribute to the understanding of the prokaryotic abundance, diversity and contribution to ecosystem functioning in those environments.

Strain isolation and growth

Enrichment cultures for mesophilic, chemolithoautotrophic organisms were obtained by inoculating 10 ml of different media, with 1 g of the sediment samples resuspended in 1 ml of anaerobic artificial seawater, which contained (l^{-1}): 28 g NaCl, 0.77 g KCl, 1.6 g $CaCl_2 \cdot 2H_2O$, 0.11 g $NaHCO_3$, 3.5 g $MgSO_4 \cdot 7H_2O$. Where field inoculation was not possible, aliquots of sediments (ca. 15-20 g) were preserved in dinitrogen atmosphere at 4°C. The primary enrichments were incubated between 30 and 55°C. When growth was observed, aliquots (0.1 ml) of the primary enrichments were subsequently transferred to fresh medium, and pure cultures were isolated by three consecutive series of dilutions to extinction, followed by isolation of single colonies on plates containing the media solidified with 1 g l^{-1} of agar, noble agar or Phytagel (Sigma). Plates were incubated in an anaerobic jar (Oxoid) pressurized with the appropriated gas mixture. Long-term stocks of the new isolates were routinely prepared by adding 150 µl sterile glycerol (Fisher Scientific) to 850 l culture and stored at –80°C. Cells were routinely stained in 0.1% acridine orange and visualized with an Olympus BX 60 microscope with an oil immersion objective (UPlanFl 100/1.3). Transmission electron micrographs were obtained as previously described (Vetriani et al., 2004).

Preliminary phylogenetic analysis of the 16S rRNA gene sequences of the obtained isolates was performed to classify, where possible the cultures with a cut of for preliminary new species definition of 97% (EzTaxon pairwise alignment). Pure cultures with a lower percentage similarity were further investigated for the description of the new isolated strain (8)

Total Prokaryotic Number and Prokaryotic Biomass

Aliquots of sediments were immediately fixed using tamponed formaldehyde (final concentration, 2%, in sterile and filtered seawater) and stored at 4°C until processed for total prokaryotic abundance (Danovaro et al., 2002). Total prokaryotic counts were performed using a staining technique with Acridine Orange (Pearson et al., 2008). Briefly, 0.5 g sub-samples were added with tetrasodium pyrophosphate and incubated for 15 min before sonication. The samples were then stained with Acridine Orange (final concentration, 0.025%), and filtered on 0.2 m pore-size Nucleopore black polycarbonate filters, under low vacuum (100 mm Hg). The filters were analyzed as described by Fry (1990), using epifluorescence microscopy (Zeiss Axioskop 2; 1000× magnification). Total prokaryotic abundance was normalized to g^{-1} sediment dry weight after

desiccation. Prokaryotic biovolume and total count were estimated either by direct count and assignment of prokaryotes to dimensional classes (Danovaro et al., 2002; Chapter 4 and 5) or using an ImageJ algorithm developed by Giovannelli and D'Errico (see Statistical section for code details; Chapter 6 and 8). Average C content was assumed to be 310 fgC μm^{-3} (Fry, 1990). The prokaryotic biomass was normalized to dry weight after desiccation.

Virus enumeration

Aliquots of sediment for virus count were immediately frozen upon arrival on board. Direct counts of virus-like particles were carried out using the method described by Danovaro et al. (2002). The viruses were separated from the sediment samples using tetrasodium pyrophosphate and ultrasound treatment, and then centrifuged for 60 s (800 ×g). Extracellular DNA interference in virus counting was removed by incubating the samples with bovine pancreas Dnase I (final concentration, 10 U ml^{-1} for 15 min at room temperature. The filters were stained with 20 ml SYBR Green I (diluted 1:20 in virus-free Milli Q water), incubated in the dark for 20 min, and then mounted on glass slides. Direct counting of virus-like particles in sediment samples was carried out by examining at least 10 fields per slide (e.g. ca. 400 viral particles per filter), under epifluorescence microscopy (Zeiss Axioskop 2; magnification, 1,000× magnification). The virus counts were normalized to sediment dry weight after desiccation.

FISH and CARD-FISH

To investigate the prokaryotic community structure, the sediment sub-samples (0.5 g) were fixed in 4.5 ml formaldehyde (final concentration, 2%) in phosphate-buffered saline, pH 7.4 (PBS) for 1 h at room temperature. These fixed samples were then washed three times with PBS, with centrifugation at 10,000 ×g for 5 min between washes, and then stored in PBS/ethanol (1:1; v/v) at -20°C until further processing (Ishii et al., 2004). To investigate the prokaryotic community structure, fluorescence in-situ hybridization (FISH) was used with rRNA-targeted oligonucleotide probes. Signal amplification (CARD, CAtalyzed Reporter Deposition) was adopted for difficult samples. The samples were resuspended, diluted and sonicated for 1 min (Branson 3510 sonicator, 100 W, 42 kHz), and then shaken for 30 s. This sonication and shaking sequence was repeated three times. After samples were filtered through 0.2 μm pore size polycarbonate filters (Millipore), washed twice with Milli-Q water, dried, and stored at -20°C until further processing. Procedure for FISH and CARD-FISH substantially differed for the permeabilization step required to allow the CARD-FISH bigger probe to enter the cell membrane.

Probes used were EUB338-mix (EUB338, 5'-CTG CCT CCC GTA GGA GT-3', EUB338-II, 5'-GCA GCC ACC CGT AGG TGT-3', and EUB338-III, 5'-GCT GCC ACC CGT AGG TGT-3')

targeting total *Bacteria* (Amann et al., 1995), ARCH915 (5'- GTG CTC CCC CGC CAA TTC CT-3') targeting total *Archaea* (Stahl and Amann, 1991), NON338 (5'-ACT CCT ACG GGA GGC AGC-3') as negative control (Amann et al., 1995), CREN537 (5'-TGA CCA CTT GAG GTG CTG-3') targeting *Crenarchaeota* Marine Group I (Teira et al., 2004) and EURY806 (5'-CAC AGC GTT TAC ACC TAG-3') targeting *Euryarchaeota* Marine Group II (Teira et al., 2004).

In CARD-FISH to avoid cell loss during cell-wall permeabilisation, the filters used for all of the treatments were initially dipped into low-gelling-point agarose (0.1% w/v in Milli-Q water), dried face up on glass slides at 35°C, and subsequently dehydrated in 96% (v/v) ethanol for 1 min. For cell wall permeabilization, filters were incubated either with lysozyme (10 mg/ml; Sigma) or with proteinase K (final concentration 0.04 mU/ml; 7.5 U/mg, Fluka) solution (0.05 EDTA, 0.1 Tris-HCl pH 8) at 37 °C for 1 h. After the permeabilisation steps, the filters were incubated in 0.01 M HCl at room temperature for 20 min. This incubation in HCl inhibits any intracellular peroxidases that are potentially present, and it also proved to effectively inhibit residual proteinase K activity. The samples were then processed using previously described protocols (Pernthaler et al., 2002).

FISH membrane permeabilization consisted of one minute dehydration in 96% ethanol. In both procedures the filters were cut into sections for hybridization with specific probes. The hybridization was performed in hybridization buffer (0.9 M NaCl, 20 mM Tris-HCl pH 7.5, 10% w/v dextran sulphate, 0.02% w/v sodium dodecyl sulphate, 1% blocking reagent, and 55% v/v formamide for the EUBmix and ARCH915 probes, and 20% v/v formamide for the CREN537 and EURY806 probes) containing 0.5 ng l^{-1} HRP probe, at 35 for 2 h or 8-12 h. For the washing step, the slides were immersed in washing buffer (5 mM EDTA pH 8.0, 20 mM Tris-HCl pH 7.5, 0.01% w/v sodium dodecyl sulfate, 13 mM NaCl for EUBmix and ARCH915, and 145 mM NaCl for CREN537 and EURY806) at 37°C for 10 min.

After washing, the filter sections were placed in PBS supplemented with 0.05% Triton X-100, and left at room temperature for 15 min. For tyramide signal amplification (TSA) in CARD-FISH analyses, the filter sections were placed in freshly prepared TSA working solution (1 vol. Tyramide-Cy3 and 20 vol. amplification diluent with 100 H_2O_2 (1:100 v/v), and incubated for 10 min in the dark at 37°C. After this incubation, the filters sections were washed in PBS supplemented with 0.05% Triton X-100 at room temperature in the dark for 15 min, then Milli-Q water, and then 95% ethanol.

Finally, the filter sections were air dried and embedded in low fluorescence glycerol mountant containing an antibleaching agent (50% PBS, v/v; 50% glycerol, v/v; 0.5% L-ascorbic acid, w/v). The filters were analysed using epifluorescence microscopy (Zeiss Axioskop 2; 1,000× magnification). Community structure was calculated as *Bacteria* to *Archaea* ratio (BAR) with value equal to 1 for a population consisting of 50% of each domain in order to give a synoptic view of the structure in term of relative abundance. Similarly, *Archaea* community structure was

calculated using a *Euryarchaeota* to *Crenarchaeota* ratio (ECR) on the same principle (Molari et al., 2012).

DNA extraction and 16S rRNA PCR amplification

Genomic DNA was extracted from sediment biomass by the phenol:chloroform method (Maniatis, 1989). Briefly, aliquots of frozen sediments (ca. 0.5 g) were resuspended in extraction buffer (100 mM Tris-HCL, 100 mM EDTA, 1.5 M NaCl pH 8.0), supplemented with 10 mg ml^{-1} lysozyme and incubated for 30 min at 37°C. Subsequently, 20% SDS was added and each sample was incubated with agitation for 1 h at 60°C. Sediments were removed by centrifugation (5 min at 14,000 ×g) and supernatants were collected and extracted with 1 volume of phenol:chloroform:isoamyl alcohol (25:24:1) followed by one extraction with chloroform:isolamyl alcohol (24:1). DNA was then precipitated overnight with 0.1 volumes of sodium acetate and 0.7 volumes isopropanol, washed with 70% ice-cold ethanol, resuspended in PCR grade water and visualized on 1% agarose gel.

The bacterial 16S rRNA gene was amplified by polymerase chain reaction (PCR) using universal bacterial primer 8F (5'-AGA GTT TGA TCC TGG CTC AG-3') and 1517R (5'-ACG GCT ACC TTG TTA CGA CTT-3') (Weisburg et al., 1991). Aliquots of 5 µl of PCR products were visualized by staining with ethidium bromide on 1.5% agarose gel.

Denaturing Gradient Gel Electroforesis

A preliminary assessment of the diversity of the sediment bacterial communities was carried out by Denaturing Gradient Gel Electrophoresis (DGGE) analysis of the bacterial 16S rRNA gene. The full-length 16S rRNA gene was obtained as described above, gel-purified and used as a template for nested PCR to amplify the V3 region using the GC-clamp primer 338F-(GC) (5'-CGC CCG CCG CGC GCG GCG GGC GGG GCG GGG GCA CGG GGG GAC TCC TAC GGG AGG CAG CAG-3') and 519R (5'-GWA TTA CCG CGG CKG CTG-3'). DGGE was performed with a D Gene system (Bio-Rad Laboratories, Hercules, CA). PCR products (15 µl) were applied directly onto 6% (wt/vol) polyacrylamide gels in 1X TAE (0.04 M Tris base, 0.02 M sodium acetate, 1 mM EDTA pH 7.4), with denaturant gradient from 40 to 60% (where 100% denaturant contains 7 M urea and 40% formamide).

Electrophoresis was performed at a constant voltage of 45 V for 14 h. After electrophoresis, the gels were incubated for 15 min in 0.5 mg l^{-1} ethidium bromide, rinsed for 10 min in distilled water, and photographed with a UV Foto Analyst system (Fotodyne, Inc., Hartland, WI).

16S rRNA Clone Libraries

Purified DNA fragments greater than 1 kb were recovered via preparative gel electrophoresis (Maniatis, 1989). The obtained DNA fragment was cloned into pCR2-TOPO Vector using the TOPO-TA Cloning Kit (Invitrogen, Inc., Carlsbad, Calif.) following manufacturers protocols and the resulting ligation products were used to transform competent *Escherichia coli* TOP10F cells. Cloned *E. coli* cells were grown on Luria-Broth media (10 g Triptone, 5 g Yeast Extract, 5 g NaCl, dd H_2O up to 1 l) added with Ampicillin. From each library 60 to 90 recombinant clones were randomly chosen and analyzed for insert-containing plasmids. A loopful of cells of each clone was suspended and lysed in 2% SDS. The lysate was extracted with an equal volume of chloroform:isoamyl alcohol (24:1). A sample from the resultant aqueous layer was electrophoresed in a 1% (w/v) agarose gel and compared with a molecular weight marker. Plasmid from positive clones was extracted using the Qiagen mini-prep kit following manufacturers protocol. Positive clone plasmids were screened further by RFLP analysis. Briefly plasmids were separately digested with HaeIII and MspI (Promega, Inc., Madison, Wis.) at 37°C. The reaction products were visualized by electrophoresis on a 3% (wt/vol) low-melting agarose gel, stained with ethidium bromide and photographed for evaluation. Each enzyme generated 3-10 bands. For groups of clones possessing the same RFLP pattern, random representatives clones were selected for sequencing. Sequencing was carried out using the Big Die terminator technology. The average number of nucleotides of sequence determined was 900 bp.

454 pyrotag 16S rRNA libraries

Amplicon pyrosequencing was performed on a 454 GS FLX Titanium system (Roche, Penzberg, Germany) according to manufacturer specification. Briefly, barcoded amplicons for multiplexing were prepared using the universal primers 338f (5'- 3') and 506r (5'- 3') extended with the respective A or B adapters, key sequence and multiplex identifiers (MID) as recommended by Roche. Emulsion PCR and sequencing of the PCR amplicons was performed at Mr. DNA sequencing facilities following the manufacturer's instructions for the Roche (Branford, CT, USA) 454 GS Titanium technology (Allgaier et al., 2010). Amplicons were purified using Agencourt AMPure-XP beads (Beckman Coulter, Brea, CA) and pooled in an equimolar ratio of 109 molecules µl−1 as quantified by the Quant-iT PicoGreen dsDNA quantification kit (Invitrogen, Paisley, UK). Emulsion PCR, emulsion breaking and sequencing were performed applying the GS FLX Titanium chemistry following supplier protocols.

Hydrocarbon sediment content

Aliphatic hydrocarbons (AHs) and polycyclic aromatic hydrocarbons (PAHs) were measure in

all pockmark sediment layers, while volatile organic carbons (VOC) were measured only on top layer. VOC were measured by warming the about 1 g of sediments kept in a gas tight container (Bellco systems) at 80°C for 15 minutes. The Headspace content, containing the volatile hydrocarbons was then injected in a gas chromatographer, and the compound identified by its retention time calibrated against a standard. AH and PAH were obtained by a similar procedure, bygas chromatography (AH) or HPLC (PAH). Briefly, 1 g sediment (wet weight) was extracted in 5 mL (0.5 M) potassium hydroxide in methanol with a microwave (150 W for 10 min). Samples were centrifuged at 1,000×g for 5 min. Methanolic solutions were concentrated in a SpeedVac (RC1009; Jouan, Nantes, France) and purified with solid phase extraction (Octadecyl C18, 500 mg × 6 mL, Bakerbond; Mallinckrodt Baker, Phillipsburg, NJ, USA). A final volume of 1 mL was recovered with acetonitrile, and HPLC analyses were carried out using a water:acetonitrile gradient and fluorimetric detection. Individual hydrocarbons were identified by the retention time of appropriate pure standard solutions, and the quality assurance/quality controls were tested by processing blank and references samples (mussel tissues SRM 2977, NIST). The concentrations obtained for the SRM were always within the 95% confidence interval of certified value. The water content of sediments was determined during preparation of samples and used to normalize hydrocarbons concentration (micrograms per gram) to dry weight.

Mono aromatic compounds (BTEX) are composed by benzene, toluene, ethyl-benzene, xylens and phenols like phenol, 2-methylphenol, 3-methylphenol, 4-methylphenol, 2,4-dichlorophenol and 4-dichlorophenol and were determined by gas-mass spectrometry (GC-MS). Briefly 200-500 mg of frozen sediments were mixed with an exane and acetone solution (2:1) and shaken for 2h. The slurry are inserted into gas-high Teflon containers and extracted for 15 minutes at 110°C in a CEM Mars-5 Microwave Digestion/Extraction System. The coled samples are thus centrifuged (1,000 ×g for 5 min) and supernatant estracted on C18 solid phase extraction columns. Purified BTEX are collected using an esane:acetone solution, concentrated on speedvac rotator and analyzed in a gas-mass spectrometer (GC ramp 40°C for 4 min; 2°C/min ramp up to 65°C; 65°C/min ramp up to 280°C kept for 3 min before cooling). Mass-spectra are compared to a certified database for compound recognition (NIST/EPA/NIH Mass Spectra Search Program Version 2.0f).

Sedimentary organic matter

Sub-samples of sediments were immediately frozen at -20°C in the field, until determination of the organic matter composition (total protein, carbohydrate and lipid and phytopigments). Total protein (Prt) concentration were determined on sediment sub-samples according to Hartree (1972). Protein concentrations were expressed as bovine serum albumin (BSA) equivalents. Total carbohydrates (Cho) were analyzed according to Gerchakov and Hatcher (1972) and expressed as

glucose equivalents. Total lipids (Lip) were extracted from the sediment by direct elution with chloroform:methanol (1:1 v/v) according to Bligh and Dyer (1959) and then determined according to Marsh and Weinstein (1966). Analyses were performed spectrophotometrically.

Carbohydrate, protein and lipid concentrations were converted into carbon equivalents using the conversion factors 0.40 and 0.49 and 0.75 mgC mg^{-1}, respectively, and normalized to sediment dry weight (Fabiano et al., 1995). Biopolymeric organic C (BPC) was calculated as the sum of the C equivalents of protein, lipid and carbohydrate.

Chlorophyll-a and feopigments were extracted from sediment sub-samples according to Plante-Cuny (1974). Briefly few mg of $MgCO_3$ are added to ca. 1 g of wet sediment to avoid chlorophyll-a degradation. Samples are added with 90% acetone, sonicated and incubated in the dark at 4°C for 12 h. After the incubation the samples are centrifuged to remove the sediment and the supernatant is determined spectrofluorimetrically (ex. 650 nm, em. 750 nm) before and after acidification with HCl 0.1 N. Concentration are calculated against a standard curve and normalized to sediment dry weight. Total phytopigments (CPE) are obtained from the sum of chlorophyll-a and feopigments.

Extracellular Enzymatic activities

Extracellular enzymatic activities of key prokaryotic enzymes were carried out in order to determine the mobilization of organic matter. L-aminopeptidase and D-glucosidase activities were carried out on sediment sub-samples. Sediment slurry (prepared with per-filtered sterilized sea water, 1:1 v/v) were incubated for 1 h (enzymatic activity increased linearly with time) in the dark and at in situ temperature with, respectively, L-Leucine-4-methylcoumarinyl-7-amide (Leu-MCA) and 4-methylumbelliferone-D-glucopyranoside (MUF-Glu) as substrates. After incubation, samples were centrifuged (800 ×g) and the supernatant was analyzed fluorometrically.

Heterotrophic Carbon production

Heterotrophic C production (HCP) was measured using [^{3}H]-leucine incorporation (Danovaro et al., 2002). Briefly, sediment sub-samples (0.2 ml) were added to a saturating aqueous solution of [^{3}H]-leucine (final concentration, 6 mCi), and incubated for 1 h in the dark at in-situ temperature. After incubation, prokaryotic C incorporation was stopped by adding 1.7 ml 80% ethanol. The samples were then washed and immediately filtered under low vacuum (<100 mm Hg) on 0.2 m pore-size Nucleopore filters. The filters were treated with 2 N NaOH and incubated at 100°C for 2 h, then centrifuged (800 ×g, 10 min), and added to scintillation fluid (Hionic fluor; Packard Bioscience). Sediment blanks were stopped with ethanol immediately after addition of [^{3}H]-leucine. The data were normalized to sediment dry weight after desiccation. The radioactivity incorporated was measured by determining the counts min^{-1} in a liquid scintillation counter

(Packard Tri-Carb 300). Data of [^{3}H]-leucine incorporation are converted into heterotrophic Carbon production (HCP) by using the following formula:

$$HCP\ g^{-1} = [nmol - leu \cdot (100/7.3) \cdot M \cdot 0.86 \cdot R \cdot 2]/g$$

Where: "nmol-leu" is calculated as follows: DP M inc/(S.A. · 2.22×10^2) where: DPM inc is "DPM sample – DPM blank"; S.A. is the specific activity (in Ci mmol^{-1}) of the [^{3}H]-Leucine; the ratio "100/7.3" is the percentage of leucine into the total bacterial aminoacid pool; "M" is the molar weight of leucine; "0.86" is the conversion factor of bacterial protein production to bacterial C production; "R" is the correction for radioactive decay of the ^{3}H-Leucine; "2" is the intracellular isotope dilution "g" is sediment dry weight (grams).

Specific growth rate (μ, days^{-1}) were calculated from HCP and PBM using the following formula: $\mu=[\ln(1+HCP/PBM)]/t$ where t is the time over which HCP is considered.

Surface primary production

Estimates for surface primary production were obtained from the Ocean Productivity database (url: http://www.science.oregonstate.edu/ocean.productivity/) for the sampling area and period, and use the Vertically Generalized Production Model (VGPM) as described in Behrenfeld and Falkowski (2001). This model estimates depth-integrated net primary production (gC m^{-2} d^{-1}) based on surface chlorophyll (mg m^{-3}), surface PAR, and SST.

Statistic and phylogenetic analyses

All statistical analyses were performed using the statistical R-Software (R-Cran project, http://cran.r-project.org/). In order to test for differences among samples and factors analysis of variance (ANOVA) was carried. Significantly different samples were subjected to the Tukey HSD post-hoc test. When ANOVA assumptions were rejected, a more conservative level of p was chosen (Underwood, 1991).

In order to investigate the presence of trends in our sampling design, multivariate ordination analysis was performed in Chapter 5 and 8. Non-metric Multi Dimensional Scaling (nMDS) is an ordination technique in which variables describing a multidimensional space are scaled based on their similarity on a two-dimension plot, in order to maximize distance among points (Clarke and Gorley, 2001). This analysis was performed using the nMDS function from the Vegan package (Oksanen et al., 2012; http://cran.r-project.org/package=vegan).

In Chapter 5 environmental and trophic variables were superimposed with the ordisurf function in the Vegan package, to fit GAMs surfaces to the ordination. Generalized additive models (GAMs) analysis was performed, using the mgcv package (Woods, 2006) to understand the

importance of environmental and trophic variables in describing community structure and functioning. GAMs are an advancement of generalized linear model in which for every parameter added to the model a spline function is applied in order to perform a smooth (i.e. non-linear) fitting. The added complexity in resulting models is balanced by the increased accuracy in model prediction power. Models were built through successive additions of describing variables. Model selection was effectuated using Akaike Information Criterion (Akaike, 1974), GCV score (Woods, 2006) and increased accuracy of the model.

DGGE profiles were analyzed with ImageJ (Schneider et al., 2012) and R-software for cluster analysis to identify significant differences in the composition of bacterial communities. Briefly, the position of each DGGE band was recorded using the ImageJ Gel plugin and the resulting matrix was fed to R for the determination of the distance matrix based on Jaccard dissimilarity and used for cluster analysis.

Sequences obtained from libraries were manually checked for quality, primers were removed and the resulting sequences were aligned using ClustalW (Larkin et al., 2007) and SeaView (Gouy et al., 2010). The software Bellerophon (Huber et al., 2004) was used to identify chimeric sequences, which were removed from the dataset. Neighbour-Joining trees were constructed using the Jukes-Cantor correction and tree topologies were tested using 1000 bootstraps replications. Sequences of cultured bacteria retrieved as top blast hits against our sequences were included as references in the alignment (Chapter 6). Phylogenetic designation of the sequences to a specific group was obtained by integrating blastn and EzTaxon results with phylogenetic analyses (Chun et al., 2007). Chao1 non-parametric diversity estimator and rarefaction curves were computed using Rarefaction software (Brzustowski, 2003; http://www2.biology.ualberta.ca/jbrzusto/ rarefact.php).

Pyrotag libraries were analyzed using Qiime software (Caporaso et al., 2010) default parameters. Briefly, 16S rRNA gene sequences were clustered with uclust (Edgar, 2010) and assigned to operational taxonomic units (OTUs) with 97% similarity. Representative sequences from each OTU were aligned with Pynast using the Greengenes (DeSantis et al., 2006) core set and chimeric OTUs were identified. Taxonomy was assigned using the Greengenes 16S rRNA gene database (version October 2012). The resulting data set was processed in QIIME for OTU abundance. Alpha diversity was obtained in Mothur.

Automatic prokaryotic counts and biomass measurement (TPN and PBM) were performed using a custom made plugging for ImageJ. Briefly 20 color micrograph of the sample were obtained using a color CCD connected to the epifluorescence microscope. The obtained images were loaded into ImageJ and the three color channel separated. The green channel was selected due to Acridine Orange fluorescence and converted to binary image using a fixed threshold. The obtained image was counted using the analyze particles function of ImageJ. The obtained prokaryotic area was converted to biovolume of an equivalent projected area sphere. In order to test the validity of the

automatic count, numerous samples from different location where counted manually from 3 different experienced operator and assessed using the newly written code in ImageJ. The variability among operators (8-10%) was comparable with the variability between automated and manual count (7-10%). Results obtained from manual counts were plotted against automated ones and the resulting regression evaluated. On average, the two results where similar with a regression r of 0.987. Below the code of the written ImageJ macro:

```
//This macro count and measure the area of prokaryotes (or any other cell
particles present in the picture) using the particle analyzer and splitting image
channel according the fluorescence recorded. In this case the macro is set to work
with the green fluorescence of Acridine Orange used to count prokaryotes in
sediments.
Dimension, circularity and threshold level are sample/tissue/cells specific and
should be evaluated accordingly in a preliminary phase before to set up the macro
parameters. At the end of the measurement save the summary windows containing the
results.
//©2011 Giovannelli & d'Errico - ISMAR CNR

macro "Batch Prokaryote Count" {
dir1 = getDirectory("Choose Source Directory");
list = getFileList(dir1);
for (i=0; i<list.length; i++) {
       open(dir1+list[i]);
       imgname = list[i];
       number=i+1;
       status=number/list.length*100;
selectImage(imgname);
run("Split Channels");

//Select channel occording to fluorochrome used:
       selectWindow(""+imgname+" (red)");
       close();
       selectWindow(""+imgname+" (blue)");
       close();
       selectWindow(""+imgname+" (green)");
       run("Invert");
       setAutoThreshold();

//Specify at which level you like to threshold the image (img specific):
       setThreshold(0, 120);
       run("Convert to Mask");
       run("Watershed");
       run("Set Scale...", "distance=0 known=0 pixel=1 unit=pixel");

//Specify the dimension and circularity of the desired particles/cells to be
counted:
       run("Analyze Particles...", "size=40-600 circularity=0.50-1.00 show=Nothing
       summarize");
       close();
}
```

Chapter 4

Factors influencing prokaryotic community structure composition in sub-surface coastal sediments

Introduction[1]

The Earth's sub-surface represents a substantial portion of the biosphere (Whitman et al., 1998) and it can have a major influence in carbon (C) cycling and global biogeochemistry (Parkes et al., 1994; D'Hondt et al., 2004). At least 50% of all prokaryotes reside in this sub-surface layer (Whitman et al., 1998). Despite this, most studies have focused on the water column and the surface sediments, and hence there is little information on the prokaryotic distribution and community structure of this marine sub-surface (Schrenk et al., 2010). While the importance of *Bacteria* in biogeochemical cycles is well established (Gasol et al., 1997; DeLong et al., 1999; Biddanda et al., 2001), the role of *Archaea* in the functioning of marine systems is still poorly understood. *Archaea* have usually been regarded as organisms that inhabit extreme environments (Murray et al., 1998), although they are now known to be widespread throughout the oceans (DeLong, 1992; Fuhrman, 1992; Massana et al., 1997; Murray et al., 1998), where they constitute a relevant fraction of the microbial community. To date, all studies on marine sediments have reported that *Bacteria* dominate prokaryotic assemblages, with *Archaea* providing relatively small contributions (Llobet-Brossa et al., 1998; Sahm and Berninger, 1998; Vetriani et al., 1999; Ravenschlag et al., 2001; Ishii et al., 2004). In contrast, sub-surface sediments appear to be dominated by *Archaea* (Lipp et al., 2008), although not all studies have been in agreement and the informations available are contrasting (Schippers et al., 2005; Musata et al., 2006).

Environmental, predatory and trophic variables control prokaryotic distribution, abundance and community composition (i.e. Pernthaler, 2005; Fuhrman et al., 2006). The availability of organic

[1] This chapter has been published as Molari et al. in *Estuarine and Coastal Shelf Science, 97 (2012) 141-148.* Giovannelli and Molari are equally contributing autors.

matter in marine sediments is recognized as a major factor that affects the metabolism, distribution and dynamics of benthic organisms, from prokaryotes to megafauna (Dell'Anno et al., 2000). In particular, the biopolymeric fraction of sedimentary organic C, as the sum of the protein, carbohydrate and lipid C equivalents, has often been reported as the fraction of total organic C potentially available to benthic consumers (Fabiano et al., 1995).

In marine subsurface sediments, the quantity and quality of organic matter is largely dependent upon seasonal deposition and burial of organic matter produced in the photic layer, and upon the complex biochemical transformations of the particles as they sink down the water column and once on the sub-surface (Thiel et al., 1988). In this regard, the quality and quantity of the organic C drive the distribution of heterotrophic prokaryotes in marine sediments (Deming and Carpenter, 2008). However, chemoautotrophy is a common characteristic among many diverse microbial isolates from subsurface environments (Schrenk et al., 2010). Whether the energy sources are organic or inorganic, life in the absence of light in the sub-surface biosphere should be dependent upon chemical energy (Bach et al., 2006). Thus, environmental variables such as redox potential, pH and temperature should be also crucial in the shaping of prokaryotic community structures living in dark ecosystems. Among the predators, viruses can have important effects on prokaryotic assemblage composition, although how these effects are controlled remains controversial (Weinbauer, 2004; Middelboe et al., 2011). Viral infection is believed to be responsible for most of the C removal from prokaryotic production (Danovaro et al., 2008), and is potentially a driver of evolution through lateral gene transfer and species selection (Thingstad and Lignell, 1997; Middelboe and Jøgensen, 2006). We present here a study on the quantitative estimate of *Bacteria* and *Archaea* down a vertical profile from shallow sub-surface sediments. Unlike deep-sea sub-surface sediments sampled to date, marine coastal sediment receives a high input of photosynthetic organic carbon that sustains high microbial abundances and activities. Hence the coastal marine sub-surface represents an ideal study site to investigate how the transition from light energy to chemical energy shapes the prokaryotic community. The aim of this study was to investigate the biotic, trophic, and environmental factors that control prokaryotic abundance and metabolism down 1-m sediment cores sampled from a coastal area of the southern Adriatic Sea. Multiple regression analysis has been used to determine the factors associated with the variance along the sediment layers. These data help to clarify the interactions between biotic and abiotic factors in the control of prokaryotic community moving from surface to sub-surface sediment environments.

Study site and sampling

The present study was carried out in Manfredonia Gulf (southern Adriatic Sea) during the SAMCA-2 (System Approach to Mediterranean Coastal Areas) cruise of the Pit-Agem Project (Integrated Methodologies for the Study of Marine Trophic Processes, and Deployment and

Management of Oceanographic Platforms for Marine Monitoring). Three independently replicated sediment cores were collected at an area along the inner reaches of the Gulf of Manfredonia (15 m depth; coordinates, 41° 32' 59" N, 16° 02' 58" E), using an SW-104 spade corer. The three 100-cm-long sediment cores obtained were sliced into 21 horizontal layers: 0-0.5; 0.5-1; 1-1.5; 1.5-2; 2-3; 3-4; 4-5; 5-6; 6-8; 8-11; 11-15; 15-20; 20-25; 25-30; 30-35; 35-40; 40-45; 45-50; 50-60; 60-70; 70-100 cm. We measured a total of 14 different variables, each in replicates. This leads to a dataset of more than 2500 independent measures, which were used for the statistical analyses. The variables measured down the 100-cm cores where divided into conceptual classes: environmental (sediment water content, %; sediment temperature, °C; Eh, mV; pH; grain size distribution, %), trophic (carbohydrate, lipid, protein, mg g^{-1}; chlorophyll-a, pheopigments, mg g^{-1}), functional (HCP, mgC g^{-1} h^{-1}) and biological (prokaryote abundance, cell g^{-1}; prokaryotic biomass, mgC g^{-1}; virus abundance, vlp g^{-1}), according to Fuhrman et al. (2006), with a few modifications. Multiple regression analysis was used to identify the subset of variables that best described the variation of the community composition down the vertical profiles. Different conceptual models were applied to the regression analysis to test the reliability and robustness of the data obtained; model 1 was the least restrictive model tested. Model 1 used all of the measured variables to describe the variance of the community structure variation (expressed as *Bacteria* to *Archaea* ratio; BAR) and HCP. In this model, no logical exclusion of variables was made, even if potential interdependence was suspected due to laboratory analytical procedures (e.g. prokaryotic abundance and biomass obtained from the same slide by epifluorescence microscopy). Model 2 was more restrictive, as the community structure variation down the vertical profile was analysed using the variables not directly related to the prokaryotic assemblages (e.g. prokaryotic abundance, biomass, and metabolically active cells were excluded from the biological factors group). Model 2 was also used to describe other prokaryotic parameters and activities. Alternatively, prokaryotic abundance, biomass, metabolically active cell number, and HCP were used as dependent variables for the analyses. For each model, factor groups and single factors were analyzed, and their significance in explaining the variance of the dependent variables are reported. All statistical analyses were performed using R software (R development Core Team, 2010).

Results

The sediment-water interface had a temperature of 23.5 ± 0.5°C (0 cm), which then showed a decrease down the vertical core profiles (to 20.9 ± 0.32°C at 100 cm). In all of the cores, the sediments had negative redox potential (mean, 279.5 ± 37 mV) with a decrease in the first 11 cm below the sea floor (bsf), and than an increase back to the original value. The water content ranged from 36.5% to 63.6% (in bottom and sediment surface, respectively). In all of the cores, the sediment grain size was prevalently silt-clay (mean, 97%; Figure 4.1). Analysis of the vertical

profiles for the BPC content showed a decrease down cores (data not shown). In all three cores, protein was the ruling class of biochemical organic matter (mean, 67.7%), followed by carbohydrate (mean, 24.2%) and lipid (mean, 8.1%), and these showed irregular patterns down the vertical profiles of the sediment cores. Carbohydrate concentrations showed a clear decrease down the vertical profiles, from 0 cm bsf to 100 cm bsf. A similar pattern was seen for the lipid concentrations (Figure 4.1), as was also seen for the chlorophyll-a and phaeopigment concentrations. The phytopigment content decreased by two orders of magnitude with depth in the sediment core. Statistical analyses showed no differences among the three cores down the vertical profiles (Kruskal-Wallis rank sum test, $p>0.5$).

Prokaryotic abundance (Figure 4.2) was significantly higher in the top layers of the cores (Kruskal-Wallis rank sum test; $p<0.001$), with values ranging from $0.3 \pm 0.15 \times 10^8$ to $15.7 \pm 2.0 \times 10^8$ cell g^{-1}. In all of the cores, the prokaryotic abundance showed a strong significant decrease (up to two orders of magnitude) down the sediment profile from 0 cm bsf to 11 cm bsf, with values ranging from $0.3 \pm 0.15 \times 10^8$ to $15.7 \pm 2.0 \times 10^8$ cell g^{-1} (Figure 4.2).

Prokaryotic abundance was significantly higher in the top layers of the cores (Kruskal-Wallis rank sum test; $p<0.001$). Previous studies of other marine sediments have reported gradually decreasing cell numbers with increasing sediment depth (Boetius et al., 2000; Quèric et al., 2004; Ishii et al., 2004; Deming and Carpenter, 2008).

Table 4.1: Multiple regression analysis using single factors. ns, $p>0.05$; , $p = 0.05$; *, $p<0.05$; **, $p<0.01$; ***, $p<0.001$

		Model 1[a]		**Model 2**			
Factor group	**Factor**	**BAR[b]**	**HCP**	**BAR**	**Biomass**	**Active cells**	**HCP**
Biological	Abundance	ns	*	np	np	np	np
	Biomass	ns	*	np	np	np	np
	Active cells	ns	ns	np	np	np	np
	Virus Abun.	ns	***	ns	ns	*	***
Functional	HCP	°	ns	*	ns	*	-
Environmental	Temperature	ns	***	ns	ns	***	**
	Water content	*	*	*	*	***	ns
	Silt-Clay %	***	ns	**	ns	*	ns
	pH	ns	ns	ns	ns	ns	ns
	Eh	ns	***	ns	ns	***	**
Trophic	Carbohydrate	ns	ns	ns	ns	ns	ns
	Lipid	ns	°	ns	ns	ns	ns
	Protein	°	°	ns	ns	ns	ns
	Chl-a	ns	ns	ns	ns	ns	ns
	Pheopigment	°	ns	ns	ns	ns	ns

a- The table show multiple regression analysis for Model 1 and Model 2. See Study site and sampling section for details;
b- BAR: *Bacteria* to *Archaea* ratio used as descriptor of community structure;
ns, $p>0.05$; °, $p = 0.05$; *, $p<0.05$; **, $p<0.01$; ***, $p<0.001$;
np- analysis not performed, see Study site and sampling section for details.

The prokaryotic abundance in the deeper layers of the cores was in line with other studies, and the abundance did not show any significant trends from 11 cm bsf to 100 cm bsf (Schippers et al., 2005; Biddle et al., 2006). There was a similar decrease in prokaryotic biomass down the cores, from 132.3 ± 34.5 mgC g^{-1} to 2.4 ± 0.8 mgC g^{-1} (data not shown). No statistically significant differences were seen across the three cores for either prokaryotic abundance or biomass (Kruskal-Wallis rank sum test, $p>0.5$). HCP showed a clear decrease down the vertical profiles from the top layers (from 1.23 ± 0.23 to 0.19 ± 0.03 mgC g^{-1} h^{-1}), while in the deeper layers of the sediment cores the pattern was again constant (mean, 0.03 ± 0.01 mgC g^{-1} h^{-1}; data not shown). As before, the three cores showed no differences (Kruskal-Wallis rank sum test, $p>0.5$). The numbers of viruses ranged from $0.5 \pm 0.26 \times 10^8$ to $17.5 \pm 2.8 \times 10^8$ virus g^{-1}, and these showed only a slight decreased with increasing depth down the sediment cores (Figure 4.1).

Overall, the number of cells visualized using the EUB338 and ARCH915 probes accounted for 80% e 94% of the total prokaryotic abundance (Figure 4.2). The highest contribution of *Bacteria* to the total prokaryotic counts (70%) was seen at 4 cm bsf. With increasing depth down the sediment cores, the *Bacteria* relative abundance decreased to ca. 23% (from 50 to 100 cm bsf). In contrast, in the top sediment cores, the percentage of *Archaea* was lower than in the deeper sediment layers (means, 32%, 47% and 65%, for 0-4 cm bsf, 5-35 cm bsf and 50-100 cm bsf, respectively). Using model 1 to describe the variation of the community structure down the vertical profiles, the grain size distribution and water sediment contents best described the variance. HCP, protein and pheopigment content showed close-to-significance levels (Table 4.1). Interactions within groups were always significant for the biological and environmental groups; however, in single factor analyses, no biological factor was detected, which suggested strong internal factor interactions. When HCP was used as a dependent variable, again the biological and environmental within-groups interactions were significant (Table 4.2; $p<0.001$). The single factors responsible for the HCP distribution down the vertical profiles were virus abundance, temperature and redox potential (Table 4.1; $p<0.001$), followed by prokaryotic abundance, biomass, and sediment water content ($p<0.05$). Protein and lipid showed close-to-significance levels.

Excluding prokaryotic-related parameters from the analysis, and using them as dependent variables in model 2, the community structure variance was described by the same subset of single factors, supporting the previous results (Table 4.1). The grain size distribution and water content of the sediment, together with HCP, were associated with most of the variance, followed by protein at close-to-significance levels. HCP was associated in model 2 to a subset of factors similar to those in model 1. Virus abundance, temperature and redox potential were the best descriptors of the vertical variation (Table 4.1; $p<0.01$ and $p<0.001$). When the prokaryotic biomass was used as a dependent variable, only the water content of the sediment was significant in the analysis output. Active cells were influenced by a complex array of factors; temperature, water content and redox potential were identified as significant through the multiple regression analysis ($p<0.001$),

followed by grain size distribution of the sediment, HCP and virus abundance (Table 4.1). Interactions within the environmental group were significant for all of the dependent variables used. All factor groups were significant when the number of metabolically active cells was used in the analysis as a dependent variable (Table 4.2).

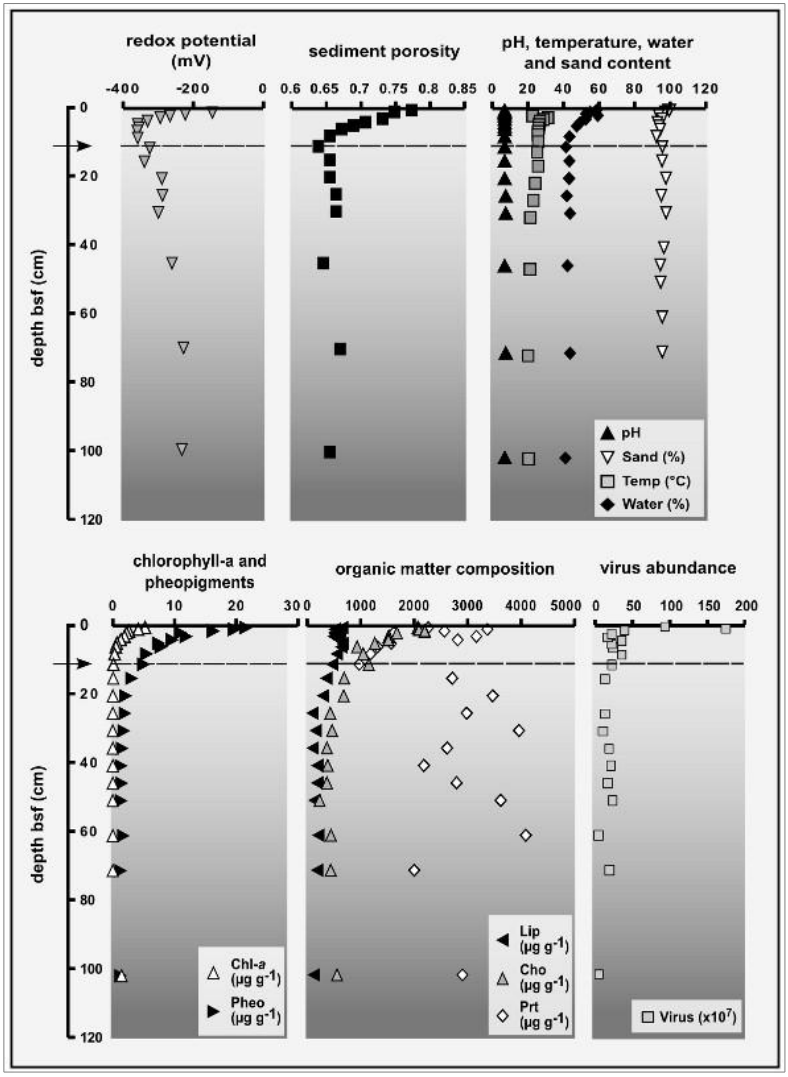

Figure 4.1: Vertical profile of the environmental and trophic variables down the 100-cm bsf sediment cores, as indicated. Data are reported as means (for clarity, standard deviations are not shown). The arrow points the layer in which the community showed significant changes in structure (11 cm bsf) and co-variables.

Discussion

The in situ identification of prokaryotic cells in sub-surface sediments is hampered by the low cellular rRNA contents of the target organisms (Ishii et al., 2004). Fluorescent in situ hybridisation catalysed reporter deposition (CARD-FISH) has the potential to overcome this limitation (Ishii et al., 2004; Hoshino et al., 2008), and was therefore used to detect and quantify bacterial and

archaeal cells. In this study, the fraction of cells targeted by CARD-FISH represented a high percentage of the total prokaryotic stained cells (~80%) and was relatively constant down the vertical profiles.

Although some previous studies based on hybridisation analysis have shown strong decreases in cell-detection frequencies down sediment profiles (Llobet-Brossa et al., 1998; Sahm and Berninger, 1998; Ravenschlag et al., 2001) as result of lower amount of rRNA, more recent CARD-FISH marine sediment studies have shown that the detectable cell fraction does not decrease, or decreases only slightly, with sediment depth (Ishii et al., 2004; Schippers et al., 2005). There are a few studies that have used FISH-based-technique to describe the bacterial and archaeal abundances along sediment profile, and most of them are focused on first 5-40 cm (Llobet-Brossa et al., 1998; Sahm and Berninger, 1998; Ravenschlag et al., 2001; Ishii et al., 2004) or below 1 m (Mauclaire et al., 2004; Schippers et al., 2005; Biddle et al., 2006) of sediments depth. In this study, for the first times, the application of CARD-FISH as a finescale study of shallow sub-surface prokaryotic community structures has provided a detailed description of the prokaryotic assemblage distribution down to the 100-cm sediment depth.

In agreement with all previous similar hybridization studies carried out in upper buried marine sediments, B*acteria* were the dominant prokaryotic domain (Llobet-Brossa et al., 1998; Sahm and Berninger, 1998; Ravenschlag et al., 2001; Ishii et al., 2004); however, in the present study, *Archaea* represented an important fraction of the sediment prokaryotic assemblages, and their importance increased with increasing sediment depth (Figure 4.3). The contribution of *Archaea* to the sub-surface prokaryotic abundance tended to increase down the sediment profiles due to the drop in the bacterial abundance (Figure 4.2), and *Archaea* dominated the prokaryotic assemblages below 60 cm bsf (Figure 4.3). Overall, our data highlight that already below 11 cm bsf there is a shift in the metabolically active prokaryotic community composition. Moving down into the sediments, the upper prokaryotic assemblages, dominated by *Bacteria,* shift towards a prokaryotic community with increasing contribution of *Archaea.*

As a general rule, decrease of microbial cell counts along sediment profile and shift in community structure are probably a result of decreasing organic carbon quality and availability in aged, deeply buried sediments (Parkes et al., 2000). Hence the change in prokaryotic community structure observed in our samples could not be addressed only to organic matter availability, but other abiotic and biotic factors must be taken into consideration.

The driving force that determines the decrease in prokaryotic abundance and community structure variation down the vertical profiles can arise from a complex mixture of biotic and abiotic factors: low mixing or bioturbation, sediment composition (e.g. grain size distribution, sediment water content), energy-stressed conditions (low food, electron acceptors, dissolved substrate and metabolite availability), and/or predatory pressures and competition.

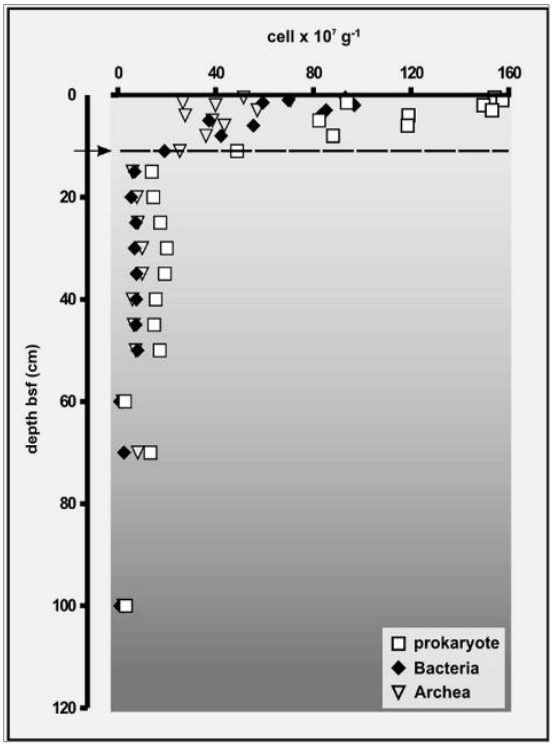

Figure 4.2: Vertical profiles of total prokaryotic, *Bacteria* and *Archaea* abundances down the 100-cm bsf sediment cores, as indicated. The arrow indicates the layer in which the community showed significant changes in abundances (11 cm bsf). Data are reported as means (for clarity, standard deviation are not shown).

In the present study, we divided and measured the co-variables in conceptual classes, and used them to understand the distribution patterns of the microbial assemblages. Our data clearly indicate a dominant role of environmental factors in controlling of the community structure. Sediment water content and grain size distribution were indicated by both models as the main forcing factors to explain the vertical distribution of prokaryotes. This result was expected, as pore-water volume has already been proposed as the main driver of prokaryotic abundance in sediments (Schmidt et al., 1998). Grain size distribution and pore-water volume are strictly related parameters that influence the mechanical and chemical stress that cells undergo. Water is essential for the functioning of cells, favoring catabolite and metabolite exchange, and electron exchange, and it is the primary solvent for all biological reactions.

The water content has been indicated in various models as also influencing active cell numbers, together with redox potential. Redox disequilibrium creates the main chemical energy source that sustains life in the absence of light in the sub-surface biosphere (Schrenk et al., 2010). Both tested models consistently indicated environmental factors as the main drivers of microbial assemblages changes in the present study.

Surprisingly, trophic factors were never significant; nevertheless, burial of organic matter produced in the photic layer is the main source of electron donors and the main organic C source in the subsurface sediments (Blair et al., 2007). Protein and lipid were close to significance only for explaining heterotrophic production, which suggests their importance in heterotrophic metabolism. Heterotrophic metabolism could also be sustained by fresh organic material produced in situ by viral lysis of prokaryotic cells. Our data indicate that viral infection is strongly related to HCP down the sediment layers. Together with temperature variations, redox potential and sediment water content, virus abundance best describe the variability of the HCP down the sediment profiles, which suggests a strong influence of viral infection on prokaryote metabolism (Mei and Danovaro, 2004).

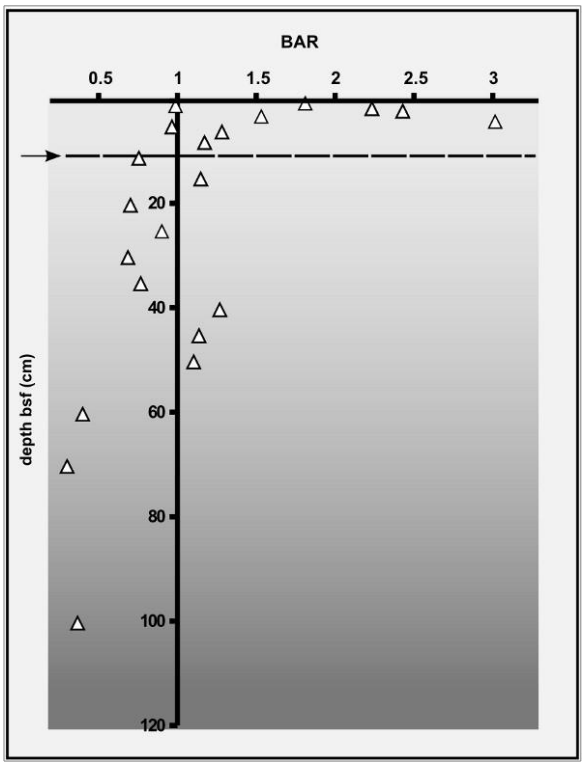

Figure 4.3: Community structure variation down the 100-cm bsf sediment cores, as indicated. Data are expressed as Bacteria to Archaea ratio (BAR). Note the dominance of Bacteria in the upper layers (BAR>1), and the dominance of Archaea in the deeper layers (BAR<1). The arrow points the layer in which the community showed significant changes (11 cm bsf).

Danovaro et al. (2008) recently showed how viral predation is the main source of bioavailable organic materials in energy-stressed environments such as deep-sea sediments. It can be hypothesised that the subsurface sediment ecosystems undergo similar mechanisms, in which viruses are responsible for the in-situ turnover of the organic materials. In contrast, virus abundance was not significant in explaining the community structure, although this has been suggested in many studies (Weinbauer, 2004; Winter et al., 2005; Danovaro et al., 2008), while there have also been several studies with controversial results (see Weinbauer, 2004, and

references therein).

The decrease in bacteria abundance and HCP in the first 15 cm bsf suggests a shift in prokaryotic community metabolism: the upper prokaryotic assemblages dominated by *Bacteria* and heterotrophic metabolism that are strongly influenced by trophic resources, and the deeper prokaryotic assemblages where buried organic matter is not the driving force for microbial abundance and activity, and where *Archaea* have major importance in the prokaryotic community structure. It has been proposed that *Archaea* are united by a universal ecological ability to cope with energy stress (Gold, 1992).

Table 4.2: Summary of the multiple regression analysis using groups. ns, p>0.05; , p = 0.05; *, p<0.05; **, p<0.01; ***, p<0.001

	Model 1[a]		**Model 2**			
Factor group	**BAR[b]**	**HCP**	**BAR**	**Biomass**	**Active cells**	**HCP**
Biological	***	***	°	***	***	***
Functional	°	ns	*	ns	*	-
Environmental	***	***	***	***	***	***
Trophic	°	ns	ns	ns	***	ns

a- The table show multiple regression analysis for Model 1 and Model 2. See Study site and Sampling section.
b- BAR: Bacteria to Archaea ratio used as descriptor of community structure.
ns, p >0.05; °, p = 0.05; *, p <0.05; **, p <0.01; ***, p <0.001

In this context our results support the hypothesis that adaptation to chronic energy stress is the crucial factor that distinguishes *Archaea* from *Bacteria* (Valentine, 2007). Indeed the sub-surface environment is poor in food and energy resources (labile organic compounds, electron acceptors, dissolved substrates and metabolites), and thus the increase in *Archaea* importance down the sediment profiles (this study) and their dominance in the deeper buried sediments (this study; Lipp et al., 2008) provide further evidence that adaptation to energy stress drives the ecology and evolution of *Archaea.* With regard to metabolism, one of the key unresolved issues from all of the subsurface studies has been the balance between production and respiration, and in particular, whether such life is capable of primary production based on lithotrophy (Schrenk et al., 2010). Tens and hundreds of meters below the sediment surface there are potential geofuels (or inorganic energy sources) that can replace the light energy in driving productivity (Bach and Edwards, 2003; Edwards et al., 2005; Bach et al., 2006). In near-surface sediments, organic carbon substrates should sustain microbial abundance and activity (D'Hondt et al., 2002, 2004), resulting in removal of organic matter across sediment column. In spite of high biopolymeric organic C amount, our results showed the major importance of the environmental factors influencing the availability of

inorganic electron donors/acceptors (water content and redox disequilibria) as a driving force of active cell abundance, suggesting that lithotrophy could be an important metabolic pathway yet in shallow sub-surface sediments. In similar works carried out in different environments (i.e. tidal-flat sediment) redox state and trophic resource have been identified as key factor driving community shifts (Wilms et al., 2006a, b).

In conclusion the application of CARD-FISH on 1 m coastal sediment cores allowed us to observed a shift on community structure between surface and bottom layers of cores, furthermore using active cells abundance and multiple regression analysis we were able to identify the principal abiotic and biotic parameter shaping prokaryotic community. Although results of this study do not allow drawing definitive conclusions on the metabolism of shallow sub-surface prokaryotes, they raise questions concerning the possible shift from organotrophic to lithotrophic metabolism accompanying prokaryotic community structure changes observed below coastal superficial marine sediments.

Chapter 5

Large-scale distribution and activity of prokaryotes in deep-sea surface sediments of the Mediterranean Sea and adjacent Atlantic Ocean

"Out of clutter, find simplicity."

Albert Einstein

Introduction[2]

The deep-sea floor represents a substantial portion of the biosphere, covering approximately 65% of Earth's surface. It constitute a dynamic environment linked to upper water column processes (Smith et al., 2009), and has a major influence in carbon cycling and global biogeochemistry (del Giorgio and Duarte, 2002; Parkes et al., 1994; D'Hondt et al., 2004). Moreover, it has also become clear that the microbial processes occurring along the deep-sea floor are essential in sustaining oceanic primary and secondary production.

Recent estimates indicate that at least 6.6×10^{29} prokaryotes reside in the first few meters of sediment depth (Whitman et al., 1998). Prokaryotes are key player in all ecosystems and in the deep-sea they have a crucial role recycling POM and DOM sinking from the photic zone (Azam and Malfatti, 2007). Despite their importance, little is known about the large-scale distribution of prokaryotes in deep-sea surface sediments (Schauer et al., 2010; Kouridaki et al., 2010), as most scientific literature is focused on the water column (De Corte et al., 2008; De Corte et al., 2012; Tamburini et al., 2009; Teira et al., 2004).

[2]This chapter is part of a manuscript Giovannelli et al. - Large-scale distribution and activity of prokaryotes in deep-sea surface sediments of the Mediterranean Sea and adjacent Atlantic Ocean. *In prep.*

Even less is known, on large scale, about the ratio between *Bacteria* and *Archaea* domain in top sediment layers (Molari et al., 2012; Molari and Manini, 2012). *Bacteria* dominance in surface sediments is generally accepted (Molari et al., 2012; Bowman et al., 2003; Chapter 4 pf this thesis) and *Archaea* account for 5 to 30% of the total prokaryotic abundance (Molari et al., 2012). This value increases with increasing sediment depth (Teira et al., 2004; Tamburini et al., 2009). While the importance of *Bacteria* in biogeochemical cycles is well established (Gasol et al., 1997; DeLong et al., 1999; Turley and Stutt, 2000; Biddanda et al., 2001), the role of *Archaea* in the functioning of marine systems is still poorly understood. *Archaea* have been regarded as organisms that inhabit extreme environments (Murray et al., 1998), although they are now known to be widespread throughout the oceans of the world (DeLong, 1992; Fuhrman, 1992; Massana et al., 2002; Murray et al., 1998), where they constitute a relevant fraction of the microbial community (Karner et al., 2001).

Previous studies reported *Crenarchaea* as the most abundant component of *Archaea* population in oxygenated deep waters (De Long et al., 1999; Karner et al., 2001) and surface sediments (Vetriani et al., 1999; Corinaldesi et al., 2011; Molari et al., 2012) surpassing the *Euryarchaea* abundances of ca. five fold. *Euryachaea* are an *Archaea* group that comprises most extreme halophiles (e.g. genera Halobacterium, Haloaredivivus) and methanogens (e.g genera Methanococcus, Methanothermus), including also methanotrophs (e.g. ANME-1 cluster, Methanosarcina) and thermophiles (e.g. Thermococcus).

Prokaryotic distribution, abundance and community composition are controlled by environmental and trophic variables (Pernthaler, 2005; Fuhrman et al., 2006; Molari et al., 2012). Until now only regional and local scale driving factors have been investigated and, although depth-related trends in prokaryotic abundance distribution have been reported (Pfannkuche and Soltwedel, 1998; Quéric et al., 2004), the enduring controlling factor of the variability of prokaryotic parameters (i.e. abundance, biomass and activity), appears to be the amount and availability of organic matter settling to the seafloor (Boetius and Damm, 1998; Boetius et al., 2000; Turley and Stutt, 2000; Turley and Dixon, 2002; Deming and Carpenter, 2008). In deep-sea sediments the quantity and quality of organic matter is largely dependent upon seasonal deposition and burial of organic matter produced in the photic layer, as well as the complex biochemical transformations of the particles as they sink down the water column (Thiel et al., 1988). Thus, the quality and quantity of the organic carbon is considered to control the distribution of heterotrophic prokaryotes in marine sediments (Deming and Carpenter, 2008). To this we need to add the contribution of *in situ* and local processes, such as dark energy production (i.e. authotrophic fixation of carbon in absence of light; Molari et al., 2013), the viral shunt (Danovaro et al., 2008) diverting large quantities of organic matter back into the microbial loop, and lateral inputs and stochastic events (deep-water currents, lateral advection and cascading; Canals et al., 2006).

We present here the results of five oceanographic cruises, analyzing the influence of environmental and trophic variables on the large scale distribution of prokaryotic community structure and activity in the deep-sea surface sediments of the Mediterranean Sea and adjacent Atlantic Ocean. We assumed during our analyses that on large scale different variables can come into play, and latitude and longitude may represent important forcing variables hiding the effects of local factors (Schauer et al 2010; De Corte et al., 2012). This implies that geographical position may have a strong influence on the functioning and structure of the prokaryotic community.

Sampling

Sediments samples were collected during five oceanographic cruise in 2008 and 2009 as part of the EU funded project ESF-EuroDeep BIOFUN (Biodiversity and Ecosystem functioning in contrasting southern European deep-sea environment). For details on sampling locations and depths see Table 5.1 and Figure 5.1. Sediments were collected by box-corer (n=3) and sub-sampled on board collecting and processing the top 1 cm of sediments. Aliquots were immediately frozen at -20°C for the determination of the organic matter composition. Sediments sub-samples were directly analyzed for bacterial production, and replicates of about 1 ml wet sediment were fixed using tamponed formalin (final concentration 2%, in sterile and filtered seawater) and stored at 4°C until processed for total prokaryotic abundance and biomass (Manini and Danovaro, 2006; Pearson, 2008).

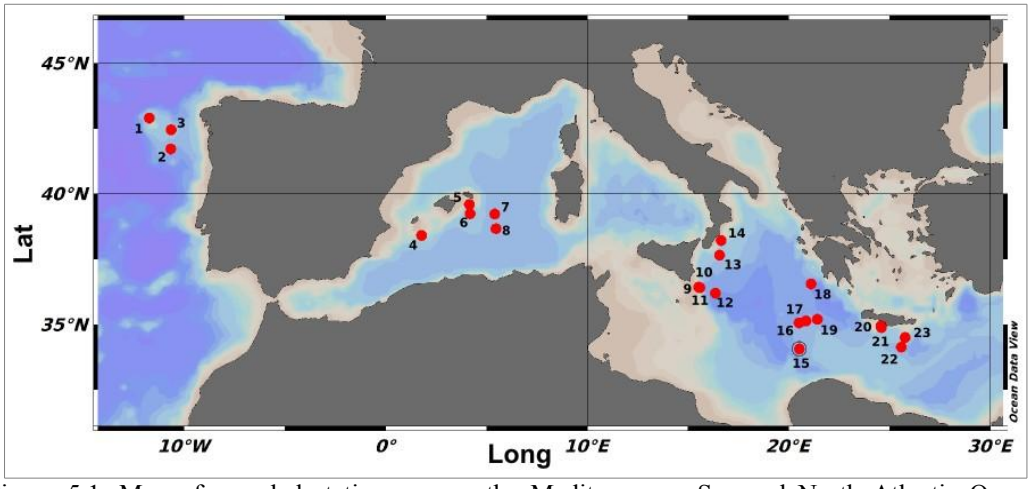

Figure 5.1. Map of sampled stations across the Mediterranean Sea and North Atlantic Ocean. Numbers were given to the station progressively, according to their longitude.

To investigate the prokaryotic community structure, sediment sub-samples (0.5 g) were fixed in 4.5 ml formaldehyde (final concentration, 2%) in phosphate-buffered saline (PBS, pH 7.4) for 1 h at room temperature. The fixed samples were then washed three times with PBS (10,000 ×g for 5

min between washes), and then stored in PBS/ethanol (1:1; v/v) at -20°C until further processing (Ishii et al., 2004).

Statistical analyses

Stations were grouped into areas on the basis of their geographic positions: North Atlantic Ocean (N, 3 stations), West (W, 5 stations), Central (C, 11 stations) and East Mediterranean Sea (E, 4 stations) and used as factor in the following analyses. Depth was also used as a factor with 4 levels (1200, 2000, 3000 and 5000 meters). Map plots were drawn using Ocean Data View (Schlitzer, R., Ocean Data View, http://odv.awi.de, 2011). Variables were divided among descriptor of the prokaryotic community (TPN, PBM, BAR, ECR, HCP), environmental (LAT, LONG, Depth, Temperature) and trophic (BPC, PRT, LIP, CHO, CPE), and used for statistical analyses using nm-MDS and GAMs analyses (see Chapter 3).

Results

Trophic variables

BPC content of surface sediment and CPE are plotted over the sampling area in Figure 5.2a and 5.2b and reported averaged for area and depth in Figure 5.3a. On average, West and Central Mediterranean accounted for the higher amount of BPC in sediment (on average 1.16±0.48 and 1.03±0.35 mgC g^{-1}, respectively) with its quantity evenly distributed among depths (Figure 5.3b). CHO were the dominant category in organic matter, constituting on average the 50% of total organic matter with the PRT following with an average contribution of 37% (Table 5.3). CPE followed a similar trend with higher value in Western and Central Mediterranean (3.75±2.05 and 2.21±2.25 μg g^{-1}), showing a higher variability along depth transects with average value higher at 2000 meters (on average 3.46±2.61 μg g^{-1}; Figure 5.3b). CPE showed a good correlation with surface primary production (SPP - Pearson moment correlation, n=69, $r=0.51$, $p<0.05$).

Prokaryotic abundance and biomass

TPN and PBM distribution along the Mediterranean Sea can be visualized in Figure 5.2c and 5.2d. No clear longitudinal gradients were present and higher values of prokaryotic abundances were present at station 11, 2000 m depth in the Central basin with 2.61±0.01 $x10^8$ cell g^{-1}. Despite the lack of significant trends, TPN varied significantly among areas, with higher value in W and C Mediterranean Sea (Figure 5.3c, ANOVA $p<0.05$). Minimum TPN of 1.32±0.21 $x10^7$ cell g^{-1} was found in the North Atlantic at 1200 m (station 1). Significant trends were also present for the depth factor with maximum values at 2000 m and minimum at 5000 m (Figure 5.3d, ANOVA $p<0.01$).

The interaction between area and depth revealed major variation across areas at 1200 m, while such differences were absent at 2000 and 3000 m depth (HSD-Tukey post-hoc test $p<0.05$).

Table 5.1. Table presenting sampling stations coordinates, depths, area, cruise, temperatures and surface primary production.

station	cruise	depth	area	Latitude	Longitude	Bottom temperature	Surface Primary Production
		m		° N	° E	°C	gC m^{-2} d^{-1}
1	Pelagia 08	1200	N	42.9118	-11.7525	9.6	480.9
2	Pelagia 08	3000	N	41.7285	-10.6835	2.7	523.3
3	Pelagia 08	2000	N	42.4607	-10.6547	4.0	546.8
4	Trans-Med 09	1200	W	38.4203	1.7704	13.0	434.6
5	Pelagia 09	1200	W	39.5997	4.1454	13.0	352.5
6	Pelagia 09	2000	W	39.2498	4.1667	13.2	315.8
7	Pelagia 09	3000	W	39.2363	5.4019	13.3	432.5
8	Trans-Med 09	3000	W	38.6776	5.4647	13.3	430.2
9	Biofun 09	1200	C	36.4327	15.5174	13.7	650.0
10	Biofun 09	2000	C	36.4222	15.5458	13.7	614.7
11	Biofun 09	2000	C	36.4168	15.5836	13.8	628.4
12	Trans-Med 09	3000	C	36.1987	16.3526	13.9	353.6
13	Trans-Med 09	2000	C	37.6539	16.5591	13.8	319.4
14	Trans-Med 09	1200	C	38.2237	16.6298	13.7	384.7
15	Biofun 08	3000	C	35.0732	20.5045	14.7	315.8
16	Biofun 08	3000	C	35.0682	20.5075	14.7	278.6
17	Biofun 08	3000	C	35.1388	20.8482	14.7	309.9
18	Biofun 08	5000	C	36.5597	21.0984	14.7	325.2
19	Biofun 08	3000	C	35.1972	21.4075	14.7	341.3
20	Biofun 08	1200	E	34.9539	24.5709	14.7	312.8
21	Biofun 08	3000	E	34.8833	24.5875	14.7	308.1
22	Trans-Med 09	3000	E	34.1459	25.5696	13.9	268.4
23	Trans-Med 09	1200	E	34.5061	25.7590	13.9	285.0

As seen in Figure 5.2d Table 5.2, PBM did not correlate with TPN, and no significant differences were found among areas (Figure 5.3c and Table 5.2), while depth related trends were consistent with prokaryotes abundance (Figure 5.3c and Table 5.2, ANOVA $p<0.001$). Once again, the highest values of PBM were present at station 11, with 9.83±0.68 µgC g^{-1}. A significant interaction was found between area and depth (ANOVA, $p<0.05$; Table 5.2).

Prokaryotic community structure

The total number of prokaryotes counted by CARD-FISH accounted for an average of *ca.* 91% of the total prokaryotes counted by acridine orange. CARD-FISH analysis revealed a dominance of *Bacteria* over *Archaea* in all investigated sediments (on average, BAR 2.2±0.83) with exception of station 17 in the Central Med (3000 m depth) where *Archaea* dominated the community (BAR value of 0.88±0.06). Higher values of BAR were detected in station 19 in the Central Med (3.67±0.56, 3000 m depth), followed by station 11 (3.60±0.75, C Med, 2000 m depth) and 1 (3.14±0.84, N Atlantic, 1200 m depth).

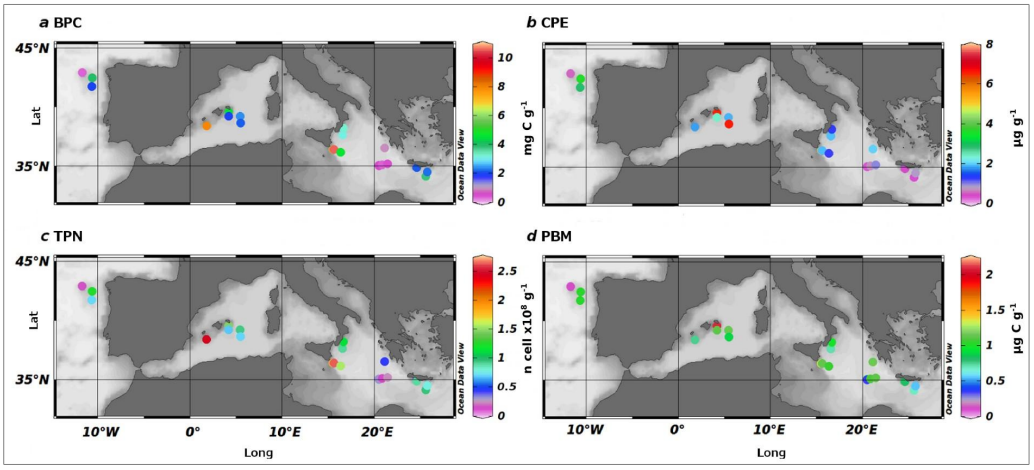

Figure 5.2. Panel of maps showing BPC (a), CPE (b), TPN (c), PBM (d) values across the sampled stations. Dots colors represent variables value as expressed in the side axis.

BAR varied significantly between areas (ANOVA $p<0.01$, Table 5.2; Figure 5.3e), but not depths (Figure 6.3f). No interaction between area and depth was identified. North Atlantic and East Mediterranean Sea were significantly different (Figure 5.3e, Table 5.2, HSD-Tukey post-hoc test $p<0.01$), while West and Central Mediterranean were a blend of the two values.

The *Archaea* community was described using the *Euryarchaeota* to *Crenarchaeota* ratio (ECR). ECR was constant among areas with an overall mean of 0.57±0.35 (Figure 6.3e). *Crenarchaeota* dominated the community in all the investigated station with the exception of station 18 in the Central Mediterranean Sea (1.64±0.58, Matapan-Vavilov Deep, 5137 m depth). Influenced by these results, ECR changed significantly among depths (ANOVA $p<0.001$, Table 5.2 and Figure 5.3f) with 5000 m being different from all other depths ($p<0.001$, HSD-Tukey post-hoc test) and no other statistical significant difference between 1200, 2000 and 3000 m depth was found (Table 5.2).

Prokaryotic activity in surface sediments

HCP in surface sediments ranged from 3.83±0.84 to 54.81±0.85 ngC g^{-1} h^{-1} (in station 3, North Atlantic at 2000 m and station 17, Central Mediterranean at 3000 m depth, respectively) with an overall average of 16.32±16.20 ngC g^{-1} h^{-1}. HCP showed significant changes among areas (ANOVA $p<0.001$, Table 5.2 and Figure 5.3g), with the North Atlantic surpassing other areas of ca. 3 folds (HSD-Tukey post-hoc test $p<0.001$, Figure 5.3g). Significant differences were also found among depths (ANOVA $p<0.001$, Table 5.2 and Figure 5.3h) with higher value at 1200 and 2000 m depth (23.92±19.76 and 26.14±18.09 ngC g^{-1} h^{-1}, respectively) than at 3000 and 5000 m (8.3±5.84 and 6.01±1.03 ngC g^{-1} h^{-1}, respectively).

Specific growth rate (μ) ranged between 0.02±0.001 to 6.88±3.52 d^{-1} for station 12 at 3000 m depth in the Central Mediterranean and station 1 at 1200 m in the North Atlantic respectively. Average growth rate was 0.51±1.61 d^{-1}.

Table 5.2. Results of ANOVA analyses on the dataset.

	area			**depth**			**area x depth**		
	df	**F**	**P**	**df**	**F**	**P**	**df**	**F**	**P**
TPN	3	3.17	ns	3	11.56	***	5	6.96	**
PBM	3	2.82	ns	3	10.79	***	5	4.33	**
HCP	3	60.92	***	3	23.64	***	5	14.25	***
BAR	3	4.71	**	3	2.37	ns	5	1.15	ns
ECR	3	0.69	ns	3	17.82	***	5	3.89	**

df= degree of freedom; F= F test, P= probability level (*** $p<0.001$, ** $p<0.01$, ns not significant).

Using PRT concentration in sediments and HCP activities, we calculated protein turnover time in the sediment assuming steady state conditions (i.e. no input of fresh proteins to the system) using the following formula: PRT/HCP. The lowest protein turnover time of 0.05±0.03 y was detected in station 1 (North Atlantic, 1200 m), while maximum turnover of 13.7±5.9 y was detected for station 12 (Central Med., 3000 m). A protein turnover of 6.1±0.2 y was found for station 18 at 5000 m in the Matapan-Vavilov deep.

Non-metric multi-dimensional scaling analysis between environmental factors and whole prokaryotic community

To investigate the role of trophic and environmental factors on the distribution, activity and community structure of prokaryotes we performed non-metric multi-dimensional scaling analysis

(nMDS). We plotted the nMDS of our whole dataset using prokaryotic variables (TPN, PBM, BAR, ECR and HCP) to describe the community in each sampled station (Figure 5.4a). The nMDS revealed a strong distribution of the stations along the dimension 1, with a preponderant role of the longitude in the ordination. The prokaryotic communities of stations from the East Mediterranean appeared to be very similar, as they showed in the plot as a compact group of points (Figure 5.4a). Central Mediterranean stations had the more diverse community as they are interspersed with all other samples. In order to remove depth related effects, we repeated the nMDS analysis separating the three main depths (Figure 5.4b, 5.4c and 5.4d). At 1200 m depth the stations from different areas clustered together in a discrete group, with the only exception of the West Mediterranean stations. This result highlights the presence of distinct prokaryotic populations at this depth (Figure 5.4b). At 2000 m (Figure 5.4c) and at 3000 m (Figure 5.4d) points were more interspersed. Using GAM analysis to force our trophic and environmental factors on the nMDS ordination, we found that trophic variables were the major driving factor in describing the differences in prokaryotic community between all sampled stations (Figure 6.5). Notably, LONG and SPP had a relevant effect in separating the points in the ordination in a non-linear way (Figure 6.5). Same results were found for PRT and LIP, while BPC and CPE surface fitted the ordination with linear relationship.

Generalized additive models

GAM analysis was used to identify the trophic and environmental factors explaining the BAR, ECR and HCP variation among the sampled stations (Figure 5.6). BAR variation across our dataset was best explained by a combination of environmental (LAT and LONG) and trophic (SPP, CPE and PRT) variables. An interaction effect between LAT and LONG, and SPP and CPE was identified, and PRT were fitted using a spline function. The resulting model was able to predict 89.9% of BAR variance across sampled stations (df=12.3). Other trophic variables (e.g. BPC, PRT/CHO ratio) when added to the model increased only marginally its accuracy (i.e. BPC increased only by 1.4% the variance prediction) but increased significantly the complexity of the model. The interaction of SPP and CPE together with the PRT explained more than 60% of the variance, with the remnants explained by the interaction term of LAT and LONG.

ECR variations were explained by the interaction of LAT and LONG, BAR and depth factor. This result is influenced by the presence of a significantly different composition of the *Archaea* community in station 18 at 5000 m, driving the effect of depth in explaining our ECR dataset. BAR and depth were fitted as linear variables and the overall model is able to predict 81.3% of the observed variance (df=20.2). HCP across our dataset was best explained by the abundance of *Bacteria*, interaction between SPP and CPE, PRT content and LONG. All variables were fitted as non-linear, resulting in the higher complexity if compared to the previous GAM (df=27.5). The resulting model explained 98.5% of the observed HCP variance in our dataset.

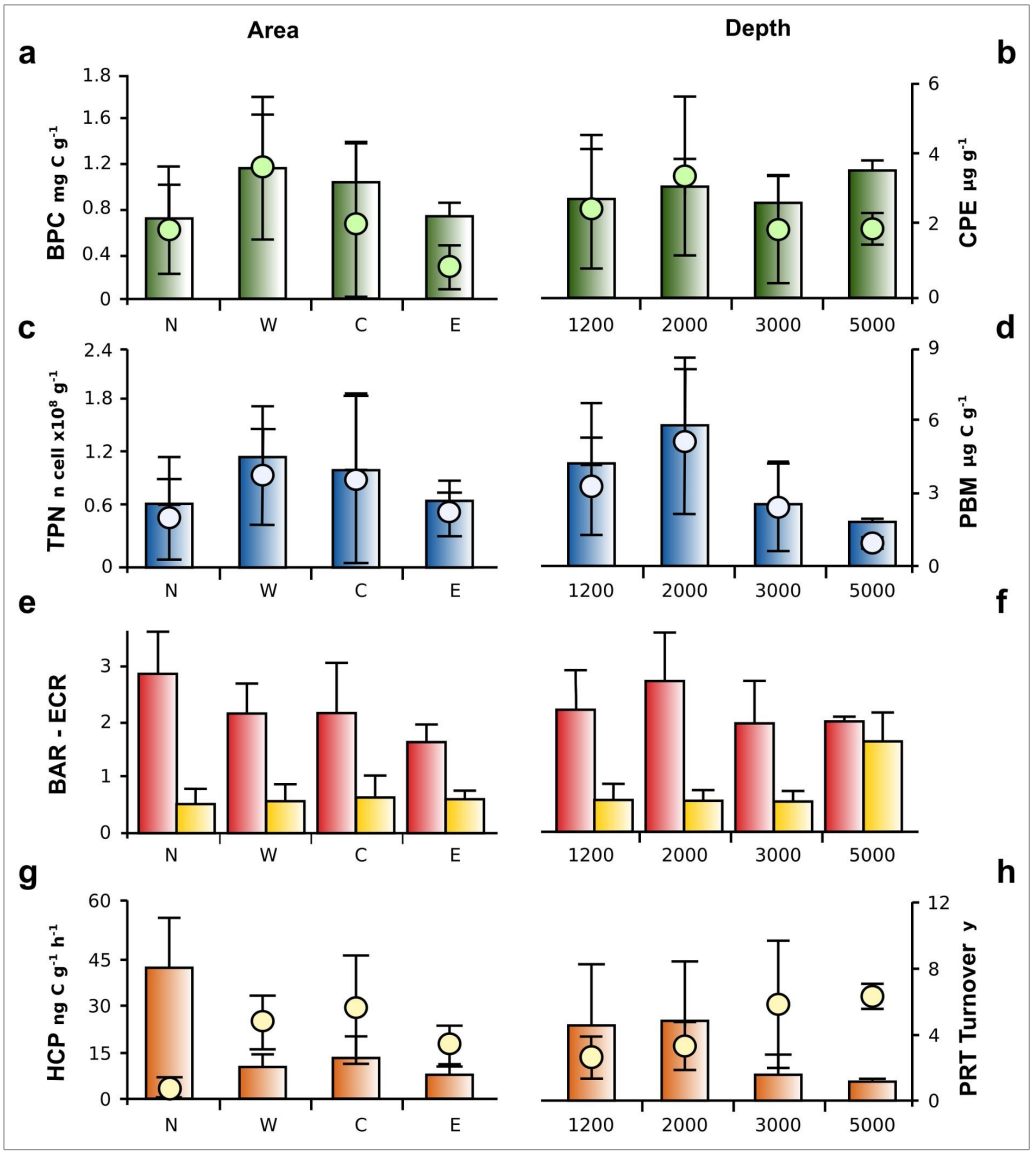

Figure 5.3. Panel of measured variables across the sampling areas (left column) and sampling depths (right column). Left side axis refers to barplot variables, right side axis to dot represented variables. BPC and CPE for area (a) and depth (b), TPN and PBM for area (c) and depth (d), BAR and ECR for area (e) and depth (f), HCP and protein turnover for area (g) and depth (h). Means and standard deviations are reported.

Discussion

Trends in prokaryotic abundance, biomass, community structure and activity

It has been widely demonstrated than the prokaryotic abundance and biomass decreases with increasing depth reaching minimum abundances and biomass in the bathypelagic waters (Reinthaler et al., 2006. This decrease in abundances and biomass, reported for the water column, has never been described on a large scale for surface sediment collected at different depths. The Mediterranean Sea is well known for its peculiar characteristics: high deep-water temperature and

homeothermy (ca. 13°C), fast deep-water turnover (in the order of 11 to 100 y; Santinelli et al., 2010) and strong trophic gradient moving from the Western to the Eastern basin (Koppelmann et al., 2004). Despite those differences with other basins the prokaryotic community in the deep-water of the Mediterranean Sea follows a similar trend to those reported for other oceans (Luna et al., 2012), with a demarcate decrease in the abundance and biomass of prokaryotes, an increase of the abundance of *Archaea* with increasing water depths (Luna et al., 2012) and a decrease in prokaryotic heterotrophic production (Tamburini et al., 2009; Luna et al., 2012).

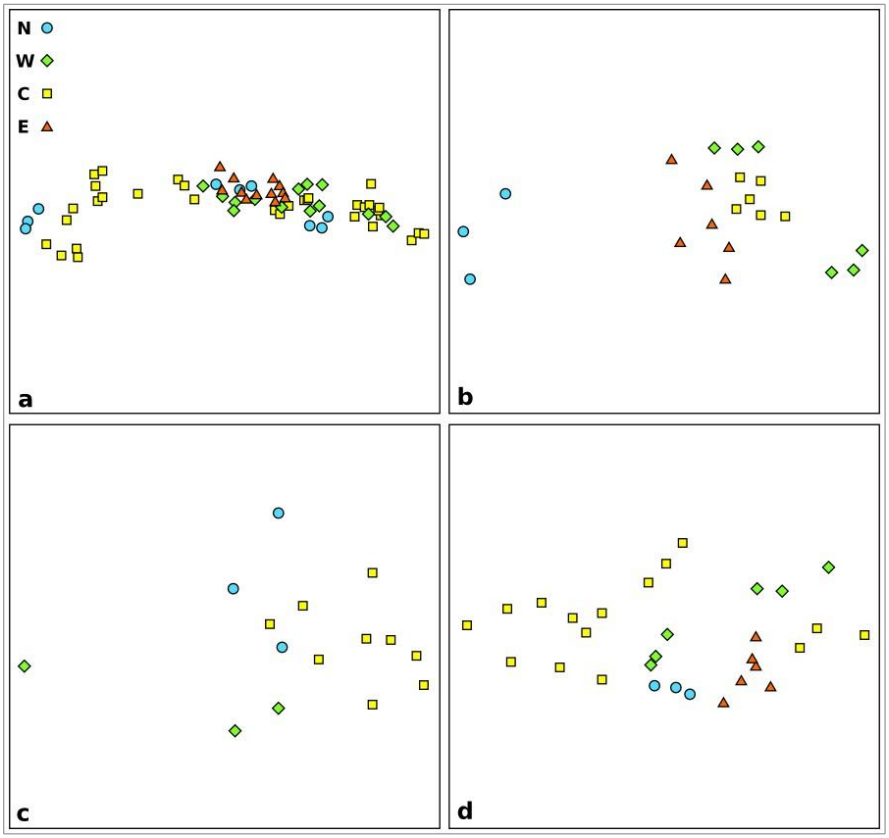

Figure 5.4. Panel of nMDS based on the biological descriptor of the prokaryotic community: all sampled stations (a), 1200 m (b), 2000 m (c) and 3000 m (d) meters depth.

We investigated for the first time the abundance, structure and activity of prokaryotic communities in deep-sea surface sediments of the Mediterranean Sea and North Atlantic Ocean on a large-scale survey. Our results show that TPN do not present difference among the sampled areas (Figure 5.3c), however a clear trend with depth is present (Figure 5.3d), with a bell shaped distribution with maxima at 2000 m depth already described for other deep-sea fauna. A similar trend was found for the PBM. The longitudinal trend appears to be related to the different trophic condition present in the Mediterranean Sea. Both results were correlated with trophic resources. Using PRT sedimentary concentration as proxy of bioavailability and freshness of organic matter (Pusceddu et al., 2010), we found a correlation between TPN and PRT (Pearson moment

correlation r=0.70, n=69, p<0.001), which highlights the heterotrophic-dominated community of deep-sea Mediterranean surface sediments. This observation is supported by our measurement of HCP, which are high compared to other measurement made in surface sediments at similar depths (Molari et al, 2013). However when we calculated the cell specific activity at each station we found value comparable to those in the literature and one order of magnitude lower on average than those reported by Luna et al. (2012) for the Mediterranean Sea water column at similar depths. This observation suggests that sediment prokaryotes are converting organic matter into biomass at a rate comparable to other oceans, despite the higher bottom temperatures (Luna et al., 2012).

The HCP in North Atlantic were instead exceptionally high, reaching a maximum at 1200 m in station 1. When calculating cell specific activities for this station, we found values 50 times higher than in any other station with 4 fg C $cell^{-1}$ h^{-1}. This is not surprising as the sampled area in the North Atlantic Ocean is positioned on the Galicia Seamount, a known upwelling highly productive area (Flach et al., 2002; Duineveld et al., 2004), and HCP has been previously positively correlated with primary production in the photic zone.

One of the major concerns in the direct count of prokaryotes is the inability to distinguish between active and dormant member of the community (Luna et al., 2002; Manini and Danovaro, 2006; Kouridaki et al., 2010). FISH and CARD-FISH techniques have the power to overcome this issue. By targeting ribosome FISH techniques stain only actively transcribing cells, leading to the counting of the active fraction of the population (Ishii et al., 2004; Hoshino et al., 2008). Our results show that, on average, 91±12% of the TPN were metabolically active. There were however big difference in the fraction of active cells between stations, with a minimum for station 12 in the Western Mediterranean at 1200 of 60±7% and a maximum of 100±19% in station 20 at 1200 m in the Eastern Mediterranean Sea. Despite those local differences no significant variations were found in the fraction of active cells between sampling areas or depths (Table 5.2). Those differences could be due to differences in the ability to permeabilize the cell membrane in different samples or more probably to the presence of different fractions of dead or dormant cells (Manini and Danovaro, 2003).

On average bacteria accounted for ca. 70% of the total prokaryotes as previously reported in other studies (Molari et al., 2012; Molari and Manini, 2012; Schauer et al., 2010). Only in station 17 at 3000 m depth in the Central basin *Archaea* outnumbered *Bacteria*, accounting on average for 53% of the total prokaryotes. Moving Eastward BAR decreased significantly with value in the Eastern Mediterranean Sea lower than those in other areas (Figure 5.3e). HCP was significantly correlated with BAR values (Pearson moment correlation r=0.531, n=60, p<0.001) suggesting on average a more heterotrophic lifestyle for the *Bacteria* present in deep-sea surface sediments. The low BAR value in the Eastern basin could be coupled with the marked oligotrophy of the East

Mediterranean surface waters (SPP in Table 5.1), reflected in the low availability of organic matter for benthic consumers (Figure 5.2a and 5.2b). This appears especially true if considering CPE and PRT content as proxy of quality and bioavailability of sedimentary organic matter. The increased importance of *Archaea* could be related to an increased contribution of dark carbon fixation in the area, as already suggested by Yakimov et al. (2007).

It is believed that *Crenarchaeota* drive the dark carbon fixation in deep water coupling CO_2 fixation with ammonia oxidation. Several studies have been published in this regard (Martínez-García et al., 2008; Pratscher et al., 2011) and an increase in the abundance of *Crenarchaeota* is considered a proxy for the increased importance of chemolithoautotrophy linked to ammonia oxidation. Recently *Crenarchaeota* Marine Group I, of which ammonia oxidizers are part, have been reported in marine sediments (Auguet et al., 2009) and marine basalts (Mason et al., 2008). So their abundance in surface sediments is not surprising. Our results show that the contribution of *Crenarchaeota* to the total pool of *Archaea* is rather constant across the investigated area (Figure 5.3e), despite the increased contribution of *Archaea* to the total prokaryotes in the Eastern Mediterranean.

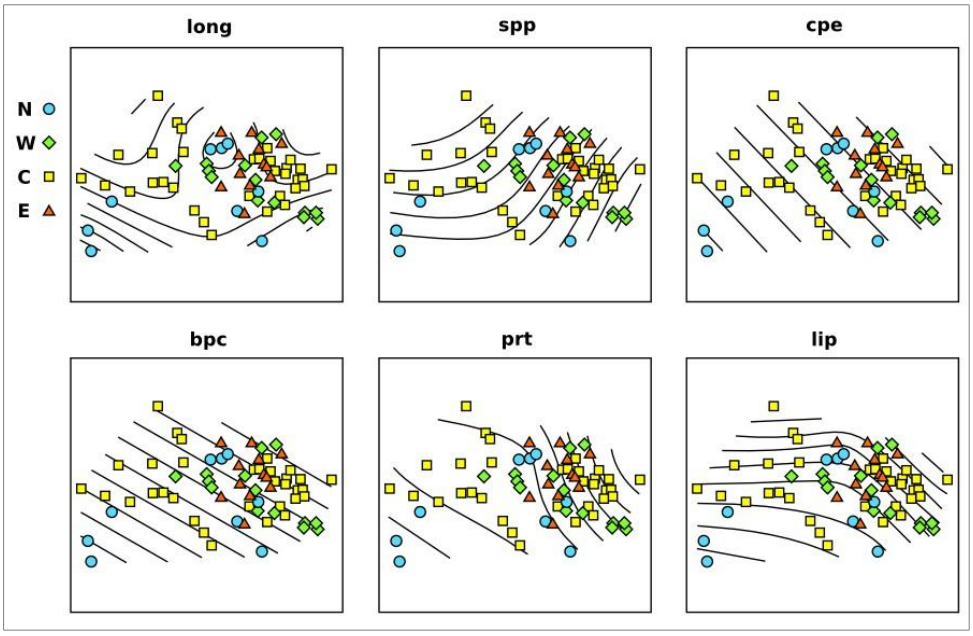

Figure 5.5. Panel of nMDS based on the biological descriptor of the prokaryotic community (all sampled stations). Surface lines in each plot represent GAM fitting of significant environmental or trophic variables explaining the observed ordination in the plots.

Previous studies have suggested that *Crenarchaeota* typically dominate over *Euryarchaeota* in oxygenated deep waters (De Long et al., 1999; Karner et al., 2001) and surface sediments (Vetriani et al., 1999;). We found the same pattern in our survey, with ECR constant between areas with value below 1 showing *Crenarchaeota* domination of the *Archaea* community, except for station 18 (Matapan-Vavilov deep) where *Euryarchaeota* accounted for 60% of the *Archaea* population.

Euryarchaeota Marine Group II has been previously reported to dominate over *Crenarchaeota* in surface waters (Stoica and Herndl, 2007; Massana et al., 2000; Pernthaler et al., 2002). In particular Masana et al. (2002) concluded that *Euryarchaeota* Marine Group II are dominant only at the surface in temperate waters. Our results clearly show an increased importance of *Euryarchaeota* at the Matapan-Vavilov deep (station 18), raising interesting question on the role of this yet-uncultured group that will require further investigation. A recently published reconstruction of a Marine Group II *Euryarchaeota* genome from metagenomic sequences (Iverson et al., 2012), suggests that this group comprises heterotrophs capable of growing on lipids and fatty acids. Interestingly we found that station 18 had one of the higher concentrations of lipids in our dataset, and the deep has been trenches have been recently reported to be a sink of OM (Glud et al., 2013).

Effect of trophic and environmental variables on prokaryotic community structure and activity

Combining all prokaryotic variables measured to describe the community as a whole, we found that communities share similarities across the entire Mediterranean basin and North Atlantic stations (Figure 5.4). In particular, the communities from Central Mediterranean stations are interspersed with all other areas (Figure 5.4a). The prokaryotic communities from the East Mediterranean stations clustered in a single condensed group, suggesting that only minor differences are present between the community at 1200 m and 3000 m in this area.

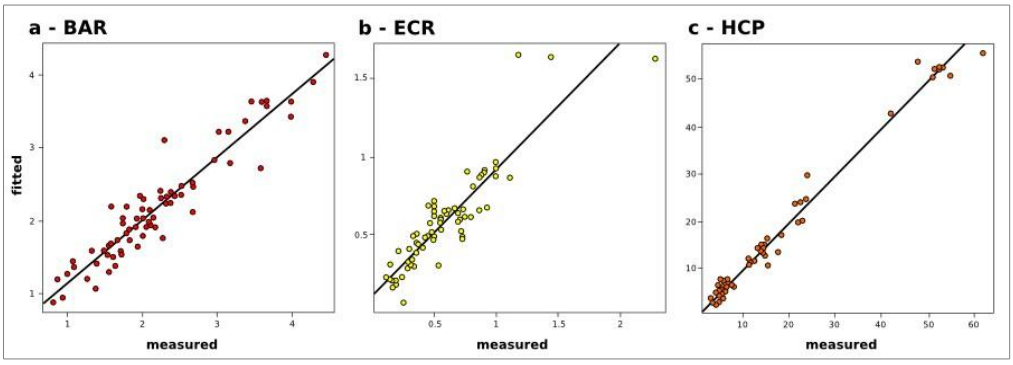

Figure 5.6. Panel of linear regressions between measured and GAM fitted values for BAR (a), ECR (b) and HCP (c). Pearson moment correlation coefficients are respectively 0.948 (df= 12.3, n= 69), 0.902 (df=20.2, n=69) and 0.972 (df=27.5, n= 60).

When we separated the plot based on the depth, we found striking differences between prokaryotic communities of the North Atlantic compared to the Mediterranean Sea at 1200 m (Figure 5.4b). Those differences were not as clear at 3000 m (Figure 5.4d) and absent at 2000 m (Figure 5.4c) where points were highly interspersed. These results suggest that deeper area of different basins share more similar communities if compared to shallower sites.

We tried to identify the trophic and environmental variables influencing the community composition and activity in deep-sea surface sediments. In energetically stressed environments, such as the deep-sea (Valentine, 2007), it is often difficult to identify processes that affect the distribution and abundance of different biotic assemblages. This is because both biological and physical factors are involved, they are not independent, and their relationships with the taxa of interest are frequently nonlinear. To identify relationships in such situations the use of most conventional correlational-type approaches is inappropriate (Zar, 1999). In this study, we used the nonlinear model-building approach of GAMs. This facilitates description of the relationship between the response variable and each predictor, while simultaneously adjusting for covariation among predictors. To our knowledge this is the first times GAMs were applied to microbial ecology in marine environments.

Trophic variables were identified by both linear regression and GAMs analyses applied to our ordination (Figure 5.5) as the main forcing variables in shaping the prokaryotic community differences among stations. BPC was effectively related with the ordination by a linear relationship (Figure 5.5) as can be observed by the presence of equidistant parallel surface lines. PRT effect on the ordination was non-linear as the effect of LIP concentration. GAM-nMDS superimposed analysis further identified LONG as an important factor, together with SPP and CPE.

The above variables were then used in GAMs analysis to identify the driving factor describing the BAR, ECR and HCP variation in our dataset. The resulting models had very powerful prediction efficiencies, as can be seen plotting measured against fitted values (Figure 5.6). Out of the three models, HCP-GAM model had the highest accuracy (Pearson moment correlation $r=0.972$, $p<0.001$, $n=60$, Figure 5.6c) with HCP variance in our dataset explained by a combination of *Bacteria* abundances, trophic variables and position along the longitudinal gradient. BAR variations were successfully explained by a combination geographical and trophic variable. The BAR-GAM model showed a good prediction accuracy (Pearson moment correlation $r=0.948$, $p<0.001$, $n=69$, Figure 5.6a) with all variables modeled as non-linear. Our results shows that the quality of organic matter is of primary importance in determining community BAR. PRT and CPE are good proxies of organic matter quality, as they are readily degradable substrate that tend to disappear as organic matter ages and undergoes burial (Pusceddu et al., 2010). The interaction between SPP and CPE increased model explained variance of ca. 10% compared to a similar model where SPP and CPE were considered independently. The amount of CPE in deep-sea sediments has been shown to be a function of SPP, depth and efficiency of removal along the water column as organic matter particle sink to the seafloor (Pusceddu et al., 2010). It is not a surprise that the two variables had an interaction effect in describing the quality of OM in surface deep-sea sediments.

ECR-GAM model was strongly influenced by the variation of ECR ratio in station 18 (Matapan-

Vavilov deep). The depth, together with BAR and geographical position had a powerful prediction power (Pearson moment correlation $r=0.902$, $p<0.001$, $n=69$) as can be seen plotting measured against fitted ECR values (Figure 5.6b).

The effect of longitude and its interaction with latitude in explaining our variance in all three models is an intriguing finding. It implies that geographical position along the Mediterranean Sea has a strong influence on the activity and structure of the prokaryotic community not related to any other variables measured in this study. Previous work analyzing differences between Western and Eastern Mediterranean basins found that the main differentiating features were primary productivity and nutrients in the water column, with a more productive area in the West Mediterranean, salinity and minor variation in bottom temperatures (Danovaro et al., 2010). Of those traditionally accounted variables, our dataset includes surface primary production, trophic resources in surface sediments and temperature. Despite this the effect of latitude and longitude is still strong, and may hide the effect of a variable or set of variables not measured in the present survey. This result suggests that overlaying water masses may play a critical role in shaping deep-sea benthic prokaryotic communities.

Chapter 6

Diversity and phylogenetic analyses of *Bacteria* from a shallow-water hydrothermal vent in Milos island (Greece)

Introduction[3]

Microbes are the most abundant life forms on Earth, account for half of the total biomass on the planet (Whitman et al., 1998) and drive major biogeochemical cycles (Staley and Reysenbach, 2002). Studies carried out in geothermal and extreme environment have shown that life on Earth is far more diverse, widespread, and resistant to extreme environments than previously thought. Prokaryotes are crucial player in extreme ecosystems and they are often the only life form able to thrive there. Despite this, current understanding of the diversity and role of prokaryotes in these environments is limited.

Deep-sea hydrothermal vent ecosystems are largely based on chemolithoautotrophic primary production (Jannasch, 1985; Bach et al., 2006; Nakagawa and Takai, 2008). Photoautotrophic contribution to these ecosystems is limited to the sinking of low-quality particulate material from the photic zone (Comita et al., 1984). In contrast, shallow-water hydrothermal vent systems are largely influenced by photosynthesis (Tarasov et al., 2005). In these environments, chemolithoautotrophy and photoautotrophy occur simultaneously and spatial separation is often influenced by steep thermal and geochemical gradients (Wenzhöfer et al., 2000).

Shallow-water hydrothermal vents are widespread ecosystems that have been so far understudied compared to their deep-sea counterparts (InterRidge vents database, http://www.interridge.org/), despite the fact that these systems were known long before the famous discovery of the deep-sea vents on the Galapagos Rift in 1977 (Lonsdale, 1977). The contribution of shallow-water hydrothermal systems to local and global biogeochemical cycles could be enormous. According to

[3] This chapter is part of a manuscript, Giovannelli et al. - Diversity and phylogenetic analyses of Bacteria from a shallow-water hydrothermal vent in Milos island (Greece), under review in *Frontiers in Extreme microbiology.*

Dando et al. (1995; 2000), the emission of carbon dioxide from the Milos venting area alone could account for 10% of the carbon dioxide emission caused by the venting associated with the Mid-Atlantic Ridge. Because of their proximity to the surface, shallow-water hydrothermal systems are influenced by both geothermal and solar energy and can be described as “high energy" environments, where microbial metabolism is fueled by different energy sources (Baross and Hoffman, 1985). Some authors even suggested that the conditions found in shallow-water hydrothermal systems could resemble those in which life originated and where metabolic divergence evolved (Nisbet and Fowler, 1996; Nisbet and Sleep, 2001; Martin et al., 2008).

To study the diversity of prokaryotic communities in shallow-water hydrothermal vents is of primary importance for evaluating their influence on biogeochemical cycles and to understand their evolution. The shallow-water hydrothermal system of Milos island was investigated in detail (Dando et al., 2000; Valsami-Jones et al., 2005). The vents in Paleochori Bay, a sandy bay off the SE coast of the island of Milos, are located in shallow waters, with temperature ranging from 25 to 119°C (Botz et al., 1996) and extensive gas and fluid seepage, and are the ideal place to study the prokaryotic communities of shallow-water vents. Early studies based on fingerprinting approaches were carried out in Milos in the late 90's and showed the presence of bacteria associated to the *Cytophaga-Flavobacteria-Bacteroides* as well as *Arcobacter* and *Thiomicrospira* (Brinkhoff et al., 1999; Sievert et al., 1999a; Sievert et al., 2000a; Sievert et al., 2000b).

In this study we carried out an environmental survey of a shallow-water hydrothermal vent located in Paleochori bay, Milos island, Greece. The site was sampled to investigate the structure and diversity of the bacterial community along a two-meter transect starting at the center of one of the vents.

Site description and sample collection

The Milos hydrothermal system is one of the largest in the Mediterranean Sea. It is part of the Hellenic arc, whose eastern section reaches the Turkish coast and the island of Kos, and Methana to the West. Extensive submarine venting occurs offshore the island, from the intertidal zone to depths of more than 100 m, with an approximate extension of 34 km^2 of seabed (Dando et al., 2000).

Inside the Paleochori bay (Figure 6.1), the venting area is characterized by strong degassing activities coupled with fluid seepage (Valsami-Jones et al., 2005). The entire shallow venting area is surrounded by patches of the seagrass, *Posidonia oceanica* and the vents occur as areas of high temperature and degassing on the sandy bottom (referred to hereafter as the center of the vent) that gradually decrease to ambient conditions as the distance from the spot increases. Steep thermal and redox gradients occur vertically, with temperature increasing with the depth of the sediment, while more gradual temperature and redox changes occur horizontally as the distance from the center of

the vent increases (Sievert et al., 1999a; Dando et al., 2000; Sievert et al., 2000a; Wenzhöfer et al., 2000). Temperatures of up to 119°C at a vent site in 10 m water depth have been reported (Botz et al., 1996).

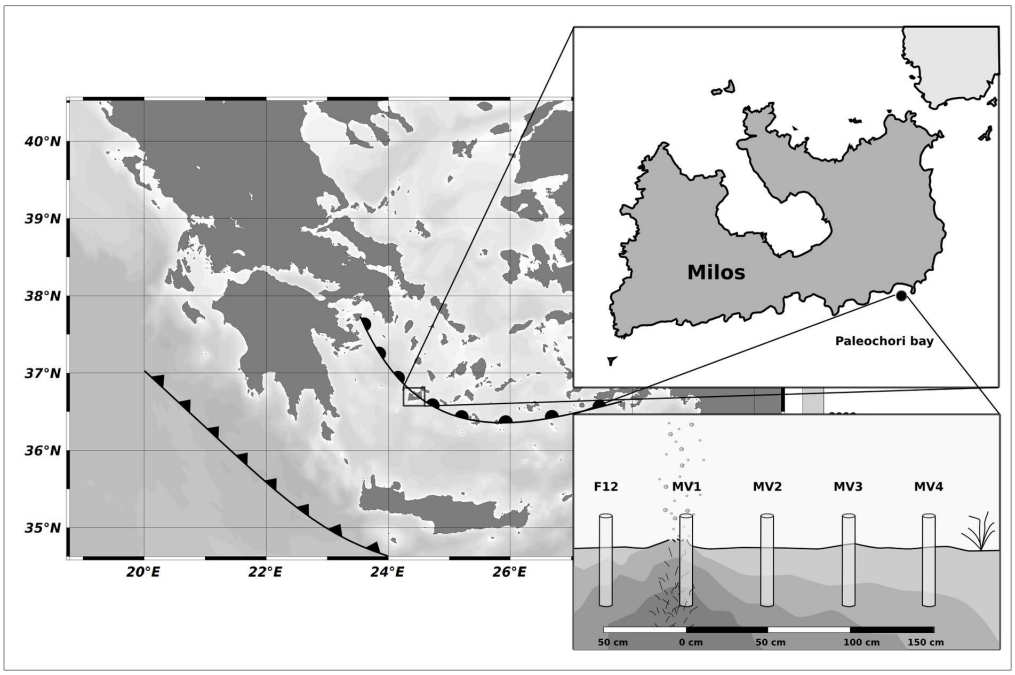

Figure 6.1. Map showing the position of Milos (Greece) respect to the Hellenic back-arc (circles) and Hellenic Fault (triangles), the location of Paleochori Bay and the sampling strategy along the transect. Cores were placed at interval of 50 cm moving away from the vent orifice.

Venting fluids are enriched with freshwater and their salinity varies. The mean composition of the gases released with the fluids is 95.5% CO_2, 1.2% H_2S, 0.8% CH_4 and 0.4% H_2 (Botz et al., 1996; Dando et al., 2000). In addition, the hydrothermal fluids have been shown to contain elevated concentrations of reduced inorganic chemicals, such as NH_4^+ (up to 1 mM), H_2S (up to 1 mM) and Mn^{2+} (up to 0.4 mM) (Fitzsimons et al., 1997). Arsenic and sulfur precipitates are common in proximity of vent orifices and dense brines can be found in sediment depressions (Dando et al., 2000).

SCUBA divers collected sediment samples with push-cores during the MAMBA cruise in 2010. Starting from the center of a vent (designated as MV1; 36° 40.351' N, 24° 31.108' E) located at a depth of 12 m, a horizontal transect consisting of four stations located 50 cm apart from each other was sampled (MV1, 0 cm distance from the center of the vent; MV2, 50 cm distance; MV3, 100 cm distance; MV4, 150 cm distance; Figure 6.1 and Table 6.1). Additionally, a single station was sampled at ca. 50 cm from the center of the vent in a yellow sediment patch (F12). The transect was characterized by a 20°C thermal gradient (45 and 25°C at stations MV1 and MV4, respectively) and differences in sediment color were observed. Station MV4 appeared only marginally influenced by hydrothermal activity as the temperature of its surface sediments was

close to background and *P. oceanica* was observed in close proximity (Table 6.1). Cores were collected and retrieved on board, sediment horizons separated (0-1 cm, 3-5 cm and 10-15 cm) and processed according to the analytical procedure described in following paragraphs. The sequences from this study are available through GenBank under accession numbers from KC463698 to KC463741.

Results

Organic matter composition

Biopolymeric organic carbon (BPC) in the surface sediments decreased along the transect from the center of the vent (MV1) towards the background station (MV4) with values ranging from 0.45±0.03 to 0.23±0.08 mg C g^{-1} at station MV1 and station MV4, respectively (Table 6.1). At station F12, BPC was highest (1.51±0.08 mg C g^{-1}). The observed horizontal gradients were significant (ANOVA $p<0.001$), and a BPC minimum at a depth of 3-5 cm was observed at all stations. Proteins dominated the carbon pool at all stations with an average contribution to BPC of 55%, followed by lipids and carbohydrates. Protein contribution to the carbon pool decreased along the transect from MV1 to MV4 (Table 6.1).

In contrast, total phytopigments (CPE) concentration increased along the transect from MV1 to MV4 (ANOVA $p<0.001$). Chlorophyll-a concentrations were extremely low, and phaeopigments were the most abundant class. The quantity and composition of the organic matter of the yellow surface sediments at station F12 differed from that of the other stations with proteins contributing near 95% of the BPC (Table 6.1).

Prokaryotic abundance and biomass

In general, total prokaryotic abundances decreased as the depth of the sediment increased at all stations, despite their proximity to vent orifice (Figure 6.2a; ANOVA $p<0.001$). Values ranged from 0.8±0.4 x10^8 to 2.7±1.1 x10^8 cell g^{-1} in the surficial sediments for MV1 and MV4, respectively, indicating higher abundances in the surface sediment layers and an increasing trend along the transect from MV1 to MV4. These trends were statistically significant (ANOVA $p<0.001$).

Prokaryotic biomass in surficial sediments ranged from 1.61±1.06 to 11.95±6.3 µg C g^{-1} in station MV2 and MV4, respectively (Figure 6.2b). Again, a trend of decreasing biomass with increasing sediment depth and increasing biomass along the transect toward the periphery of the vent was observed (Figure 6.2b; ANOVA $p<0.01$). Prokaryotic abundance in station F12 was comparable to station MV1, while prokaryotic biomass was significantly higher. The decreasing trend along the vertical sediment profile was more evident at stations located further away from the

center of the vent. Inter-replicate variability was also higher at those stations.

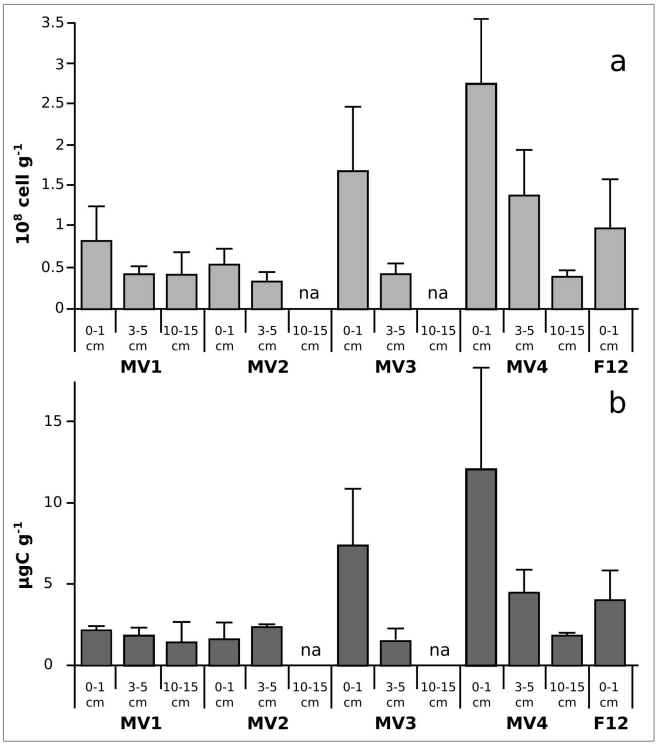

Figure 6.2. Prokaryote abundance (TPN; a) and biomass (PBM; b) along the sampled stations. Mean values are reported with standard deviation. na = data not available.

Prokaryotic diversity

We used DGGE to investigate the diversity of the sediment bacteria from the 0-1, 5-10 and 10-15 cm layers along the transect stations, and that from the 0-1 cm layer of station F12 (Figure 6.3). We obtained similar DGGE profiles from stations MV1, MV3 and MV4 and F12 (we did not obtain data for station MV2). Cluster analysis based on the DGGE profiles indicated that the bacterial communities from the same sediment layers tend to group together (Figure 6.3). A main group included communities from the 0-1 cm sediments from the transect stations and from F12, while the 3-5 and 10-15 cm layers from MV1 and MV4 formed a second group (Figure 6.3). The bacterial communities from the 0-1 cm layer of stations MV1 (center of the vent) and MV4 (periphery of the vent) were selected to construct 16S rRNA gene libraries.

Both the MV1 and MV4 libraries were dominated by sequences that could be assigned to the *Epsilonproteobacteria* (60 and 59% for MV1 and MV4, respectively; Figure 6.4). Other common phyla in both libraries were sequences belonging to the *Bacteroides* (16% and 6% for MV1 and MV4, respectively) and *Gammaproteobacteria* (7% and 21% for MV1 and MV4, respectively; Figure 6.4). The number of gammaproteobacterial clones increased at the periphery of the vent. The ratio of *Epsilon*- to *Gammaproreobacteria* was used as proxy to describe the observed shift,

and values of 8.2 and 2.9 were obtained at stations MV1 and MV4, respectively. Sequences related to the *Deltaproteobacteria*, *Flavobacteria-Cytophaga* cluster, high G+C Gram-positive bacteria, *Actinobacteria* and *Chlorobi* were also found. Two percent of the sequences retrieved from station MV1 could not be assigned to any known lineage (Figure 6.4).

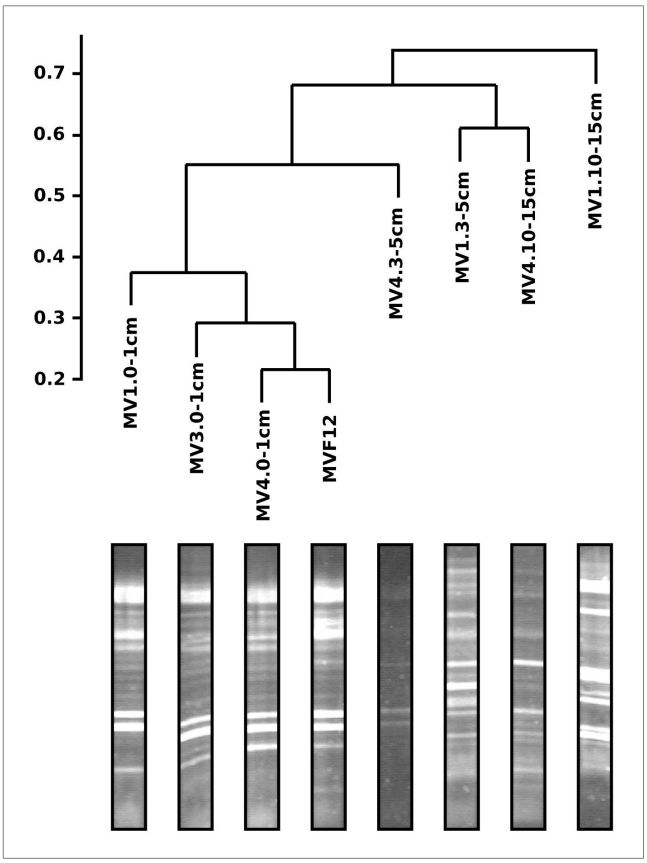

Figure 6.3. Bacterial DGGE gel profile and cluster analysis of the resulting diversity. Scale represents distance computed as Jaccard dissimilarity on the presence/absence matrix.

The sequences were further analyzed by aligning them against closest cultured relatives and a neighbor-joining tree was constructed (Figure 6.5). Both libraries are well represented in the tree, with numerous sequences clustering together despite their different origins. Most of the sequences obtained from the libraries were related to *Sulfurovum lithotrophicum* (Inagaki et al*.,* 2004), and clustered around this sequence on the tree (average similarity of 93%; Figure 7.5 and Table 7.2). The *Sulfurovum*-related sequences were organized in two discrete clusters, each containing clones from both libraries, and represented 44% of the clones in each library. The same clusters had best hits in the non-redundant database to sequences identified during environmental surveys in a variety of submarine geothermal environments such as the Logatchev field on the Mid-Atlantic Ridge (Nakagawa et al*.,* 2005; Hügler et al*.,* 2010), Vailulu seamount in the Samoa and submarine volcanoes on the Kermadec Arc (Hodges and Olson, 2009).

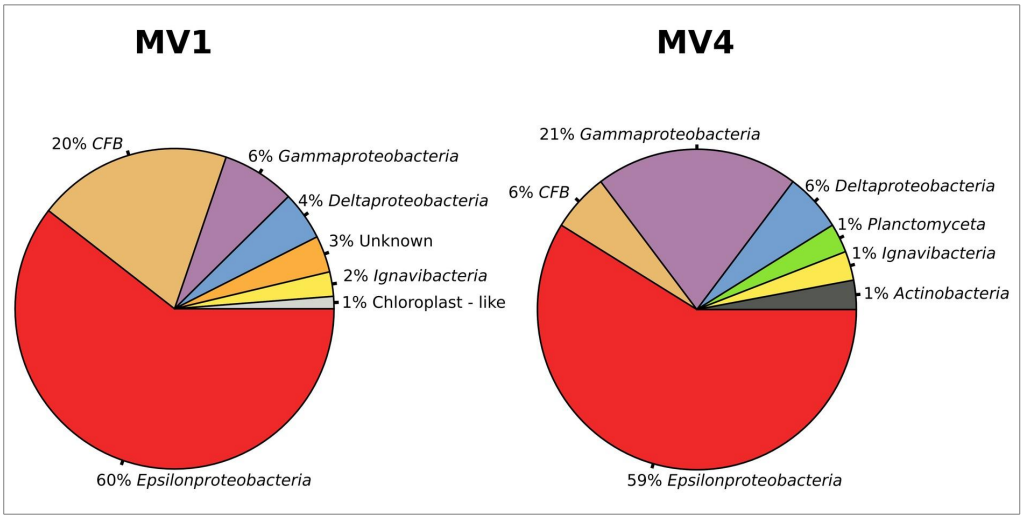

Figure 6.4. Bacterial community structure at station MV1 and MV4 surface sediments (0-1 cm) as obtained by the analysis of the sequences. Groups are shown at the phylum level based on the results of blast and position on the phylogenetic tree. *CFB = Cytophaga-Flavobacteria-Bacteroides* group.

A second major group of epsilonproteobacterial sequences was related to *Sulfurospirillum* spp. (90.8% average similarity), and clustered outside of the *Sulfurospirillum* group, constituting 13.6% and 5.8% of the two libraries respectively (Figure 6.5 and Table 6.2). Clones closely related to the Epsilonproteobacterium *Sulfurimonas authotrophica* were found exclusively in library MV1 (2.5% of the library sequences), while sequences related to *Sulfurimonas paralvinellae* constituted 8.8% of the MV4 library (93% similarity).

Sequences related to the *Gammaproteobacteria* constituted the second largest group in the MV4 library and were mainly related to *Pseudomonas* spp. and *Thioalophilus*/*Thioprofundum* cluster (98.5% and 91.7% average similarity, respectively) constituting 20.6% of the clones sequenced from this library. In the library from MV1, the *Gammaproteobacteria*-related sequences were related to *Thioalkalivibrio denitrificans* and *Thiothrix eikelboomii* (average similarity 90%), constituting only 6.2% of the library. The remaining gammaproteobacterial clones were associated with *Acinetobacter sp.* FR-W5Bb (98% similarity, 1.2% of the library) and a cluster that included clones MV1.01-C9 and MV1.01-F10, related to *Thioalkalivibrio denitrificans* (90% average similarity, 3.7% of the library, Figure 6.5 and Table 6.2).

Sequences related to the *Flavobacteria-Bacteroides-Cytophaga* cluster were the second major group in library MV1, with an average similarity of 90% to *Cythophaga* sp. BHI60-95B (constituting 16% of the clones in the library). Sequences related to the same species were also found in library MV4 (5.9% of the library). Unique sequences related to the *Flavobacterium Gaetbulibacter jejuensis* and *Polaribacter sp.* j2-11 were present at station MV1 (93% and 91% similarity, respectively). *Deltaproteobacteria* were represented in library MV4 by sequences related to *Geothermobacter ehrlichii* (87.5% similarity, 5.8% of the clones in the library) and

Ferrimicrobium acidiphilum (96% similarity, 3% of the library). MV1sequences related to the *Deltaproteobacteria* represented 5% of the clones in this library and were associated to *Eubacterium* sp. OS (84% similarity). Clones related to the *Ignavibacterium album* (87.7% similarity on average) were retrieved from both libraries, MV1 and MV4.

Despite the lower number of clone sequenced at station MV4, computed Chao1 diversity estimate indicated that diversity at MV4 was higher if compared to MV1 (Chao1, 63.7±22 and 28.8±4.2 respectively). This can be also inferred from the slope visible on the rarefaction curves computed for both libraries (Figure 6.6).

Discussion

Shallow-water hydrothermal vents are distributed worldwide and, while understudied relative to their deep-sea counterparts, they represent unique ecosystems where primary productivity is supported both by chemosynthesis and photosynthesis (Tarasov et al., 2005). In this study we investigated the abundance, biomass, community structure and diversity of the prokaryotic community at a shallow-water hydrothermal vent in Paleochori Bay, Milos island, Greece (Figure 6.1).

Prokaryotic abundances were as high as 2.7±1.1 x10^8 cell g^{-1}, with average values comparable to those reported in previous studies of the same area and other shallow-water hydrothermal systems, as well as at deep-sea vents (Figure 6.2a; Sievert et al., 1999b; Sievert et al*.,* 2000a; Sievert et al*.,* 2000b; Nakagawa et al*.,* 2005; Manini et al*.,* 2008; Williamson et al*.,* 2008; Maugeri et al*.,* 2009; Maugeri et al*.,* 2010). Prokaryotic abundances decreased with depth in the sediments at all stations, a general trend previously reported for shallow-water marine sediments (Molari et al*.,* 2012). In contrast, prokaryotic abundances increased along the transect from MV1 (center of the vent) to MV4 (periphery of the vent; Figure 6.2a). Prokaryotic biomass followed similar spatial patterns, with higher values at the surface (0-1 cm) and at station MV4 (Figure 6.2b). A previous report of the Milos vents indicated that deeper sediments tend to be hotter (Sievert et al., 2000b), while surface sediments along the transect became gradually cooler at the periphery of the vent (Table 6.1). Hence, it appears that temperature and prokaryotic biomass are inversely correlated (Figure 6.2, Pearson moment correlation $r=-0.617$, $p<0.05$).

Biopolymeric organic carbon (BPC), as well as proteins, decreased along the transect from the center (MV1) to the periphery of the vent (MV4), while carbohydrates and lipids remained fairly stable (Table 6.1). In contrast, phytopigments (CPE) followed an opposite pattern, increasing along the transect from MV1 to MV4 (Table 6.1).

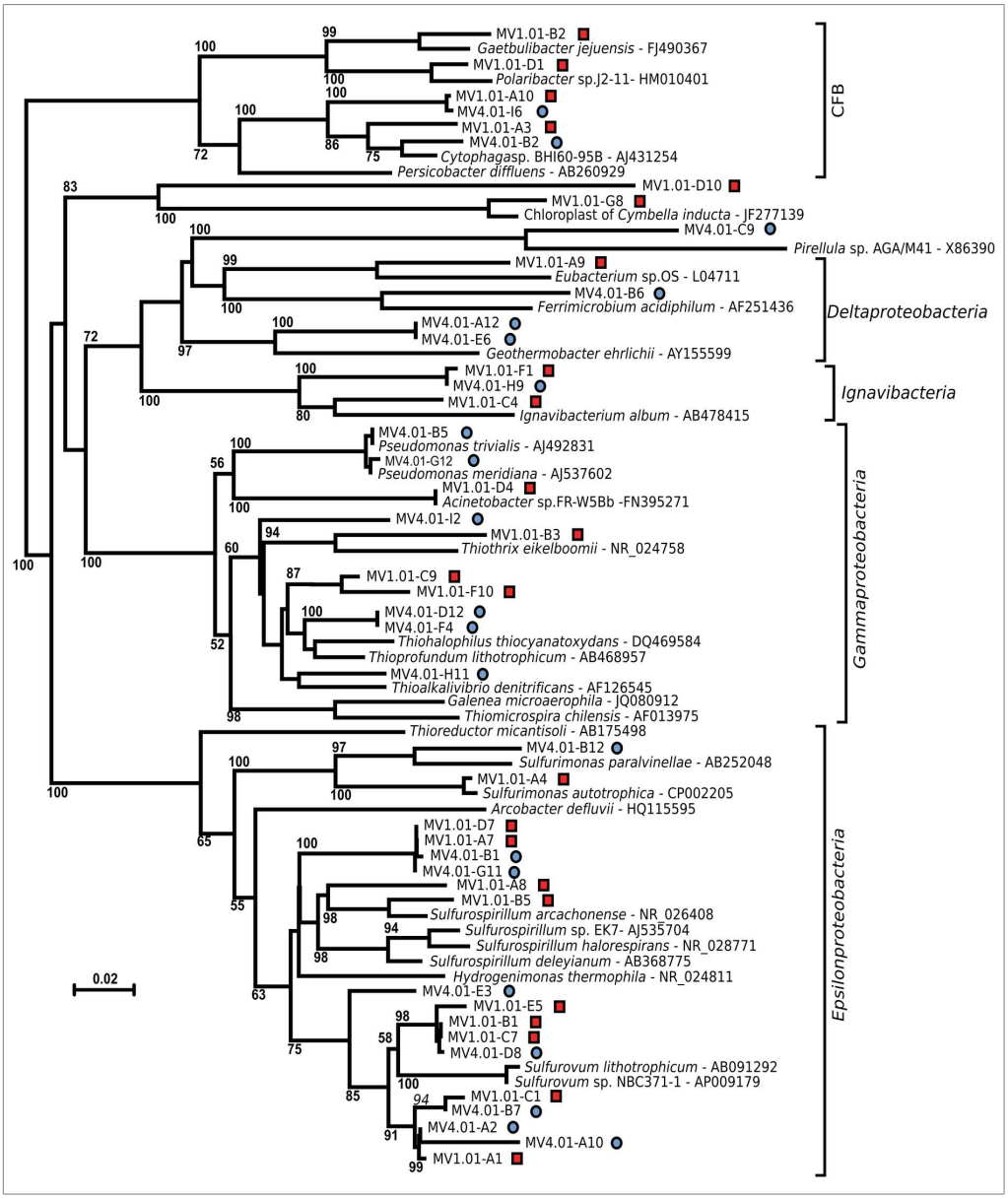

Figure 6.5. Unrooted Neighbor-joining tree of the bacterial diversity at station MV1 (squares) and MV4 (circles) surface sediments (0-1 cm) with cultured relatives. The tree was obtained using Jukes-Cantor correction and 1000 bootstrap. Bar, 2 % substitution rate. Bootstrap values below 50 are not shown. *CFB = Cytophaga-Flavobacteria-Bacteroides* group.

At station F12 (yellow sediments, temperature 34°C), we measured the highest concentrations of proteins and BPC and lowest concentration of CPE (Table 6.1). The increasing concentration of CPE as the sediment temperature decreases implies an increase of phototrophic organisms in the lower temperature regions of the vent system, probably due by the presence of previously described diatoms and cyanobacteria mats in the outer rings of similar vents (Thiermann et al.,

1997). This is consistent with the general notion that photoautotrophs are less tolerant to elevated temperatures than chemoautotrophic or chemoheterotrophic microorganisms. These findings suggest a shift from chemotrophic to phototrophic organisms along the decreasing thermal gradient. While BPC and proteins decreased along the transect from MV1 to MV4, prokaryotic abundance and biomass increased (Table 6.1 and Figure 6.2a and 6.2b) and no significative correlation was found among the two parameters (Pearson moment correlation $r=-0.214$, $p>0.05$). Being the transect relatively short and all sampling stations at the same depth, it is safe to assume that the input of organic matter from the water column and lateral advection is constant in all stations.

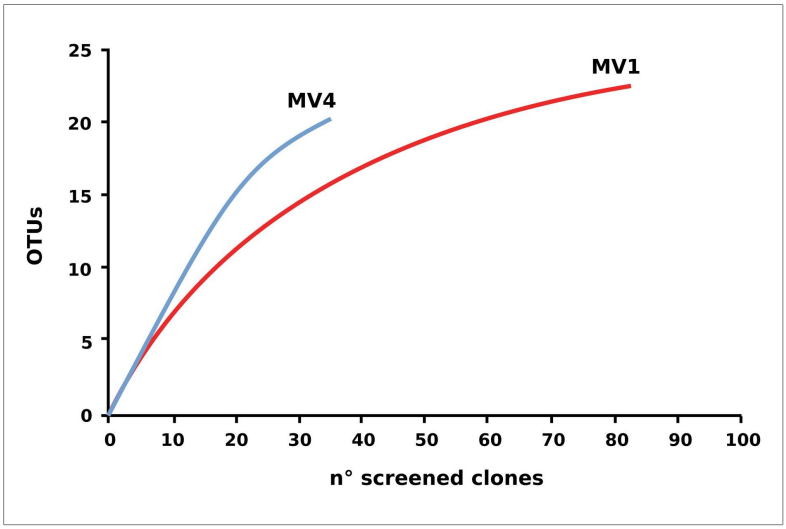

Figure 6.6. Rarefaction curve of the 16S rRNA gene libraries. Rarefaction curves were computed using Rarefaction software (Brzustowski, 2003; http://www2.biology.ualberta.ca/jbrzusto /rarefact.php).

We hypothesize that the decreasing prokaryotic biomass in the hottest section of the vent may lead to a decrease in carbon consumption, which is reflected in the higher concentration of measurable proteins and BPC. Our hypothesis implies that temperature, rather than trophic resources, mainly controls the distribution of prokaryotes in this system. Bacterial diversity, investigated by DGGE profiles, showed that the main DGGE banding pattern was highly conserved, while the highest number of unique bands was obtained from the 3-5 and 10-15 cm depth profiles at station MV1 (Figure 6.3). Overall, our results suggest that the deeper sediments of the hottest part of the vent hosted a prokaryotic community low in biomass but highly diverse (Figures 6.2b and 6.3). In total, we obtained 30 unique bands with distinct electrophoretic mobility. This is an underestimation of the actual bacterial diversity, since DGGE bands that have the same electrophoretic mobility may contain more than one type of sequence. As expected, our DGGE analysis highlights the presence of distinct bacterial populations in surface and deeper sediments, which likely reflect different thermal and redox regimes (Figure 6.3). Similar findings have been

reported for a variety of environments, including shallow-water and deep-sea hydrothermal vents (Moyer et al., 1995; Sievert et al., 1999b; Sievert et al., 2000a; Manini et al*.,* 2008).

Previous studies of the Paleochori bay vents based on DGGE and fingerprinting analyses reported a population dominated by the *Cytophaga-Flavobacteria-Bacteroides* cluster, *Gammaproteobacteria* of the genus *Thiomicrospira* and *Epsilonproteobacteria* of the genus *Arcobacter* (Brinkhoff et al*.,* 1999; Sievert et al., 1999a; Sievert et al*.,* 2000a). Here, we integrated fingerprinting, sequencing and phylogenetic analyses to assess the bacterial diversity of the shallow-water vent ecosystems of Milos island. Our survey of the bacterial 16S rRNA gene sequences of the surface sediments of stations MV1 and MV4 showed that *Epsilonproteobacteria* were the dominant phylum in both libraries. *Epsilonproteobacteria* are well adapted to sulfidic conditions and are commonly detected in environmental surveys of geothermal environments, as well as isolated as pure cultures from deep-sea hydrothermal vents (Campbell et al*.,* 2006; Sievert and Vetriani, 2012). In contrast, *Gammaproteobacteria* constituted only 7 and 21% of the MV1 and MV4 clone libraries, respectively. However, it is worth noting that the relative abundance of gammaproteobacterial clones increased along the transect from the center to the periphery of the vent (Figure 6.4). The *Epsilon-* to *Gammaproteobacteria* ratio decreased accordingly, from 8.8 at station MV1 to 2.9 at station MV4. Overall, the expected diversity, calculated as Chao1 and rarefaction analyses (Figure 6.6), appears to be higher at MV4. Sievert et al. (1999a) reached a similar conclusion, as they found that the microbial diversity based on DGGE profiles was higher at the periphery of the vent. Despite this, the beta-diversity within the transect appears to be relatively low, as, in general, clones retrieved from both MV1 and MV4 were closely related (Figure 6.5).

Phylogenetic analysis showed that most of the sequences retrieved from both libraries were placed in the *Sulfurovum* cluster, although the average similarity of our clones to the type strain, *Sulfurovum lithotrophicum*, was only 93% (Figure 6.5). *S. lithotrophicum* is a sulfur-oxidizing *Epsilonproteobacterium* isolated from deep-sea hydrothermal sediments of the Okinawa trough (Inagaki et al., 2004) and it has since then been identified in deep-sea vent communities worldwide (Campbell et al., 2006; Huber et al., 2007; Tokuda et al., 2007; Huber et al., 2010). Our finding of *Sulfurovum*-related clones in the Milos vents shows that the distribution of this group of *Epsilonproteobacteria* extends to shallow-water hydrothermal systems.

A large number of the sequences retrieved in this study have low similarity to currently cultured bacterial strains (on average 90.1% similarity), while only four sequences (two for each library, 12.5% of the total investigated clones) had similarities equal or above 97%, a value considered as cut-off for closely related species/strains (Rossello-Mora and Amann, 2001). When we searched the non-redundant database, the closest relatives to our sequences were clones retrieved in the course of microbial diversity surveys of deep-sea hydrothermal vents (Lopez-Garcia et al., 2003;

Nakagawa et al., 2005; Hügler et al., 2010), cold-seeps (Wegener et al., 2008) and seamounts (Hodges and Olson, 2009). However, the average similarity with those sequences was rather low (93.6% and 96.7% for MV1 and MV4, respectively). This was particularly true for station MV1, where the average similarity between cultured and uncultured best hits was comparable (Table 6.2). This suggests that the Milos shallow-water hydrothermal vents harbor previously undiscovered taxa, and raises questions on the physiology and metabolism of the *Bacteria* at this site. Beside temperature, the quantity and quality of organic matter found at the Milos vent (Table 6.1) are likely a key factor in selecting for heterotrophic or facultative heterotrophic bacteria. This observation is supported by the abundance of member of the *Cytophaga-Flavobacteria-Bacteroides* (CFB) cluster in our libraries (Figure 6.4). Since all cultured members of the *CFB* are heterotrophs, it is reasonable to speculate that the Milos *CFB* have a similar metabolism.

Currently, all the cultured *Epsilonproteobacteria* isolated from geothermal environments are chemolithoauthotrophs, although some of these bacteria have the ability to use one-carbon compounds (and in some rare cases complex organic carbon compounds; Campbell et al., 2006; Sievert and Vetriani, 2012). Given the phylogenetic distance between the *Epsilonproteobacteria* identified in this study and both cultured and uncultured relatives, it is possible that the shallow-water hydrothermal vents of Milos harbor member of the *Epsilonproteobacteria* with novel metabolic characteristics. One interesting possibility is that such *Epsilonproteobacteria* might be mixotrophic or facultatively heterotrophic. To this end, an effort to use alternative strategies to culture and isolate key members of the community is needed to understand their physiology and metabolism, and ultimately elucidate their role in these ecosystems. None of the 16S rRNA gene sequences identified in this study were related to the newly described genus *Galenea,* isolated from the same sediment samples (Giovannelli et al., 2012; Chapter 7). Surprisingly, none of the gammaproteobacterial 16S rRNA gene sequences was related to the genus *Thiomicrospira*, and none of the epsilonproteobacterial sequences was related to the genus *Arcobacter*, both of which were previously reported to be abundant in the Milos vents (Brinkhoff et al., 1999; Sievert et al., 1999b; Sievert et al., 2000a). This suggests that spatial and/or temporal differences in the composition of the microbial communities of these vents could be enormous. Shallow-water hydrothermal vents are characterized by fluctuating condition with elevated temporal and spatial variability of oxygen, salinity, composition of fluids, and venting regimes (Wenzhöfer et al., 2000), and they are affected by weather conditions, swell, tides and currents. Such variability creates micro-niches and high spatial and temporal heterogeneity, possibly leading to an increase of the overall community variability and gamma-diversity.

In conclusion, we showed that prokaryotic abundances at the shallow-water vents of Milos island are comparable to those reported in other shallow-water and deep-sea hydrothermal systems. Temperature appears to be the main driving factor in controlling prokaryotes distribution in proximity of the vent and photoautotrophy seems to increase in the lower temperature regions of

the vent system. For the first time, we report *Sulfurovum*-related sequences in shallow-water hydrothermal sediments, which underscores their possible relevance in the microbial communities of both shallow-water and deep-sea hydrothermal vents. The Milos shallow-water hydrothermal vent investigated in this study harbor previously undescribed and unexpected diversity, as most of the clones retrieved had a very low similarity to previously reported sequences. We speculate that this may be due to the abundance of organic matter in these systems, which may support *Epsilonproteobacteria* with novel metabolic characteristics. Further attempts to isolate key species in those ecosystems are critical to shed light into their evolution and functioning and to understand the ecology of these environments.

Table 6.1. Sampled stations, temperature, organic matter content and main characteristic of the area. Means are reposted with standard deviation. Prt = Proteins, Cho = Carbohydrates, Lip = Lipids, BPC = Biopolymeric organic Carbon, CPE = total phytopigments.

Station	**Sediment depth**	**Surface temp.**	**Prt**	**Cho**	**Lip**	**BPC**	**CPE**	**Notes**
	cm	**°C**	**mg g^{-1}**	**mg g^{-1}**	**mg g^{-1}**	**mg C g^{-1}**	**µg g^{-1}**	
MV1	0 - 1	45	0.70±0.05	0.07±0.00	0.18±0.02	0.45±0.03	11.84±1.35	Vent orifice – dark gray sediment
	3 - 5		0.27±0.20	0.06±0.01	0.07±0.00	0.19±0.08	6.17±3.29	
	10 - 15		0.39±0.00	0.12±0.02	0.10±0.03	0.29±0.03	6.12±0.64	
MV2	0 - 1	32	0.53±0.15	0.03±0.01	0.10±0.01	0.30±0.06	9.31±0.94	
	3 - 5		0.21±0.03	0.02±0.00	0.07±0.04	0.15±0.05	12.97±0.64	
	10 - 15		0.88±0.63	0.01±0.00	0.14±0.01	0.46±0.25	2.14±0.51	
MV3	0 - 1	28	0.42±0.17	0.05±0.01	0.21±0.02	0.34±0.09	25.69±2.24	Presence of white precipitate
	3 - 5		0.10±0.05	0.02±0.00	0.09±0.02	0.12±0.01	11.37±0.38	
MV4	0 - 1	25	0.20±0.03	0.08±0.03	0.15±0.15	0.23±0.08	154.6±3.89	Proximity to *P. oceanica*
	3 - 5		0.21±0.04	0.08±0.02	0.24±0.11	0.30±0.11	72.21±4.45	
	10 - 15		0.32±0.03	0.05±0.01	0.17±0.08	0.28±0.05	12.67±0.63	
F12	0 - 1	34	3.62±0.23	0.03±0.00	0.06±0.01	1.51±0.08	7.6±1.1	Yellow sediments

Table 6.2. Sequenced clones, top blast hits to the non-redundant database (closet relative) and best hit among cultured bacteria (closest cultured relative).

Clone Group	% lib.	Closest relative (top blast hit)	% sim.	Closest cultured relative	% sim.
MV1.01-A1	24.7	Unc. *Epsilonproteobacterium* FN562857	92	*Sulfurovum lithotrophicum* AB091292	94
MV1.01-A3	13.6	Unc. bacterium clone VS_CL-76 16S FJ497327	93	*Cytophaga* sp. AJ431254	91
MV1.01-A4	2.5	Unc. bacterium clone VS_CL-308 16S FJ497560	95	*Sulfurimonas autotrophica* DSM 16294 CP002205	98
MV1.01-A7	8.6	Unc. *Epsilonproteobacterium* AB175533	90	*Sulfurospirillum* sp. EK7 AJ535704	92
MV1.01-A8	2.5	Unc. *Epsilonproteobacterium* AB247847	96	*Sulfurospirillum halorespirans* NR_028771	90
MV1.01-A9	4.9	Unc. bacterium clone C13S-4 16S EU617730	95	*Eubacterium* sp. (OS type K) L04711	84
MV1.01-A10	2.5	Unc. bacterium partial 16S rRNA AM176864	93	*Cytophaga* sp. BHI60-95B AJ431254	90
MV1.01-B1	1.2	Unc. bacterium partial 16S rRNA AF449240	95	*Sulfurovum lithotrophicum* 42BKT AB091292	93
MV1.01-B2	2.5	Unc. bacterium partial 16S rRNA FM179896	93	*Gaetbulibacter jejuensis* CNURIC014 FJ490367	93
MV1.01-B3	2.5	Unc. bacterium clone 16S HQ225056	95	*Thiothrix eikelboomii* AP3 NR_024758	90
MV1.01-B5	1.2	Unc. *Epsilonproteobacterium* AJ969489	92	*Sulfurospirillum arcachonense* F1F6 NR_026408	95
MV1.01-C1	4.9	Unc. epsilon clone AT-co11 AY225616	95	*Sulfurovum lithotrophicum* 42BKT AB091292	93
MV1.01-C4	1.2	Unc. bacterium clone SIMO-2441 AY711807	92	*Ignavibacterium album* Mat9-16 AB478415	87
MV1.01-C7	2.5	Unc. Epsilonproteobacterium AB197179	93	*Sulfurovum lithotrophicum* 42BKT AB091292	94
MV1.01-C9	1.2	Unc. Gamma clone GU230337	95	*Thioalkalivibrio denitrificans* ALJD AF126545	91
MV1.01-D1	1.2	Unc. marine bacterium clone HM437670	91	*Polaribacter* sp. J2-11 HM010401	91
MV1.01-D4	1.2	Unc. bacterium clone JF221689	98	*Acinetobacter* sp. FR-W5Bb FN395271	98
MV1.01-D7	1.2	Unc. Epsilonproteobacterium AB175533	91	*Sulfurospirillum deleyianum* AB368775	88
MV1.01-D10	3.7	Unc. bacterium clone TF-33 16S FJ535257	94	*Thioreductor micantisoli* AB175498	78
MV1.01-E5	11.1	Unc. Epsilonproteobacterium AB197179	94	*Sulfurovum lithotrophicum* 42BKT AB091292	93
MV1.01-F1	1.2	Unc. bacterium clone TS-31 16S FJ535328	95	*Ignavibacterium album* Mat9-16 AB478415	88
MV1.01-F10	2.5	Unc. bacterium clone D13S-50 EU617758	94	*Thioalkalivibrio denitrificans* ALJD AF126545	89
MV1.01-G8	1.2	Unc. bacterium clone 16S HQ178788	94	*Cymbella inducta* NJCI77 chloroplast JF277139	94
MV4.01-A2	26.5	Unc. *Epsilonproteobacterium* BH8 FN562857	96	*Sulfurovum lithotrophicum* 42BKT AB091292	94
MV4.01-A10	5.9	Epsilon ectosymbiont of Symm. GU253366	94	*Sulfurovum lithotrophicum* 42BKT AB091292	90
MV4.01-A12	2.9	Unc. bacterium clone SMI1-GC205-Bac66	98	*Geothermobacter ehrlichii* SS015 AY155599	88
MV4.01-B1	2.9	Unc. *Epsilonproteobacterium* AB175533	94	*Sulfurospirillum deleyianum* AB368775	91
MV4.01-B2	2.9	Unc. *Bacteroidetes* clone VS_CL-132 FJ497383	97	*Persicobacter diffluens* NBRC 15940 AB260929	84
MV4.01-B5	5.9	Pseudomonas sp. VS05_25 FJ662886	99	*Pseudomonas trivialis* DSM 14937 AJ492831	99
MV4.01-B6	2.9	Unc. *Actinobacterium* AB099989	97	*Ferrimicrobium acidiphilum* T23 AF251436.2	96
MV4.01-B7	5.9	Unc. *Epsilonproteobacterium* FN562857	97	*Sulfurovum* sp. NBC37-1 AP009179	93
MV4.01-B12	8.8	Unc. bacterium clone KM51 AY216438	98	*Sulfurimonas paralvinellae* GO25 AB252048	93
MV4.01-C9	2.9	Unc. bacterium clone NT2_C15 HM630159	97	*Pirellula* sp. AGA/M41 X86390	87
MV4.01-D8	2.9	Unc. *Epsilonproteobacterium* clone AF449240	97	*Sulfurovum lithotrophicum* 42BKT AB091292	93
MV4.01-D12	2.9	Unc. sediment bacterium clone HQ191081	97	*Thiohalophilus thiocyanatoxydans* DQ469584	92
MV4.01-E3	2.9	Unc. *Epsilonproteobacterium* clone DQ295546	93	*Hydrogenimonas thermophila* EP1-55 NR_024811	88
MV4.01-E6	2.9	Unc. bacterium clone DQ521800	98	*Geothermobacter ehrlichii* SS015 AY155599	87
MV4.01-F4	2.9	Unc. sediment bacterium clone HQ191081	97	*Thiohalophilus thiocyanatoxydans* DQ469584	92
MV4.01-G11	2.9	Unc. *Epsilonproteobacterium* AB175533	95	*Sulfurospirillum deleyianum* DSM 6946 CP001816	89
MV4.01-G12	2.9	Unc. bacterium clone nbw124b GQ024593	99	*Pseudomonas meridiana* CMS 38 AJ537602	98
MV4.01-H9	2.9	Unc. bacterium clone TS-31 FJ535328	98	*Ignavibacterium album* Mat9-16 AB478415	88
MV4.01-H11	2.9	Unc. *Gammaproteobacterium* clone JF344515	99	*Thiohalophilus thiocyanatoxydans* DQ469584	91
MV4.01-I2	2.9	Unc. bacterium clone SSW84Ap EU592359	97	*Thioprofundum lithotrophicum* 108 AB468957	92
MV4.01-I6	2.9	Unc. *Bacteroidetes* clone DQ351801	94	*Cytophaga* sp. BHI60-95B AJ431254	90

Chapter *7*

Galenea microaerophila gen. nov., sp. nov., a mesophilic, microaerophilic, chemosynthetic, thiosulfate-oxidizing bacterium isolated from a shallow hydrothermal vent[4]

Sulfur-oxidizing bacteria are widely represented within the *Gammaproteobacteria* and they are found in a variety of marine environments, both as free-living bacteria and in symbiotic associations with invertebrates (Brinkhoff et al., 1997; Dando et al., 1998; Brinkhoff et al., 1999; Schulz et al., 1999; Takai et al., 2004; Nagakawa and Takai, 2008; Crespo-Medina et al., 2008). The most common sulfur-oxidizing *Gammaproteobacteria* belong to the order *Thiotrichales* within the families *Thiotrichaceae* and *Piscirickettsiaceae*, and include the genera *Achromatium*, *Beggiatoa*, *Thiobacterium*, *Thiomargarita*, *Thioploca*, *Thiospira* and *Thiomicrospira* (Jannasch et al., 1985; Muyzer et al., 1995; Brinkhoff et al., 1997; Dando et al., 1998; Wirsen et al., 1998; Brinkhoff et al., 1999; Schulz et al., 1999; Sievert et al., 1999; Sievert et al., 2000; Takai et al., 2004). Representatives of the genera *Thiomicrospira* are among the aerobic, chemosynthetic, thiosulfate-oxidizing bacteria most commonly isolated from hydrothermal vent samples (Ruby and Jannasch, 1982; Jannasch et al.,1985; Teske et al., 2000).

In this study, we describe a novel mesophilic, strictly microaerophilic, chemosynthetic, thiosulfate oxidizing Gammaproteobacterium, isolated from the sediment of an active shallow hydrothermal vent in Paleochori bay, Milos (Greece).

---

[4] This chapter has been published in as Giovannelli et al. In the *International Journal of Systemtic and Evolutionary Microbiology, 62(2012):3060-3066.*

Sediments of a active vents were collected during the summer of 2010 from Paleochory Bay, Milos, Greece (36˚40.351' N, 24˚31.108' E, depth 12 m) during the MAMBA2010 Oceanographic cruise, and from Faial, Azores, Portugal (38˚32.401' N, 28˚35.338' W, depth 44 m), by scuba divers using hand held Plexiglas pushcores. The Paleochory Bay site has been described in details in Sievert et al. (1999a) and Dando et al. (2000), while the Faial site has not yet been characterized. On the surface, samples were transferred to the laboratory and subsamples from different sediment layers were stored at 4 °C under a dinitrogen atmosphere.

Enrichment cultures for mesophilic, chemolithoautotrophic organisms were obtained by inoculating 10 ml of modified medium 1011 (Inagaki et al., 2004) supplemented with 10 % w/v nitrate under CO_2/O_2 (95:5; 200 kPa), with 1 g of the sediment samples resuspended in 1 ml of anaerobic artificial seawater, which contained (l^{-1}): 28 g NaCl, 0.77 g KCl, 1.6 g $CaCl_2 \cdot 2H_2O$, 0.11 g $NaHCO_3$, 3.5 g $MgSO_4 \cdot 7H_2O$. Medium 1011 contained (l^{-1}): 30 g NaCl, 0.14 g K_2HPO_4, 0.14 g $CaCl_2 \cdot 2H_2O$, 3.4 g $MgSO_4 \cdot 7H_2O$, 4.18 g $MgCl_2 \cdot 6H_2O$, 0.33 g KCl, 0.5 mg $NiCl_2 \cdot 6H_2O$, 0.5 mg $Na_2SeO_3 \cdot 5H_2O$, 0.01 g $Fe(NH_4)_2(SO_4)_2 \cdot 6H_2O$, 0.25 g NH_4Cl, 1.5 g $NaHCO_3$, 1.5 g $Na_2S_2O_3 \cdot 5H_2O$, 10 ml trace mineral solution 151 and 1 ml of trace vitamins 197 (http://www.dsmz.de/). The primary enrichments were incubated at 35 °C. Aliquots (0.1 ml) of the primary enrichments were subsequently transferred to fresh medium, and pure cultures were isolated by three consecutive series of dilutions to extinction followed by isolation of single colonies on plates containing modified medium 1011 solidified with 1 g l^{-1} Phytagel (Sigma). Plates were incubated in an anaerobic jar (Oxoid) pressurized with CO_2/O_2 (95:5; 200 kPa). During the isolation procedures the cultures were incubated at 35 °C. Two independent cultures, from the Paleochory Bay and Faial vents, respectively, were obtained using this procedure and were designated as strain $P2D^T$ and P3D. No colonies were obtained when agar was used to solidify the medium. Long-term stocks of the new isolates were prepared by adding 150 µl sterile glycerol (Fisher Scientific) to 850 µl culture and were stored at –80 °C.

Preliminary phylogenetic analysis of the 16S rRNA gene sequences indicated that strains $P2D^T$ and P3D were closely related (sequence identity: 99.5 %, EzTaxon pairwise alignment); $P2D^T$ was chosen for further characterization.

Cells were routinely stained in 0.1 % acridine orange and visualized with an Olympus BX 60 microscope with an oil immersion objective (UPlanFl 100/1.3). Transmission electron micrographs were obtained as previously described (Vetriani et al., 2004). $P2D^T$ cells were short rods, approximately 0.8-1.3 µm in length (mean 1.0 µm) and 0.4-0.5 µm in width (mean 0.45 µm: Figure 7.1a). Cells stained Gram-negative. The organism was motile and possessed one polar flagellum, which was observed in electron micrographs of platinum-shadowed cells (Figure 7.1b).

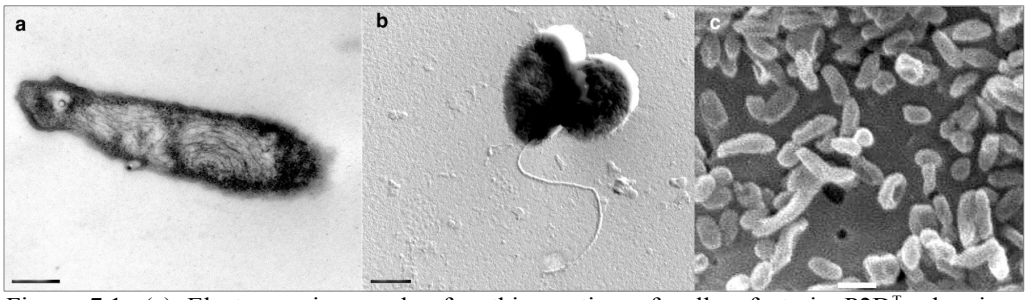

Figure 7.1. (a) Electron micrograph of a thin section of cells of strain P2D^T, showing cell morphology. Bar, 0.2 □m; (b) electron micrograph of platinum-shadowed P2D^T cells, showing a single polar flagellum. Bar 0.5 □m.

Cells grouped together to form a biofilm at the liquid/gas interphase. Biofilm flakes were sampled and observed in scanning electron microscope micrograph, and what appeared to be large sulfur crystals were present (data not shown). On solid medium 1011, P2D^T formed distinct round shaped colonies with a cream to yellow color.

Growth rates (μ; h^{-1}) were estimated as $\mu = (\ln N_2 - \ln N_1)/(t_2 - t_1)$, where N_2 and N_1 are numbers of cell ml^{-1} at times (in h) t_2 and t_1. Generation times (t_g; h) were calculated as $t_g = (\ln 2)/\mu$. All growth experiments were carried out in duplicate in modified liquid medium 1011 under CO_2/O_2 gas phase (95:5; 200 kPa), unless stated otherwise. Samples were collected at regular intervals and subjected to direct cell counts.

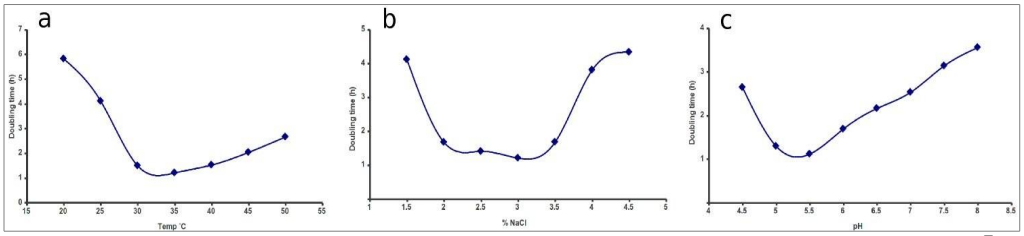

Figure 7.2. Generation time (in h) of *Galenea microaerophila* gen. nov., sp. nov. P2D^T under different growth conditions. (a) Temperature; (b) NaCl concentration; (c) pH.

The optimal growth temperature for strain P2D^T was determined by incubating cultures between 20 and 55ºC (at 5ºC intervals). Strain P2D^T grew at temperatures between 20 and 50°C, with optimal growth at 35°C. No growth was observed below 20 or above 50°C (Figure 7.2a). All subsequent experiments were carried out at 35 °C. The optimal salt requirement was determined by varying the concentration of NaCl between 10 and 50 g l^{-1}, at 5 g l^{-1} intervals. P2D^T grew at NaCl concentrations between 15 and 45 g l^{-1} with optimal growth at 30 g l^{-1} (no growth was observed at 10 and at 50 g l^{-1}; Figure 7.4b). The optimal pH for growth was determined between pH 4.0 and pH 8.5 (at pH 0.5 intervals) as previously described (Voordeckers et al., 2005).

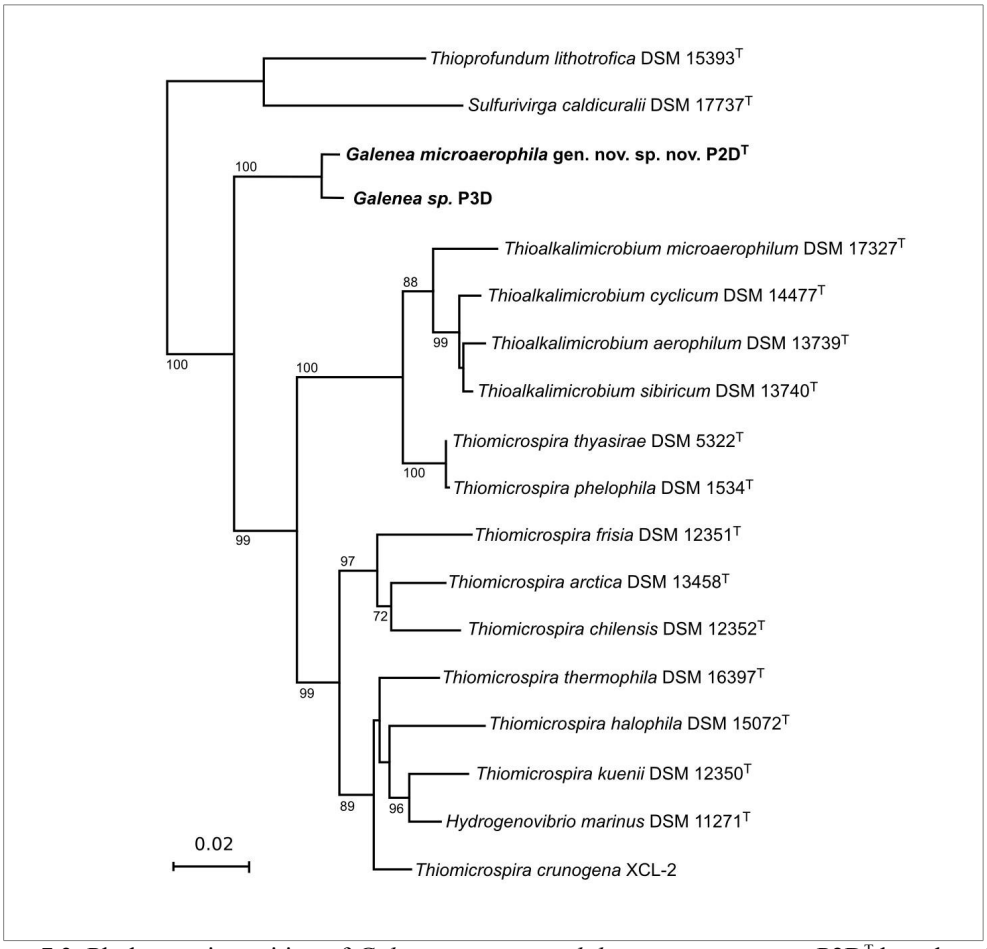

Figure 7.3. Phylogenetic position of *Galenea microaerophila* gen. nov. sp. nov. P2D^T based on 16S rRNA gene sequences. Neighbor-joining three (Jukes-Cantor correction, 1000 bootstrap) constructed with Plylo_Win. Bar, 2 % estimated base substitutions.

Growth of strain P2D^T occurred between pH 4.5 and pH 8.0, with an optimum at pH 5.5 (Figure 7.4c). Under optimal conditions, the generation time of isolate P2D^T was 1.1 hours. Strain P2D^T was a microaerophilic, chemolithoautotrophic bacterium that used thiosulfate as the electron donor and oxygen as the terminal electron acceptor. Antibiotic resistance was tested in liquid cultures in the presence of ampicillin, chloramphenicol, streptomycin and kanamycin (all 100 µg ml^{-1}). All antibiotics were added aseptically before incubation at 35 °C and an ethanol control was carried out for chloramphenicol. Strain P2D^T was inhibited by chloramphenicol, ampicillin, streptomycin and kanamycin. Catalase activity, detected by the formation of gas bubbles after concentrated cells were resuspended in 70 µl of a 3 % solution of H_2O_2 at room temperature, was not observed.

The effect of organic substrates on the growth of strain P2D^T was investigated by adding the following substrates to the medium under an CO_2/O_2 (95:5; 200 kPa) gas phase: lactate, peptone, tryptone, acetate, formate, D(+)-glucose, sucrose (each at 2 g l^{-1}) and yeast extract (0.1 and 1 g l^{-1}). Under an CO_2/O_2 gas phase, no growth of P2D^T occurred in the presence of lactate, peptone,

tryptone, acetate, formate and yeast extract (1 g l^{-1}), while sub-optimal growth occurred in the presence of yeast extract (0.1 g l^{-1}) (generation time was several hours). No inhibition of growth was observed in the presence of D(+)-glucose and sucrose. These substrates were also tested as possible energy and/or carbon sources by using the following conditions: CO_2/O_2 (95:5; 200 kPa) gas phase with no thiosulfate added to the medium, and N_2/O_2 (95:5; 200 kPa) gas phase without the addition of sodium bicarbonate to the medium. Out of all the conditions tested, strain P2D^T only grew in the presence of D(+)-glucose and sucrose under a N_2/O_2 gas phase. No growth was observed in the presence of D(+)-glucose and sucrose when thiosulfate was removed from the medium. Strain P2D^T did not grow when thiosulfate was replaced with either S_0 (3% w/v) or H_2 (80% gas phase) as alternative energy sources. The ability of P2D^T to use alternative electron acceptors was tested by adding sulfate (7 mM), sulfite (4.1 mM), arsenate (5 mM), selenate (5 mM), sulfur (3 % w/v) and potassium nitrate (9.9 mM) to oxygen-depleted medium (N_2/CO_2; 200 kPa). Strain P2D^T did not grow in the presence of any electron acceptor other than 5 % O_2, or in the presence of 0.5 % or 21 % O_2. However, cultures of strain P2D^T survived exposure to air for several hours, indicating that the organism was aerotolerant. In conclusion, strain P2D^T is a strict microaerophile and a facultative mixotroph, capable of using CO_2, D(+)-glucose or sucrose as carbon sources and thiosulfate as the sole electron donor.

The DNA G + C content of P2D^T was determined by the Identification Service of the DSMZ (Deutsche Sammlung von Mikroorganismen und Zellkulturen GmbH, Braunschweig, Germany) by HPLC analysis of deoxyribonucleosides as described by Mesbah, et al. (1989). The G+C content was 44.9 mol%. Chemotaxonomic analyses of strain P2D^T, which included cellular fatty acid composition, polar lipids and respiratory quinones, were carried out by the Identification Service and Dr. Brian Tindall (DSMZ, Braunschweig, Germany) on 300 mg of freeze-dried cells grown to early stationary phase under optimal culture conditions by the authors. The major cellular fatty acids of strain P2D^T were analyzed as the methyl ester derivatives using the Sherlock Microbial Identification System (MIS) (MIDI, Microbial ID, Newark, DE 19711 U.S.A.) and an Agilent model 6890N gas chromatograph (Kuykendall et al., 1988). The fatty acids of strain P2D^T, analyzed using the version 6.1 of the MIDI Inc Sherlock MIS software, were $C_{16:1\omega7c}$ (39.8 %), $C_{16:0}$ (19.1 %), $C_{18:1\ \omega7c}$ (18.3 %) and $C_{18:0}$ (10.5 %) while $C_{12:0}$, $C_{12\text{-alde}}$, $C_{10:0\ 3\text{-OH}}$ and $C_{17:0}$, were present in lower amounts (2.3 %, 2.4 %, 1.8 % and 2.0 %, respectively). These results show that the overall composition of the fatty acids of strain P2D^T is different from other closely related type strains of the genera *Thiomicrospira*, *Thioalkalimicrobium* and *Sulfurivirga* (Table 7.2). The fatty acid profile was compared against the MIS library TSBA40 version 4.10 and TSBA6 version 6.10. The similarity indexes calculated between the fatty acid profile of strain P2D^T and most similar species in the database were very low. The closest profile was of *Grimontia hollisae* (formely *Vibrio hollisae*) for reference library TSBA6 (similarity index of 0.263), while *Pseudomonas huttiensis, Photobacterium leiognathi* and *Vibrio aestuarianus* were the closest in the reference library

TSBA40 (with a similarity index of 0.111, 0.089 and 0.089 respectively, in a range from 0 to 1).

The two predominant polar lipids of strain P2D^T, identified by their staining behavior on thin layer chromatography plates (Tindall, 1990a; Tindall, 1990b), were phosphatidylethanolamine and phosphatidylglycerol, while unidentified phospholipids and aminolipids constituted the minor fractions.

Analysis of the respiratory lipoquinones of strain P2D^T by thin layer chromatography followed by HPLC of the eluted products (Tindall, 1990a; Tindall, 1990b), revealed that strain P2D^T synthesized Q8 as the sole respiratory quinone, similarly to most G*ammaproteobacteria*.

Genomic DNA was extracted from cells of strain P2D^T by using the UltraClean microbial DNA isolation kit (MoBio). The 16S rRNA gene was selectively amplified from the genomic DNA by PCR and sequenced as described previously (Vetriani et al*.,* 2004). Identification of the strain was made using blastn algorithms against the public non-redundant database followed by the BLAST and megaBLAST programs against the database of type strains with validly published prokaryotic names (Chun et al., 2007). The 50 sequences with the highest scores were then selected for the calculation of pairwise sequence similarity using global alignment algorithm, which was implemented at the EzTaxon server (http://www.eztaxon.org/; Chun et al., 2007). Top hits sequences were aligned automatically using CLUSTAL X and the alignment was manually refined using SEAVIEW (Galtier et al., 1996; Thompson et al., 1997). Neighbor-Joining and Maximum-Likelihood trees were constructed to provide confidence estimates for phylogenetic tree topologies. The neighbor-joining tree was constructed by using Phylo_Win and the least-squares algorithm of De Soete from a normal evolutionary distance matrix, (DeSoete, 1983; Perriere and Gouy, 1996) the Jukes-Cantor correction and 1000 bootstraps (Figure 8.3). Phylogenetic analysis of the 16S rRNA gene sequence placed strain P2D^T and P3D within the family *Piscirickettsiaceae* with high bootstrap support (100) (Figures 8.3). Strain P2D^T and strain P3D were closely related (99.5 % similarity) and were placed in a discrete branch outside of the *Thiomicrospira/ Thioalkalimicrobium* cluster. The type strains of these two genera, *Thiomicrospira pelophila* (Kuenen and Veldkamp, 1972) and *Thioalkalimicrobium aerophilum* (Sorokin et al., 2001), had a 92.1 % and 91.5 % sequence identity to strain P2D^T, respectively (Table 8.3). These sequence identities are below the minimum range of 95 % for which a new genus is considered (Tindall et al, 2010). Based on physiological differentiating features from its closest cultured relatives (Table 7.1), on phylogenetic and chemotaxonomic analyses, strain P2D^T represents a new genus, for which we propose the name *Galenea* gen. nov. The type species is *Galenea microaerophila* sp. nov., with the type strain P2D^T (=DSM 24963^T = JCM 17795^T).

G. microaerophila gen. nov., sp. nov. strain P2D^T is a strict microaerophile,, obligate lithotroph and facultative mixotroph that depends on the oxidation of thiosulfate, whose narrow metabolic versatility is unexpected in a bacterium adapted to survive in an unstable fluctuating environment

such as a shallow water hydrothermal system. These environments are characterized by highly fluctuating physical and chemical condition compared to deep-sea hydrothermal systems, including variable organic matter load, temperature shift due to thermocline seasonal formation, hydrodynamism and fluctuation of hydrothermal emission, input of fresh water from land and perturbation of the sediment water interface due to current and wave action (Wenzhöfer et al., 2000). These conditions create a challenging environment in which ecological niches are often unstable on temporal/spatial scales (Wenzhöfer et al., 2000). Heowever, it is possible that the ecological niche occupied by *G. microaerophila* strain P2D^T is perhaps more stable than expected in term of physico-chemical gradients (Stockdale et al., 2009). *G. microaerophila* strain P2D^T shows broad physiological range in terms of temperature, pH, and salinity, and it is aerotolerant. These characteristics, along with its ability to form biofilms, may afford *G. microaerophila* strain P2D^T the ability to survive the sudden changes in environmental conditions typical of shallow-water geothermal environments.

Description of *Galenea* gen. nov.

Galenea (Gal.en'ea N.L. from Gr. fem. *Galene* one of the Nereids, generally associated with the Aegean Sea. *Galene* was known as the goddess of calm seas and shallow water).

Cells are Gram-negative, short rods and motile by mean of one polar flagellum. Mesophilic, strict microaerophiles, require thiosulfate for growth. Facultative mixotrophs. Major respiratory quinone is Q8. Major fatty acids are $C_{16:1\omega7c}$, $C_{16:0}$ and $C_{18:1\ \omega7c}$ and the predominant polar lipids are Phospatidylglycerol and Phospatidylethanolamine. Phylogenetic analyses placed the genus within the *Piscirickettsiaceae* family in the *Gammaproteobacteria*. The type species of the genus is *Galenea microaerophila.*

Description of *Galenea microaerophila* sp. nov.

Galenea microaerophila (mic.ro.aer.o'phi.la Gr. adj. *micros* small, little; Gr. masc. n. *aer* gas; Gr. adj. *philos* loving; N.L. fem. adj. *microaerophila* low-air-loving).

Cells are short rods (on average ca. 1 x 0.45 µm), with a single polar flagellum. Under optimal growth condition (35 ˚C, 3% NaCl, 5.5 pH, CO_2/O_2 95:5) the generation time is 1.11 h. Catalase negative. Growth occurs between 20 and 55 C, 15 and 45 g NaCl l^{-1} and pH 4.5 and 8.0. Growth occurs under strictly microaerophilic, chemolithoautotrophic conditions in the presence of O_2 and $S_2O_3^{2-}$ as sole terminal electron acceptor and donor, respectively. Aerotolerant. No growth occurs in the presence of lactate, peptone, tryptone, acetate, formate (each at 2 g l^{-1}) and yeast extract (1 g l^{-1}). D(+)-glucose and sucrose are utilized as carbon sources. Sensitive to chloramphenicol, ampicillin, streptomycin and kanamycin (each at 100 mg ml^{-1}). Genomic DNA G + C content is

44.9 mol%. Representative of the species are strains P2D^T and P3D. The type strain is P2D^T (=DSM 24963^T = JCM 17795^T), which was isolated from the sediment of an active shallow water hydrothermal vent orifice in Paleochory bay, Milos, Greece.

Table 7.1. Differentiating features of *Galenea microaerophila* gen. nov., sp. nov. P2D^T and genus type strains of *Thiomicrospira pelophila* and *Thioalkalimicrobium aerophilum*.

Strains: 1, *Galenea microaerophila* gen. nov., sp. nov. P2D^T (this study); 2, *Thiomicrospira pelophila* DSM 1534^T (Kuenen and Veldkamp, 1972); 3, *Thioalkalimicrobium aerophilum* DSM 13739^T (Sorokin et al., 2001). +, positive; -, negative.

Characteristic	**1**	**2**	**3**
Size (µm)	1.1-0.45	2.5-0.2	1.3-0.5
Growth on solid media	+ (phytagel) - (agar)	+ (agar)	+ (agar)
DNA G+C content (mol%)	44.9	48	49.5
Isolation area	Shallow Hydrothermal Vents Milos, Greece	Shallow mud flat of Dutch Waddenzee	Siberian soda lake sediment of Buriatia
Growth Temperature (°C) Optimum (range)	35 (20-50)	28	10 (4-40)
NaCl concentration (g l^{-1}): Optimum (range)	30 (15-45)	25 (15-30)	40 (10-65)
pH Optimum (range)	5.5 (4.5-8.0)	7.2 (5-8.5)	10 (7.5-10.6)
Terminal electron acceptors	O_2 (5%)	O_2	O_2
Electron donors	$S_2O_3^{2-}$	$S_2O_3^{2-}$, S_0, H_2S, tetrathionate	$S_2O_3^{2-}$, H_2S
Carbon source	CO_2, D(+)Glucose, Sucrose, Yeast extract	CO_2	CO_2
Optimum generation time (h)	1.1	0.3	0.3

Table 7.2. Cellular fatty acid content of *Galenea microaerophila* gen. nov., sp. nov. P2D^T and related type strains of *Gammaproteobacteria.* Values are percentages of total fatty acids.

Strains: 1, *Galenea microaerophila* gen. nov. sp. nov. P2D^T (data from this study); 2, *Thiomicrospira crunogena* XCL-2^T (Jannasch et al., 1985; Takai et al., 2004); 3, *Thiomicrospira thermophila* DSM 16397^T (Takai et al., 2004); 4, *Thioalkalimicrobium aerophilum* DSM 13739^T (Sorokin et al., 2001); 5, *Sulfurivirga caldicuralii* DSM 17737^T (Takai et al., 2006). Values are percentages of total fatty acids.

Fatty Acid	**1**	**2**	**3**	**4**	**5**
$C_{10:0}$ 3-OH	1.8				
$C_{12:0}$	2.3				
$C_{14:1}$					42.9
$C_{14:0}$	1.1	2.0	7.4		
$C_{15:0}$					
$C_{14:0}$ 3-OH					4.8
$C_{12:0}$ -alde [a]	2.4				
$C_{16:1\ \omega7c}$	39.8				
$C_{16:1}$ [b]		21.4	37.2	4.1	2.3
$C_{16:0}$	19.1	49.2	16.3	12.7	27.0
$C_{17:1\ \omega8c}$	0.7				
$C_{17:0}$	2.0				
$C_{17:0}$ -anteiso		0.9	4.0		
$C_{18:1\ \omega7c}$	18.3				
$C_{18:1}$ [b]		11.8	13.8	80.4	
$C_{18:0}$	10.5	15.2	21.3	1.3	21.1
Summed Feature 2*	39.8				
Summed Feature 3*					4.8
Summed Feature 4*	18.3				

* Summed features are groups of two or three fatty acids that cannot be separated by GLC with the MIDI system; Summed feature 2 contains $C_{16:1\ w7c}$, $C_{16:1\ w6c}$, or both, Summed feature 3 contains $C_{14:0}$ 3-OH, $C_{16:1}$ iso I, or both; Summed feature 4 contains $C_{18:1\ w7c}$, $C_{18:1\ w6c}$, or both;

a $C_{12:0}$ -alde represents a fatty acid with no reference in the MIDI system;

b It is possible that the values reported for $C_{16:1}$ and $C_{18:1}$ in the reference strains correspond to $C_{16:1\ \omega7c}$ and $C_{17:1\ \omega8c}$, respectively.

Table 7.3. Pairwise similarity values obtained using BLAST and megaBLAST algorithms against a manually annotated database of type strains (http://www.eztaxon.org/; Chun et al., 2007) and *Galenea microaerophila* gen. nov., sp. nov. P2D^T. In bold the type species of each genus used as reference.

Species	Strain DSM	Accession	Pairwise Similarity (%)	Difference in total n. of nucleotides
Thiomicrospira psychrophila	13458	AJ404732	92.8	102/1421
Thiomicrospira arctica	13458	AJ404731	92.5	106/1426
Thiomicrospira chilensis	12352	AF013975	92.5	109/1449
Thiomicrospira thermophila	16397	AB166731	92.4	109/1442
Hydrogenovibrio marinus	11271	AB266389	92.4	106/1402
Thiomicrospira crunogena	12353	L40810	92.4	106/1398
Thiomicrospira halophila	15072	DQ390450	92.1	111/1410
Thiomicrospira pelophila	1534	L40809	92.1	112/1418
Thiomicrospira frisia	12351	AF013974	92.0	116/1449
Thiomicrospira thyasirae	5322	AF016046	92.0	114/1424
Thiomicrospira kuenenii	12350	AF013978	91.8	118/1446
Thioalkalimicrobium cyclicum	14477	AF329082	91.7	118/1425
Thioalkalimicrobium aerophilum	13739	AF126548	91.5	121/1421
Thioalkalimicrobium microaerophilum	17327	DQ900623	91.2	120/1366
Thioalkalimicrobium sibiricum	13740	AF126549	91.2	127/1437
Sulfurivirga caldicuralii	17737	AB245479	89.4	153/1440
Thioprofundum lithotrophicum	15393	AB468957	89.0	159/1446

Chapter 8

Microbial assemblages of Pockmarks of the middle Adriatic Sea

Introduction[5]

Cold-seeps, mud volcanoes and pockmarks are seafloor feature linked to the seepage of thermogenic and biogenic gases (Rogers et al., 2006) and/or fluids (Harrington, 1985) from cracks and fissure on the seabed. Alternatively, such structures can be created by the seepage of dense waters, often brines (King and MacLean, 1970). Pockmarks are crater-like features on the seafloor, with dimension generally up to several hundreds of meters in diameter and tens of meters in relief (King and MacLean, 1970). Since the late 70's they have been described to occur in lakes (Pickrill, 2006), shallow bays, estuaries and fjords (e.g. Hovland and Judd, 1988; Kelley et al. 1994), on continental shelves, slopes and rises, as well as in the deep-sea (King and MacLean, 1970; Josenhans et al. 1978.; Paull et al., 2002; Loncke et al., 2004; Gay et al., 2007). Various attempts have been made to estimate the flux to the atmosphere from seabed sources. Seeps, gas hydrates, and mud volcanoes provide 30 Tg y^{-1} of methane (Kvenvolden et al., 2001), a significant portion of total naturally released methane (Etiope and Klusman, 2002; Kvenvolden et al., 2005). The majority of studies carried out on pockmark field investigated their geological and chemical settings in relation to the potential exploitation of underlying hydrocarbon-rich reservoirs (Whelan et al., 2005 and citation therein).

Hydrocarbon-rich sediments tend to have higher sulphate reduction rates and hence high concentrations of sulphides (Ivanov et al., 1989). Invertebrates which obtain their nutrition from symbiotic sulphur-oxidising or methane-oxidising bacteria have been found at hydrocarbon seeps in the Skagerrak (Schmaljohann and Flugel, 1987), off California (Davis and Spies, 1980; Kennicutt et al., 1989) and on the Louisiana Continental Slope (Kennicutt et al., 1985). In shallow (depth lower than 1000 m) seeps, pockmark and mud volcanoes no endemic macro and mega

[5] This chapter is part of a manuscript, Giovannelli et al. - Pockmark of the Middle Adriatic Sea are hotspot of prokaryotes diversity and n-damo metabolsim. *In prep.*

fauna has been reported. However the presence of locally adapted species harboring symbiont cannot be excluded.

The microbiology of cold-seeps has been extensively studied in Mexico, North Sea, Deep-Sea Nile Fan, Olimpi Field, West Africa (Schmaljohann and Flugel, 1987; Davis and Spies, 1980; Kennicutt et al., 1989; Kennicutt et al., 1985). The microbial community are generally characterized by the presence of a wide diversity of methane and sulphate oxidizer. Anaerobic methane-oxidation (AMO) is carried out trough the syntrophic relationship of sulfate reducing bacteria and archaea methane-oxidiziers (Orphan et al., 2002; Joye et al., 2004; Valentine and Reeburgh, 2008). Major groups of sulfate reducing *Bacteria* are *Desulfococcus- Desulfonema-Desulfosarcina*-like and *Desulfovibrio- Desulfomicrobium*-like, and methane oxidizing *Euryarychaeota are Methanomicrobiales*, *Methanosarcinales*, *ANME*-1 and *ANME*-2 among others (Mills et al., 2003; Knittel et al., 2005). However, despite the large number of information available on major deep-sea cold-seeps and mud volcanoes, the microbiology of pockmark, especially shallow pockmark have been so far underinvestigated.

Shallow pockmarks have been observed in the Adriatic Sea during the 80's (Curzi and Veggiani, 1985). In this area the formation of the pockmark field is believed to be caused by the underlying mud diapirs structures (Geletti et al., 2008) as suggested in other investigated areas (Dimitrov and Woodside, 2003; Hovland, 1991; Hovland and Judd, 1988). Following studies (Trincardi et al., 2004; Geletti et al., 2008) described in details the geological settings of those structures, confirming their origins and presenting indirect (e.g. sub-bottom profiler) evidence of fluid seepage. Despite this, there are no studies dealing with the chemistry of the fluids, the sedimentary content of hydrocarbons or the prokaryotic diversity in shallow-water Adriatic pockmark.

In the present work we carried out an integrated chemical and microbiological survey of the Adriatic pockmark formation aligned with the Middle Adriatic Ridge, presenting evidence of hydrocarbon seepage and microbial mediated methane-oxidation and sulphate reduction.

Sampling

Sediments samples were collected during the ARCADIA oceanographic cruise in March 2010. For details on sampling locations and depths see Table 8.1. The pockmark field along the middle Adriatic depression was inspected during the cruise by mean of multibeam (Figure 8.1). The area is characterized by numerous pockmarks surrounding the Middle Adriatic Ridge, an active fault system dividing the Middle Adriatic Depressions. Five station were sampled, two pockmark south-east of the MAR (A162 and A163), one pockmark in the north-west, proximal to the depression above the ridge (A164), and two stations (A168 and A169) in the nearby north-west sediments. Sediments were collected by box-corer and sub-sampled on board by mean of push-core. Each samples was collected in replicate. Sediment horizons were separated in top (0-1 cm), mid (3-5

cm) and bottom (5-10 cm).

Table 8.1. Details of the sampled station and sedimentary organic matter.

	Lat	Long	Depth	Layer	PRT		CHO		LIP		BPC		Chl-a		Feo		CPE	
Station	° N	° E	m	cm	mg g^{-1}	sd	mg g^{-1}	sd	mg g^{-1}	sd	mgC g^{-1}	sd	µg g^{-1}	sd	µg g^{-1}	sd	µg g^{-1}	sd
A162	42.866	15.095	189	0	1.34	0.1	0.55	0.07	0.53	0.03	1.27	0.02	0.07	0.01	6.87	0.37	6.94	0.36
				5	1.44	0.1	0.44	0.00	0.14	0.03	0.98	0.10	0.04	0.01	5.22	0.19	5.26	0.20
				10	1.74	0.0	0.52	0.18	0.38	0.06	1.35	0.15	0.08	0.02	4.68	0.18	4.76	0.17
A163	42.874	15.092	194	0	1.68	0.2	0.37	0.07	0.23	0.06	1.14	0.11	0.05	0.01	5.40	0.31	5.45	0.30
				5	1.65	0.5	0.64	0.17	0.08	0.02	1.12	0.26	0.04	0.00	4.29	0.28	4.33	0.28
				10	1.84	0.2	0.49	0.08	0.17	0.04	1.23	0.06	0.06	0.01	4.16	0.34	4.23	0.34
A164	42.907	15.072	190	0	1.40	0.1	0.53	0.17	0.24	0.06	1.08	0.08	0.13	0.02	7.17	0.52	7.30	0.53
				5	1.17	0.2	0.45	0.01	0.32	0.05	0.99	0.10	0.05	0.02	4.33	0.18	4.39	0.20
				10	1.36	0.2	0.39	0.09	0.08	0.00	0.89	0.09	0.02	0.00	1.11	0.07	1.13	0.07
A168	42.911	15.062	197	0	0.60	0.1	0.49	0.01	0.19	0.00	0.63	0.05	0.04	0.00	2.83	0.21	2.86	0.21
				5	0.60	0.1	1.73	0.44	0.19	0.04	1.13	0.14	0.02	0.00	2.13	0.09	2.15	0.09
				10	0.73	0.1	0.33	0.10	0.14	0.01	0.60	0.06	0.01	0.00	0.62	0.11	0.62	0.11
A169	42.903	15.069	190	0	0.91	0.2	0.90	0.25	0.20	0.00	0.95	0.18	0.05	0.01	4.35	0.19	4.40	0.20
				5	0.71	0.2	0.50	0.24	0.25	0.05	0.74	0.17	0.02	0.00	1.65	0.34	1.67	0.34
				10	0.75	0.1	0.54	0.02	0.10	0.01	0.66	0.06	0.01	0.00	0.60	0.18	0.60	0.18

Results

Sediment hydrocarbons content

Volatile Organic carbon, ranging from C5 to C10, were measured only in the surface sediment (0-1 cm). The concentrations were overall low (Figure 8.2), and showed no differences among the stations with the exclusion of station A164 which presented higher VOC concentrations (438.6±169.3 ng g^{-1}; HSD Tukey post-hoc, $p<0.05$). Alifatic hydrocarbons (AH) showed the higher concentrations, with levels reaching µg g^{-1} of dry sediments (Figure 8.2). In all stations the higher value of AH were measured in the deeper sediment layers (32.1±4.3 µg g^{-1}) with significant differences with the lower values measured in the intermediate 3-5 cm layer (on average 20.8±5.6 µg g^{-1}; ANOVA, $p<0.05$). Among the surface layer (0-1 cm), stations A168 and A169 showed the lower AH concentrations. BTEX value are constant among sampled stations and sediment layers, and within the range 0.5- 40 ng g^{-1}, with the notable exception of station A164 and A169 where in the deeper layer the value are sensibly higher (473.8 and 383.9 ng g^{-1} respectively; Figure 8.2).

The PAH concentrations measured in the sediment layers of the sampled stations are shown in Figure 8.2. Overall the results show a low concentration of PAH in all stations, with slightly higher value in the stations A162, A163, A168 and A169 (range 110.0-139.6 ng g^{-1}) than A164 (97.8 ng g^{-1}). Low molecular weight PAH are the most abundant fraction, and Naphthalene and its methylated forms dominate in all stations (data not shown).

Sedimentary organic matter

Biopolymeric Organic Carbon concentration in the sampled Pockmark changed significantly

among the sampled stations (ANOVA, $p<0.05$; Table 8.2, Figure 8.3). Sediment depth related trends were overall absent (Table 8.2, Figure 8.3), however in station A169 a clear vertical decrease was present. Protein concentrations, as reported for the BPC, changed significantly among stations but not among layers.

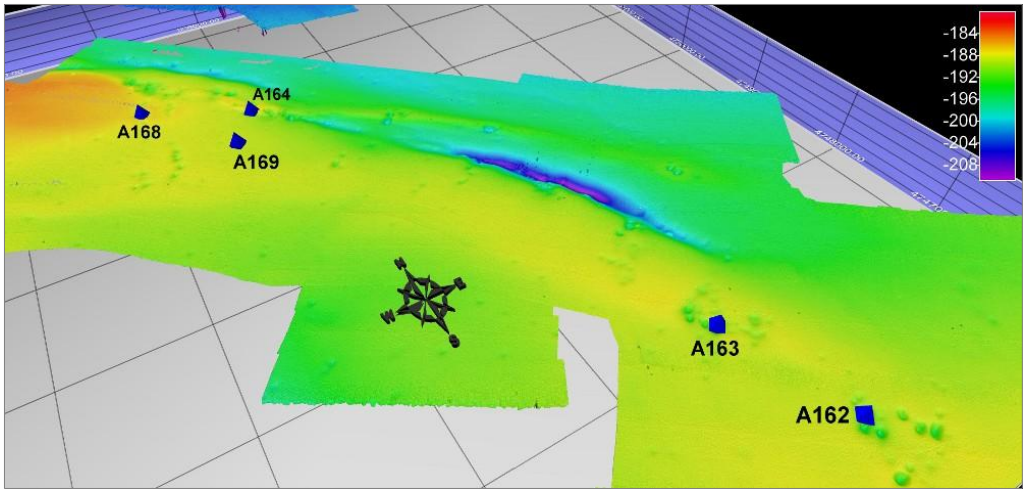

Figure 8.1. High-resolution bathymetry of the sampled pockmark field along the Middle Adriatic Depression. Several pockmarks are visible, together with the depression associated with the MAR.

The proteins concentration were higher in station A162, A163, A164, reaching the maximum in the deeper layer of station A162 (1.9±0.2 mg g^{-1}) and minimum in the superficial layer of station A168 (0.6±0.1 mg g^{-1}; Figure 8.3). Carbohydrates and lipids concentration are reported in Table 8.1. Average concentrations of carbohydrates were homogeneous among sampled stations (range 0.4-0.9 mg g^{-1}) with a maximum in the 3-5 cm layer of station A168 which showed a peak of CHO of 1.7 ± 0.4 mg g^{-1}. Lipids instead showed differences among stations (ANOVA, $p<0.05$; Table 8.2), with higher concentration in the surface layer (0-1 cm) in station A162 (0.5±0.03 mg g^{-1}), and lower in station A168 (0.2±0.03 mg g^{-1}; HSD Tukey post-hoc, $p>0.05$). Despite those difference no clear trends were observed.

Chloroplastic Pigments Equivalents (CPE) showed a clear decreasing trend with sediment depth (Figure 8.3), with higher concentrations in the surface sediment of station A164 (7.3±0.5 µg g^{-1}), and a lower value in the station A168 (2.9±0.2 µg g^{-1}). Overall station A168 and A169 showed the lower values of CPE in all sediment layers (HSD Tukey post-hoc, $p<0.05$).

Prokaryotic abundance, biomass and community structure

TPN were higher in the surficial sediments of the sampled stations (Figurs 8.3), with maximum values at station A162 and A163 (respectively, 3.3±0.8 x10^8 e 3.3±0.2 x10^8 cell g^{-1}) and minimum

at station A169 (1.2±0.4 x10^8 cell g^{-1}). TPN showed a clear trend between sediment layer, decreasing as depth in the sediment increased (ANOVA, $p<0.05$; Table 8.2). Prokaryotic biomass followed similar trends, with higher values in the surficial layers (ANOVA $p<0.05$). Both variables showed higher values for station A162 and A163, decreasing moving in the northwestern pockmarks and with lower values in the north-west sediments.

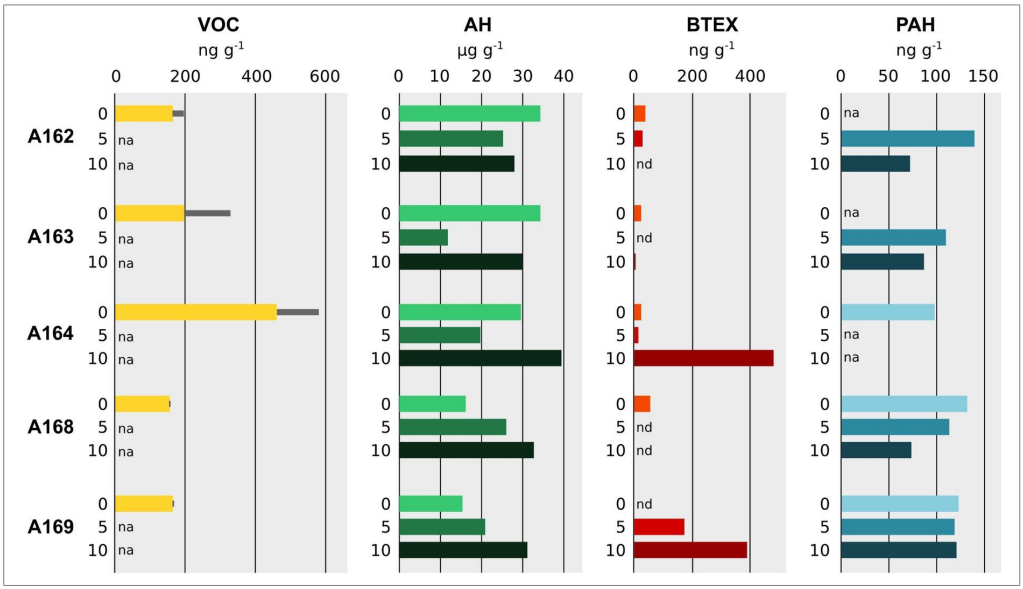

Figure 8.2. Profile of hydrocarbon in sampled stations and layers: VOC - volatile organic carbons from C5 to C10; AH – aliphatic hydrocarbons from C10 to C40; BTEX – benzene, toluene, ethyl-benzene, xylene; PAH – polycyclic aromatic hydrocarbons. Mean value and standard deviation (gray bar) are reported. na – not available. nd – not detected.

We used FISH techniques to investigate the prokaryotic community structure in the sampled stations. The community appears to be dominated by *Bacteria*, with an average contribution to total prokaryotes of 60%. Active cells, measured as the sum of *Bacteria* and *Archaea* counted by FISH accounted on average for 80% of TPN (Figure 8.3), with no significant differences among stations and sediment layers. Higher abundances of *Bacteria* and *Archaea* were respectively found in the deeper layer of station A163 and A162. *Bacteria* to *Archaea* Ratio (BAR; Figure 8.3) changed significantly among stations and layers (Table 8.2), although it did not follow clear trends.

Prokaryotic diversity

Prokaryotic diversity was investigated using 16S rRNA pyrotag libraries with universal primers in all surficial sediments of the sampled stations. We obtained 47,289 sequences that passed quality controls and were used to identify Operational Taxonomic Units (OTUs) clustering at 97% similarity (Rosselló-Mora and Amann, 2001). A total 1940 OTUs were identified among the libraries. Of those 121 OTUs were identified at the species level, with similarities to formally

described prokaryotes between 100 and 97% (6.2% of total OTUs). The 7.5% and 32.1% of total OTUs were identified to the genus or family level respectively (145 and 623 OTU with similarities between 97-95% and 95-90%). We could not identify deeper than Order level 36.5% of total OTUs (709 OTU, similarity range between 90 and 85%), and 13.1% to the Class level (255 OTU, between 85 and 80% similarity). 2.8% were identified to the Phylum level (55 OTU) and 1.6% remained unknown (31 OTU).

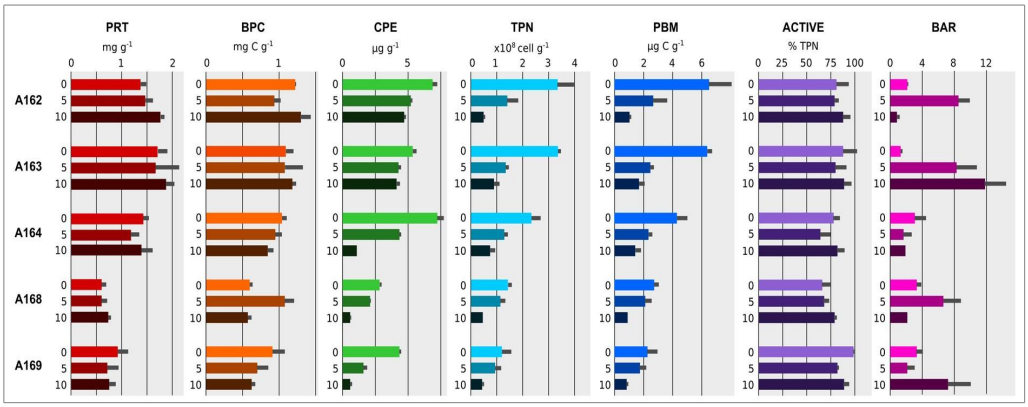

Figure 8.3. Profile of variables across the sampled stations and sediment depths: PRT – Proteins; BPC – Biopolymeric organic carbon; CPE – Total phytopigments; TPN – Total prokaryotic number; PBM – Prokaryotic biomass; ACTIVE - % of metabolically active cells; BAR – *Bacteria* top *Archaea* ratio. Mean value and standard deviation (grey bar) are reported.

The community composition in the five samples is presented in Figure 8.4. Station A164 had the higher diversity with 693 OTUs retrieved, followed by station A168, A162 and A169 with 681, 674 and 657 OTUs respectively. Station A163 presented the lower diversity, with 372 OTUs retrieved. Sequences of the phylum *Firmicutes* were numerically dominant (on average 44.2% of total sequences; Figure 8.4) in all stations, followed by *Proteobacteria* (on average 23%). Within the *Firmicutes*, *Bacillales* where the dominant class with an average abundance of 44.2% of total sequences. *Proteobacteria* were dominated by *Gammaproteobacteria* (on average 14.2% of total sequences), followed by *Alpha* and *Deltaproteobacteria* (4.3% and 4.3% respectively). *Betaproteobacteria* were low in abundances (0.15% on average) and *Epsilonproteobacteria* were below 0.1%, cut-off commonly used to define rare species in pyrotag 16S rRNA surveys (Sogin et al., 2006). Among the *Gammaproteobacteria*, the order *Chromatiales* (6.4%) was the most abundant, followed by *Thiotrichales* (0.76% on average).

Ocenospirillales abundances were low in all station (0.76% on average), except in station A169 where they were 4.2% of the total sequences. *Methylococcales* abundances were low in all stations (on average 0.7%), like the *Alteromonadales* (0.79%), although this group represented 9.6% of total sequences in station A169. Among *Deltaproteobacteria, Desulfovibrionales* were the most abundant with an average contribution to total community of 1.5%. Other abundant *Bacteria* phyla

were *Actinobacteria* (3.3%), *candidate division NC10* (2.7%), *Bacteroidetes* (1.52%) and *Verrucomicrobia* (0.79%).

Table 8.2. Results of ANOVA analysis on the main measured variables

	PRT		BPC		CPE		TPN		PBM		BAR		Active		VOC	
	F	p	F	p	F	p	F	p	F	p	F	p	F	p	F	p
Stations	49.2	***	23.4	***	335.8	***	17.0	***	17.3	***	8.9	***	6.7	***	50.3	***
Layer	2.8	ns	1.3	ns	520.9	***	104.2	***	104	***	10.2	***	5.7	**	NA	NA
Station*Layer	1.0	ns	7.6	***	43.7	***	7.5	***	7.5	***	11.2	***	0.9	ns	NA	NA

Archaea sequences accounted on average for 11.8% of the total retrieved sequences. *Thaumarchaeota* were the third most abundant phyla with an average contribution to total diversity of 11.5% (range 7.3 – 16.2% in A162 and A168 respectively). Within this phylum *Cenarcheales* and *Nitrosopumilales* dominated the community with the genus *Nitrosopumilus* being on average 9.3% of total 16S rRNA sequences.

No major differences between stations were found in the community composition at the phylum and class level considering taxa with a relative abundance above 1% (Figure 8.4). On the other hand, big differences were found when comparing low-abundance species among stations (Figure 8.5). Major differences between station were in the abundance of *Clamidyae, candidate division OP1*, *candidate division WS3* and *Nitrosospirare. Euryarchaeota* sequences abundance were low in all stations (on average 0.27%).

Discussion

Numerous studies carried out in continental margins at different latitudes evidences the fundamental role of hydrocarbon seepage in the formation of a great variety of geomorphological seabottom features, like mud volcanoes, cold-seeps, pockmarks and carbonate mounds (Judd and Hovland, 2007). Those structures and underlying hydrocarbons storages are generally discovered trough geophysiscal investigations. Current research on geomorphological sea-floor features in the central Adriatic Sea evidenced the presence of gas-seepage associated to Messinian evaporites and mud diapirs (Geletti et al., 2008). Despite this geophysical evidences, no data are available on the sediment chemistry or microbiology confirming the presence of hydrocarbon and of a specialized chemosynthetic community in the associated pockmark field.

In order to asses the presence of hydrocarbon anomalies in the sediments of the middle Adriatic Sea pockmark field, we measured the concentration of different class of hydrocarbons in pockmarks (stations A162, A163, A164, A168) and near-by sediments (station A169). The results revealed that overall hydrocarbon contents in the area is rather low, however there are differences

in term of volatile (VOC), alifatic (AH) and monoaromatic (BTEX) fractions between the sampled stations. VOC concentration showed higher level in the pockmark station A164 (Figure 8.2), situated in close proximity of the MAR. In the literature pockmark-like structures aligned with each other or with other hydrocarbon related structures are defined "aligned pockmarks", and generally are thought to be more active (Judd and Hovland, 2007). The proximity to the MAR and the underlying mud diapirs could explain the higher VOC, being the MAR an active fault where previous studies evidenced the presence of gas chimneys and the possible seepage of gas and/or fluids (Geletti et al., 2008). The higher concentration of VOC found could suggest the presence of methane in the sediments, a theory that will require further *in-situ* analysis.

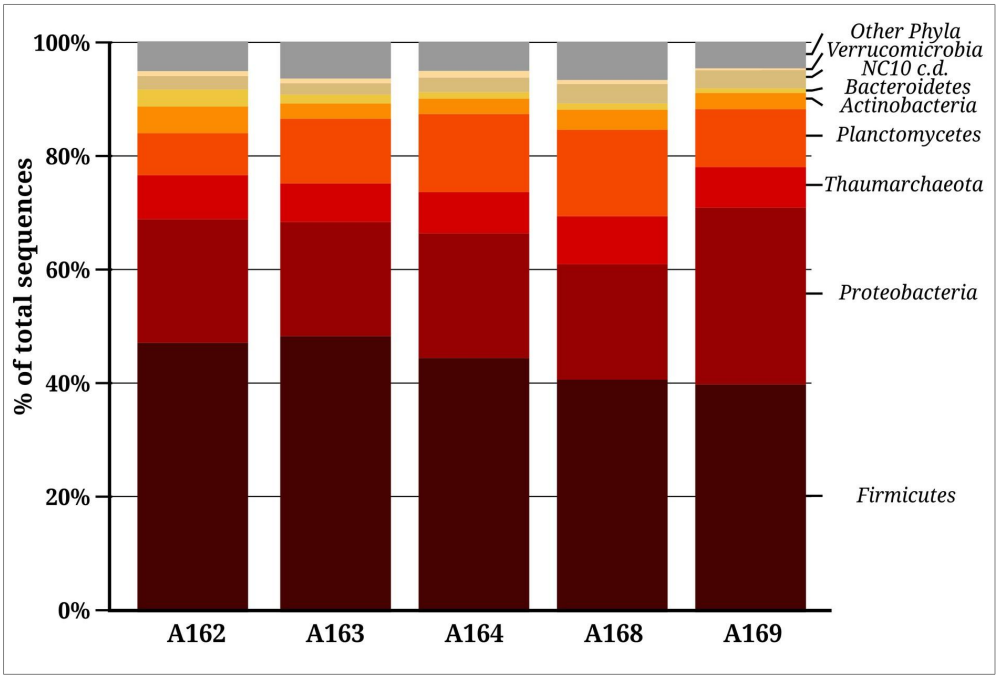

Figure 8.4. Community composition of the top sediment (0-1 cm) in the sampled stations as revealed by 16S rRNA pyrotag analysis. Only phyla with relative abundance above 1% are showed.

Organic matter concentrations are similar to those reported in other studies at similar depths (Manini and Danovaro, 2006; Pusceddu et al., 2010). BPC was dominated by proteins, and proteins to carbohydrate ratio, commonly used as a proxy for the availability of organic matter, was high in all stations (ranging between 1 and 5). While no major differences were found between station in term of BPC, the concentration of CPE showed strong differences among stations (Figure 8.3). Those differences could not be explained by differences in surface primary production or degradation during sink, being all the sampled station at the same depth and in close proximity to each other. Rather, they could be due to a differential use of resources in different stations, thus depending largely on the consumption of the sediment prokaryotic community.

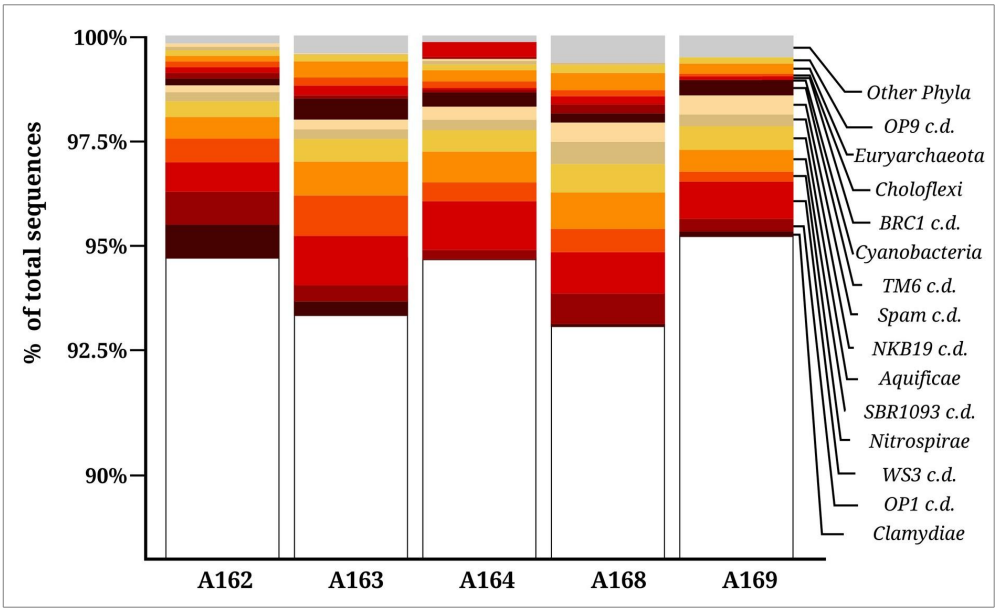

Figure 8.5. Community composition of the top sediment (0-1 cm) in the sampled stations as revealed by 16S rRNA pyrotag analysis. Only phyla with relative abundance below 1% are showed.

The abundance and biomass of the prokaryotic community are within the range of those reported for other studies in similar environments and depths (Manini et al., 2008; Danovaro et al., 1999; Pusceddu et al., 2010). Pockmark stations A162, A163 and A164 showed an higher prokaryotic abundance and biomass (Figure 8.3). This results correlated with the CPE and protein concentrations, suggesting that a relevant portion of the prokaryotic community could be dominated by heterotrophs. The measured BAR supports this theory, as a dominance of *Bacteria* over *Archaea* have been previously reported to by linked to heterotrophy (Molari et al., 2012; Chapter 4 and Chapter 5 of this thesis). Differently from most results reported in the literature (Lipp et al., 2008; Molari et al., 2012; Molari and Manini, 2013), *Bacteria* appears to increase with increasing sediment depths. This finding is controversial and will require further investigations. The observed differences between the *Archaea* contribution to total prokaryotic community calculated using FISH and 16S rRNA pyrotag libraries are likely due to the preferential amplification of B*acteria* by the universal primers, or bias in the emulsionPCR used to generate 454 libraries. FISH direct count are likely to give more reliable results.

The supposed dominance of heterotrophic lineages of *Bacteria* in the pockmark sediments is supported by the diversity analysis results. In all sampled stations sequences belonging to the *Firmicutes* were numerically dominant (Figure 8.4). Cultured *Firmicutes* are gram positive heterotrophs able to degrade or ferment a wide array of organic substrates, including recalcitrant substrates such as cellulose, lignin, amids and other complex carbohydrates. Moreover other typically heterotrophic phyla were abundant (e.g. *Planctomycetes*, *Actinobacteria* and

Verrucomicrobia; Figure 8.4).

Among the *Archaea* sequences, the phylum *Thaumarchaeota* with the genus *Cenarchaeum* and *Nitrosopumilus* were the most abundant. The genus *Cenarchaeum* contains a single described species, *C. symbiosum*, generally described to be the symbiont of marine sponges (Preston et al., 1996). The genus *Nitrosopumilus* includes numerous candidate species, all of which are chemolithoautotrophs ammonia-oxidizers (Könneke et al., 2005). Sequences related to this genus are abundant in all sampled stations evidencing the role of *Archaea* in the cycling of nitrogen in this environment. Within *Archaea* sequences retrieved we found other groups typically present in geothermal influenced sediments like *Methanobacteriales* (methano-oxidizers) and *Thermococcales* (heterotrophic thermophyles). Those groups, despite being low in abundance in our libraries (between 0.01 and 0.2 %), evidence the presence of a specialized consortia able to exploit the possible presence of methane and suggest a thermal anomaly in proximity of the water-sediment interface. This observation in further supported by the presence of other groups of *Bacteria.* Particularly the presence of numerous group of sulfate reducing bacteria of the phylum *Deltaproteobacteria*, which suggest the presence of the syntrophic couple SBR/AMO. The supposed thermal anomaly is further supported by the presence in the library of sequences related to the *Aquificales* and the *Epsilonproteobacteria,* all of which are chemolithoautotrophs and thermophiles (Sievert and Vetriani, 2012). Among the most abundant taxa, the *Gammaproteobacteria* with the order *Chromatiales*, and the genus *Thioploca* and *Thiotrix,* all of which are chemoautotrophs sulfur oxidizers, evidence the strong chemoautotrophic nature of the *in situ* pockmark community.

The oxidation of methane in the investigated stations could be carried out alternatively by the abundant members of the *candidate division NC10*, rather than by the classic SBR/AMO syntrophic couple. C*andidate division NC10* is a group of bacteria with uncertain phylogenetic placement, and containing only one genus and a single species, *Candidatus Methylomirabilis oxyfera*. This bacteria is the only known example of methane-oxidizer capable of autonomously perform this reaction in a nitrite-dependent way (Ettwig et al., 2010). This type of metabolism, called n-damo (nitrite-dependent anaerobic methane oxidation), has the peculiarity of being oxygenic, and thus could represent a possible alternatives to the photosynthesis as mean of creating our moder oxygen-rich atmosphere (Ettwig et al., 2010).

Concluding, our analyses confirmed the presence of a specialized chemosynthetic prokaryotic community at the shallow-water pockmark of the Adriatic Sea, although was not possible to identify a positive anomaly in the hydrocarbon concentrations. This however does not exclude the presence of methane seepage in the area. The abundance of archaea methane oxidizers and sulphate reducing bacteria groups evidence the presence of microbial-mediated methane oxidation at those stations. Moreover, the abundance of sequences related to the *canidate division NC10*

raises interesting question about the ecological significance in those area of n-damo metabolism, which will require further investigation to confirm its relevance.

Chapter 9

Conclusion and future perspectives

> "I never think of the future. It comes soon enough."
>
> *Albert Einstein*

Mediterranean shallow-water extreme environments were known long before the discovery of deep-sea hydrothermal vents in 1977 (Lonsdale, 1977) and Gulf of Mexico cold-seeps in the 80's. Although their popularity and accessibility makes them ideal candidates for the study of those ecosystems, research has been lagging behind their deep-sea oceanic counterparts. This nonsense is probably due to the nature of the research carried in the countries in which those systems are located and the lack of research founds in southern European countries, where the majority of those systems is located. Whichever the reason, Mediterranean shallow-water extreme environments and the deep-sea Med are key source of information for the understanding of the functioning of extreme systems, and deserve intense attention from the scientific community.

In the course of this doctorate project I tried to give my contribution to the study of Mediterranean extreme environments, with a focus on prokaryotes diversity and metabolism in those ecosystems. The idea to break open the "black box" of marine prokaryotic biodiversity, by the application of different molecular tools, has been one of the key assets in the past 20 years or so. Prokaryotes in fact play a key role in all ecosystems (Pfannkuche, 1992) and dominate most extreme environments. They posses the greatest metabolic plasticity and are the most ancient group on Earth.

In the need to connect diversity with ecosystem functioning, the main vision of microbial ecology exploration is now an integrated approach of traditional microbiology and molecular ecology (Sievert and Vetriani, 2012) to give a more in-depth understanding of the dynamics that shape the system. In this thesis I applied this approach to the whole dataset collected in different Mediterranean extreme environments.

Prokaryotic abundance, biomass and community structures

I started investigating the prokaryotic community structure and forcing variables in the low-energy sub-surface sediments (Chapter 4). The investigation of the factor driving the prokaryotic abundance, biomass and community structure in sub-surface shallow-water sediments lead to the identification of biotic (predation) and abiotic factors as main drivers. Despite being on a low-energy environments such as the sub-surface, the percentage of Active cells measure by CARD-FISH was high (~80%) and relatively constant down the vertical profile. Similar results were found on Chapter 5 along the surface deep-sea sediment of the Mediterranean and in the pockmark area in the Adriatic Sea (Chapter 8). It thus appears that the viability of cells is not influenced by the energy availability in the environments (high *vs* low energy), and suggests that the community, as expected, is highly adapted to the local conditions (Figure 9.1).

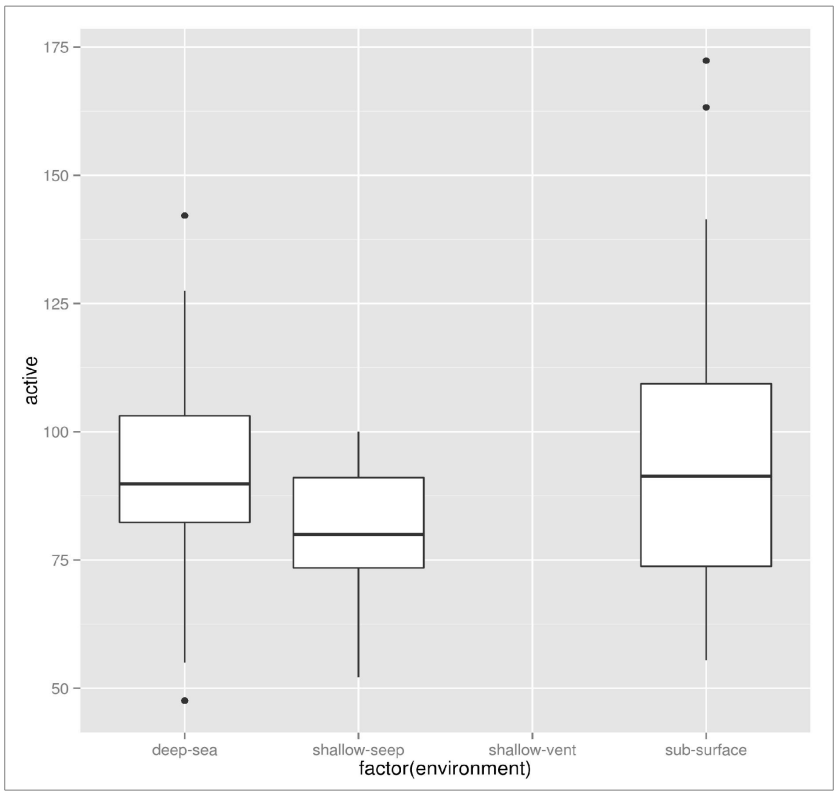

Figure 9.1. Boxplot showing relationship between active cells fraction (%) measured by FISH or CARD-FISH and sampled environments. Deep-sea and subsurface – low-energy; Shallow-seep and shallow-vent – high-energy.

Prokaryotic abundances on average did not varied significantly among sampled areas, although surface layer in shallow-water tidal flat area of the Adriatic (Chapter 4) had a significantly higher TPN (Figure 9.2). This results reveals that prokaryotic abundances are not influenced by the energy regime of the sampled areas. While the abundances are comparable, the energy availability could influence the prokaryotic biomass. Analyzing the PBM with respect to the sampled

environments did not reveal significant differences (data not shown). This surprising result is likely due by methodological bias, introduced by different approaches in measuring prokaryotic biomass during counts. Two different methods where applied in the curse of this thesis. Chapter 4 and Chapter 5 PBM was measure using a direct assignment into dimensional class by the microscope operator (Danovaro et al., 2002), and then converted into biomass using average conversion units (Fry, 1990). This methods has the disadvantage to be influenced by the relative dimension of cells in the sample, as medium cells in a low biomass per cell sample will appear as large, while will be classified as small in a large biomass per cell. To overcame this problems I developed in the curse of this thesis in collaboration with Dr. Giuseppe D'Errico an automated count approach (Giovannelli and D'Errico, unpublished). In this methods samples stained with acridine orange according to standard protocols (Danovaro et al., 2002), are photographed using an epifluorescence microscope.

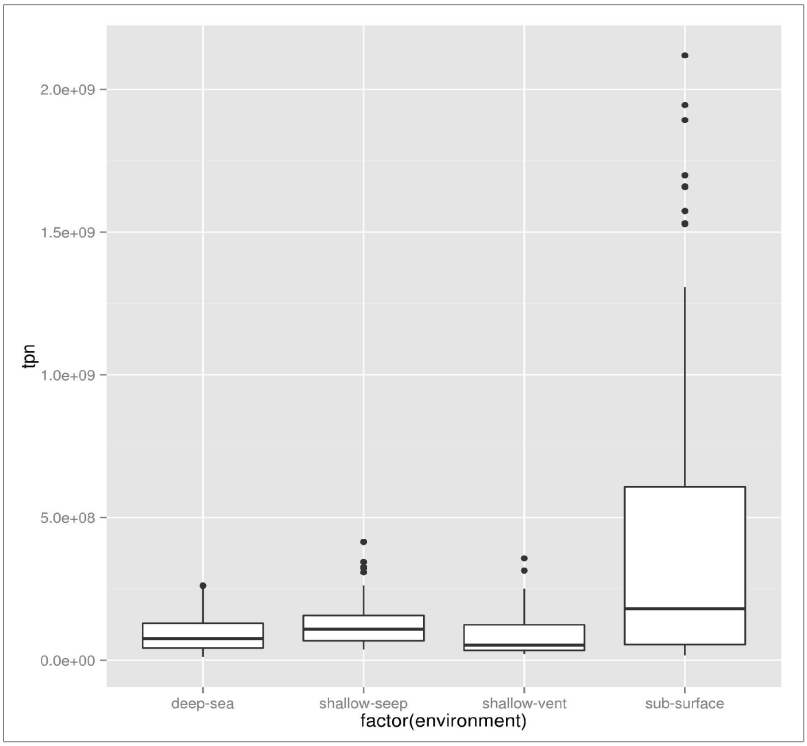

Figure 9.2. Total prokaryotic abundances grouped by sampled areas.

The pictures are automatically processed by a custom ImageJ macro (see Chapter 2 for details), which counts and measure the area of each prokaryotic cells. This measure is converted in bio-volume and thus into biomass using standard conversion factors (Fry, 1990). This approaches has the advantage of making absolute rather then relative measure of the prokaryotic biomass. Thus the absence of differences in biomass between high- and low-energy environments is likely a methodological artifacts. During the course of this thesis I tried to identify the enduring controlling

factors of prokaryotic abundance, biomass and diversity. From the results obtained in the various chapters of this thesis it appears evident that different variables come into play in different environments. Is thus the search for the ultimate controlling factors a chimera of modern microbial ecology? Are we trying to oversimplify the complexity of natural environments?

In Figure 9.3 we can observe the relationship between prokaryotic abundances measured in all sampled environments and biopolymeric organic carbon.

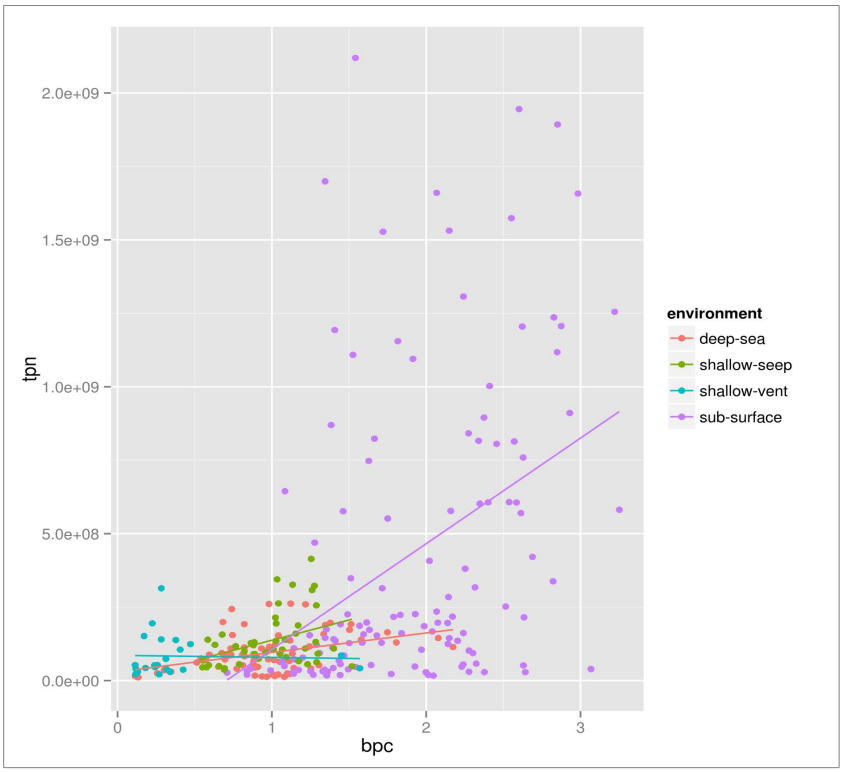

Figure 9.3. Correlation between total prokaryotic abundances and sedimentary biopolymeric carbon content. Linear regression by sampled environments are plotted.

It appears that overall TPN and BPC are linked by positive linear relationship, although the dispersion of points in the subsurface dataset evidence the role of other variable (see Chapter 4 for details) in controlling prokaryotic abundance. In a similar way in shallow-water hydrothermal vents (Chapter 6) BPC has no influence of prokaryotic abundance, which is positively correlated with temperature.

Is it possible to draw conclusion on the role of controlling factors across different environments? It appears from the results of this study that the answer may be more complex than expected.

It could be agreed that different metabolic strategies are influenced by different factors. For example distribution and abundance of heterotrophic prokaryotes is largely influenced by the availability if organic substrates, while chemoauthotrophs are dependent among the availability of

metabolism-specific compounds (e.g. nitrate, ammonia, sulfide, sulfate, methane, etc...). It is thus possible to draw a model in which dominant community metabolism will dictate the kind of relationships observed with environmental and trophic variables. From the data collected in the course of this doctorate is possible to draw conclusion of the relationship between prokaryotic abundances and trophic resources (Figure 9.4).

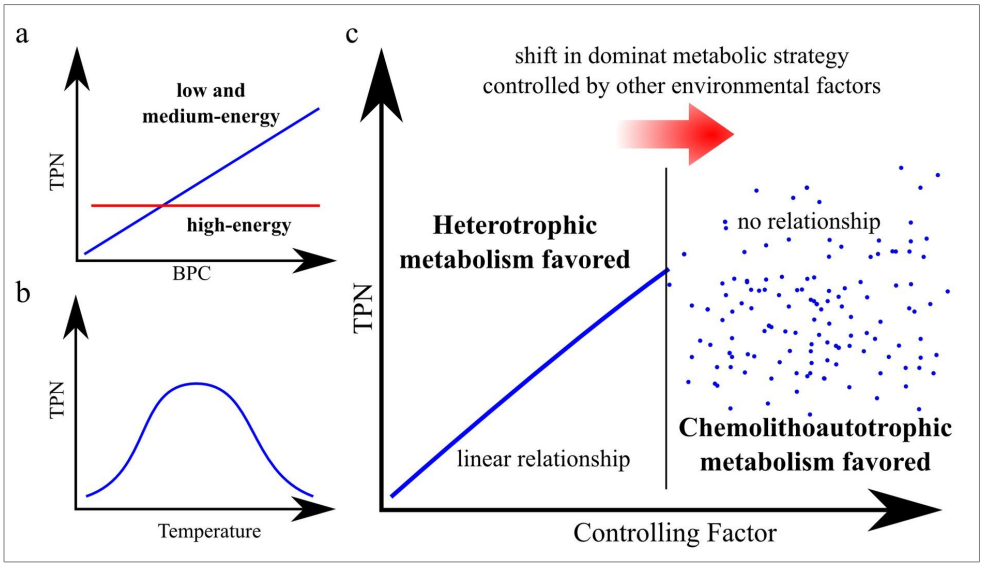

Figure 9.4. Relationships between TPN and BPC (a), TPN and Temperature (b) and proposed model describing the relationship between TPN and trophic controlling factor during shift in community metabolism (c).

As resulting from performed analyses, two types of relationships were observed between TPN and BPC (Figure 9.5a). In type one a positive relationship was present, suggesting heterotrophic dominated communities. This type of relationship was evidenced in deep-sea, pockmark and sub-surface datasets (Figure 9.4). The second type of observed results is the absence of relationships, as evidenced in shallow-water vents (Figure 9.4). In this ecosystem the primary controlling factor was temperature (Chapter 6), for which a bell shaped relationship with prokaryotic abundance is known (Figure 9.5b; *sensu* intermediate disturbance model theory, Dial and Roughgarden, 1998). In this environment, the higher temperatures and reducing conditions of the hydrothermal fluids selects for a community dominated by the chemoautotrophic *Epsilonproteobacteria* (Chapter 6, Figure 6.4). It is thus evident that, depending on the dominant community metabolism, the relationship between prokaryotic abundances and trophic resources described in some studies may be not longer verified (Figure 9.5c), and that secondary factors may come into play.

Prokaryotic diversity in extreme environments

Prokaryotic diversity gives powerful insight into the ecological role of the prokaryotes present *in situ*, despite only 1/10 of total taxonomic group has at least one cultured member. For the two environments where prokaryotic diversity was assessed, it was possible to reconstruct the metabolic processes at work. Despite the differences in used techniques (clone library in Chapter 6 and pyrotag sequencing in Chapter 8), I was able to compare the dominant groups in the two environments (Figure 9.5).

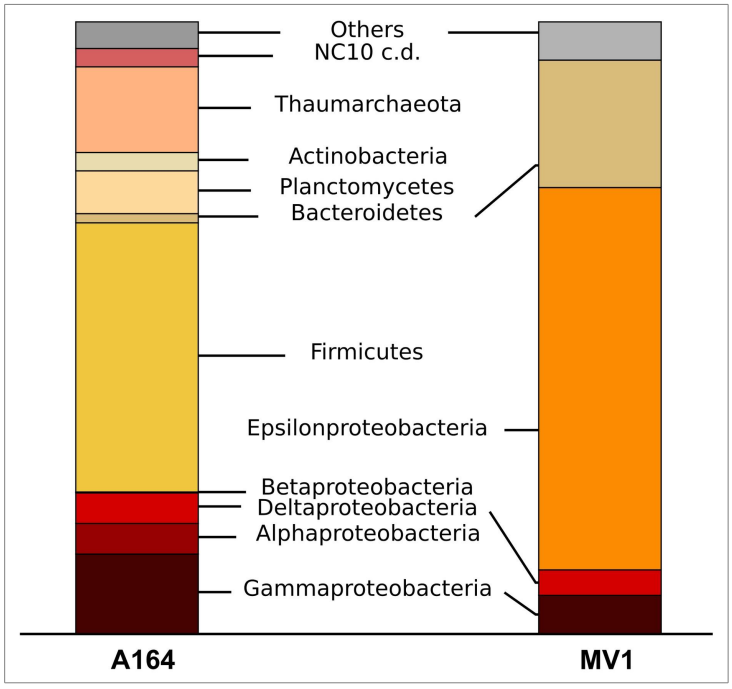

Figure 9.5. Comparison of 16S rRNA diversity at the pockmark station A164 and the shallow-water hydrothermal vent orifice MV1.

Already at the Phylum and Class levels the dominant groups at pockmark and shallow-water vent were different. The only shared taxa were *Gammaproteobacteria*, *Deltaproteobacteria* and *Bacteroidetes* (Figure 9.6). Despite this diversity the two environments, both classified in this thesis as high-energy, had much more in common in term of dominant metabolic strategies. For some of the retrieved groups of prokaryotes it was possible, based on the similarities of retrieved sequences to known species, to infer the metabolism, and thus the ecological function (Figure 9.6).

The results showed an high degree of metabolic redundancy, despite the diverse composition of the community. In both environments heterotrophy and chemoautotrophy were well represented, and metabolism like sulphate reduction and sulfur oxidation were present. Moreover it appeared that the two ecosystems where complementary in regard to the nitrogen cycle, with nitrification present at pockmarks and denitrification at shallow-water vents.

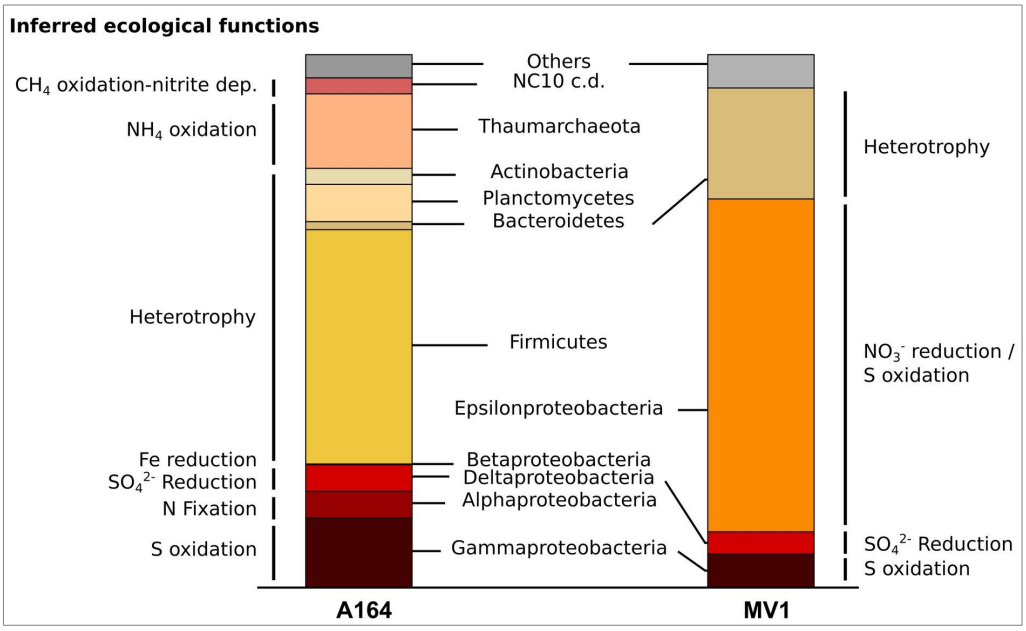

Figure 9.6. Inferred ecological function and metabolism of the dominant prokaryotic taxa at Adriatic pockmarks and shallow-water vents.

A word of caution in interpreting those results is however necessary. Despite the effort in inferring metabolism from phylogeny, this approach is biased by our limited knowledge of prokaryotic metabolisms across the tree of life. In order to increase our knowledge of the functioning of those systems, and more in general of natural ecosystems, we will need to couple environmental survey with genomic and laboratory experiments on pure cultures. Moreover we will need to increase our cultivation effort for those abundant, yet uncultured, prokaryotes.

Future perspectives

Despite the conspicuous amount of work carried out during the course of the doctorate and presented thesis, I am aware of the limited contribution given to the knowledge of Mediterranean Sea extreme environments. Reality is that, whichever the effort, the real contribution of those environments to the functioning of our biosphere will largely remain unknowable. Same holds true for the role of prokaryotes in those systems. Nowadays a big contribution in filling this knowledge gap is coming from "omics" and single cells techniques.

In a quest to add those skills to my personal toolbox, during the course of the doctorate I also worked at the reconstruction of two complete genomes. *Thermovibrio ammonificans* (Vetriani et al., 2004) and *Caminibater mediatlanticus* (Voordeckers et al., 2007) are two termophilic, chemoauthotrophic bacteria isolated from deep-sea hydrothermal vents for which the genome has

been recently sequenced[6,7]. The information contained in the genomes, and the ability to use those species in controlled laboratory experiments gives the advantage of being able to understand their metabolisms and role in the natural environments, and will serve as foundation for future environmental surveys. In the case of the environments sampled during the course of the doctorate, I tried to apply an integrated approach of traditional microbiological and ecological techniques, with an effort to isolate representative species from each environments. This resulted in the isolation and description of *Galenea microaerophila* (Chapter 7), a representative member of the gammaproteobacterial community at Milos shallow-water hydrothermal vents. The genomes of G. microaerophila will be proposed this year for sequencing. Once the metabolic pathways of this species will be clarified, it will be possible to return to the Milos environments with increased knowledge of the in situ processes. A similar integrated approach should be applied to all investigated areas.

From the results of the past thirty years ocean investigations at all scale, it appears that prokaryotes contributed substantially in shaping our ecosystems thought time, and still carry out reactions of crucial importance for global cycling of nutrients and biogeochemistry. In the future, in the daunting task of studying the mechanisms that control our planet, we will need a shift in our approach to investigate natural ecosystems, with an effort to integrate different techniques and disciplines. The integration of ecology, microbiology, geochemistry, oceanography and molecular biology will give a more accurate view of the functioning of our biosphere. For microbial ecology, we will need to move from a "human scale" to a "microbe scale" of measuring, reasoning and interpreting the microbial world, as suggested by Azam and Worden (2004). Moreover we will need to increase our effort to cultivate new species of prokaryotes to fill the gap in the knowledge of their life-style and metabolic potential.

---

[6] D. Giovannelli, S. Ferriera, J. Johnson, S. Kravitz, I. Pérez-Rodríguez, J. Ricci, C. O'Brien, J.W. Voordeckers, E. Bini and C. Vetriani. (2011). Draft genome sequence of *Caminibacter mediatlanticus* strain TB-2T, an *Epsilonproteobacterium* isolated from a deep-sea hydrothermal vent. *Standard In Genomic Science,* 5(1):135-143

[7] D. Giovannelli, I. Pérez-Rodríguez, J. Ricci, C. O'Brien and C. Vetriani. (2012). Complete genome sequence of *Thermovibrio ammonificans* strain HB-1T, an *Aquificae* isolated from a deep-sea hydrothermal vent. *Standard In Genomic Science*, 7(1):82-90

Bibliography

Akaike, H. 1974. A new look at the statistical model identification. IEEE Transactions on Automatic Control, 19:716–723

Allgaier, M., Reddy, A., Park, J. I., Ivanova, N., D'haeseleer, P., Lowry, S., ... and Hugenholtz, P. 2010. Targeted discovery of glycoside hydrolases from a switchgrass-adapted compost community. PLoS One, 5:e8812

Amann, R.I., W. Ludwig and K.H. Schleifer. 1995. Phylogenetic identification and *in situ* detection of individual microbial cells without cultivation. Microbiol. Rev. 59:143-169

Arndt, N. and Nisbet, E. 2012. Processes on the young earth and the habitats of early life. Annu. Rev. Earth Planet. Sci., 40:521–549

Auguet, J. C., Barberan, A., and Casamayor, E.O. 2009. Global ecological patterns in uncultured Archaea. ISME journal, 4:182-190

Azam, F. and Malfatti, F. 2007. Microbial structuring of marine ecosystems. Nature Reviews Microbiology, 5:782-791

Azam, F. and Worden, A.Z. 2004. Microbes, molecules, and marine ecosystems. Science, 303:1622-1624

Bach, W. and Edwards, K. 2003. Iron and sulfide oxidation within the basaltic ocean crust: implication for chemolithoautotrophic microbial biomass production. Geochimica et Cosmochimica Acta, 67:3871-3887

Bach, W., Edwards, K.J., Hayes, J.M., Huber, J.A., Sievert, S.M. and Sogin, M.L. 2006. Energy in the dark: Fuel for life in the deep ocean and beyond. Eos Transaction AGU, 87:73-78

Baross, J.A. and Hoffman, S.E. 1985. Submarine hydrothermal vents and associated gradient environments as sites for the origin and evolution of life. Origins of Life and Evolution of Biospheres, 15:327-345

Behrenfeld M.J. and Falkowski, P.G. 1997. Photosynthetic rates derived from satellite –based chlorophyll concentration. Limnology and Oceanography, 42:1-20

Biddanda, B., Ogdahl, M. and Cotner, J. 2001. Dominance of bacterial metabolism in oligotrophic relative to eutrophic waters. Limnology and Oceanography, 46:730-739

Biddle, J.F., Lipp, J.S., Lever, M.A., Lloyd, K.G., Sørensen, R.A., Fredricks, H.F., Elvert, M., Kelly, T.J., Schrag, D.P., Sogin, M.L., Brenchley, J.E., Teske, A., House, C.H. and Hinrichs, K.U. 2006. Heterotrophic Archaea dominate sedimentary subsurface ecosystems off Peru. PNAS, 103:38-46

Blair, C.C., D'Hondt, S., Spivack, A.J. and Kingsley, R.H. 2007. Radiolytic hydrogen and microbial respiration in subsurface sediments. Astrobiology 7:951-970

Bligh, E.G. and Dyer, W. 1959. A rapid method for total lipid extraction and purification. Canadian Journal Biochemistry Physiology, 37:911–917

Boetius, A. and Damm, E. 1998. Benthic oxygen uptake, hydrolytic potentials and microbial biomass at the Arctic continental slope. Deep-Sea Research Part I, Oceanographic Research Papers, 45:239-275

Boetius, A., Ravenschlag, K., Schubert, C.J., Rickert, D., Widdel, F., Gieseke, A., Amann, R., Jørgensen, B.B., Witte, U. and Pfannkuche, O. 2000. A marine microbial consortium apparently mediating anaerobic oxidation of methane. Nature, 407:623-626

Botz, R., Stoben, D., Winckler, G., Bayer, R., Schmitt, M., and Faber, E. 1996. Hydrothermal gases offshore Milos Island, Greece. Chemical Geology, 130:161-173

Bowman, J.P. and McCuaig, R.D. 2003. Biodiversity, community structural shifts, and

biogeography of prokaryotes within Antarctic continental shelf sediment. Applied Environmental Microbiology, 69:24-63

Braakman, R. and Smith, E. 2012. The emergence and early evolution of biological carbon-fixation. PLoS Computational Biology, 8:e1002455

Brinkhoff, T. and Muyzer, G. 1997. Increased species diversity and extended habitat range of sulfur-oxidizing Thiomicrospira spp. Appl Environ Microbiol, 63:3789–3796

Brinkhoff, T., Sievert, S.M., Kuever, J. and Muyzer, G. 1999. Distribution and diversity of sulfur-oxidizing *Thiomicrospira spp.* at a shallow-water hydrothermal vent in the Aegean Sea (Milos, Greece). Appl Environ Microbiol, 65:3843-3849

Brzustowski, J. 2003. Rarefaction calculator.

Callahan, M.P., Smith, K.E., Cleaves, H.J., Ruzica, J., Stern, J.C., Glavin, D.P., House, C.H. and Dworkin, J.P. 2011. Carbonaceous meteorites contain a wide range of extraterrestrial nucleobases. PNAS, doi:10.1073/pnas.1106493108

Campbell, B.J., Engel, A.S., Porter, M.L. and Takai, K. 2006. The versatile *epsilon-proteobacteria*: key players in sulphidic habitats. Nat Rev Microbiol, 4:458-468

Canals, M., Puig, P., de Madron, X. D., Heussner, S., Palanques, A. and Fabres, J. 2006. Flushing submarine canyons. Nature, 444:354-357

Caporaso, J. G., Kuczynski, J., Stombaugh, J., Bittinger, K., Bushman, F. D., Costello, E. K., ... and Knight, R. 2010. QIIME allows analysis of high-throughput community sequencing data. Nature methods, *7*:335-336

Chun, J., Lee, J.H., Jung, Y., Kim, M., Kim, S., Kim, B.K., and Lim, Y.W. (2007). EzTaxon: a web-based tool for the identification of prokaryotes based on 16S ribosomal RNA gene sequences. Int J Syst Evol Micr 57, 2259-2261

Chyba, C.F. 2005. Rethinking Earth's Early Atmosphere. Science, 308: 962–963

Ciccarelli, F. D., Doerks, T., Von Mering, C., Creevey, C. J., Snel, B., and Bork, P. (2006). Toward automatic reconstruction of a highly resolved tree of life. Science, 311:1283-1287.

Clarke, K. R., and Gorley, R. N. (2001). Primer. Plymouth Marine Laboratory, Plymouth.

Cleaves, H. J., Chalmers, J.H., Lazcano, A., Miller, S.L., Bada, J.L. 2008. A Reassessment of Prebiotic Organic Synthesis in Neutral Planetary Atmospheres. Origins of Life and Evolution of Biospheres 38:: 105-115.

Comita, P.B., Gagosian, R.B., and Williams, P.M. 1984. Suspended particulate organic material from hydrothermal vent waters at 21 N. Nature, 307:450-453

Corinaldesi, C., Dell'Anno, A. and Danovaro, R. 2011. Viral infections stimulate the metabolism and shape prokaryotic assemblages in submarine mud volcanoes. The ISME Journal, 6:1250-1259

Crespo-Medina, M., Chatziefthimiou, A., Cruz-Matos, R., Perez-Rodrıguez, I., Barkay, T., Lutz, R.A., Starovoytov, V. and Vetriani, C. 2009. Salinisphaera hydrothermalis sp. nov., a mesophilic, halotolerant, facultatively autotrophic, thiosulfate-oxidizing gammaproteobacterium from deep-sea hydrothermal vents, and emended description of the genus Salinisphaera. Int J Syst Evol Microbiol, 59:1497–1503

Curzi, P.V. and Veggiani, A., 1985. I pockmark nel mare Adriatico centrale. Acta nat. 'Ateneo Parmense' 21, 79-90. (In Italian)

D'Hondt, S., Jørgensen, B.B., Miller, D.J., Batzke, A., Blake, R., Cragg, B.A., Cypionka, H., Dickens, G., Ferdelman, T., Hinrichs, K., Holm, N.G., Mitterer, R., Spivack, A., Wang, G., Bekins, B., Engelen, B., Ford, K., Gettemy, G., Rutherford, S.D., Sass, H., Skilbeck, G., Aiello, I.W., Guèrin, G., House, C.H., Inagaki, F., Meister, P., Naehr, T., Niitsuma, S., Parkes, R.J., Schippers, A., Smith, D.C., Teske, A., Wiegel, J., Naranjo Padilla, C., and Solis Acosta, J.L., 2004. Distributions of Microbial Activities in Deep Subseafloor Sediments. Science, 306:2216-2221

D'Hondt, S., Rutherford, S. and Spivack, A.J. 2002. Metabolic activity of subsurface life in deep-

sea sediments. Science, 295:2067-2070

Dando, P. R., Thomm, M., Arab, H. and other authors 1998. Microbiology of shallow hydrothermal sites off Palaeochori Bay, Milos (Hellenic Volcanic Arc). Cah Biol Mar, 39:369–372

Dando, P., Aliani, S., Arab, H., Bianchi, C., Brehmer, M., Cocito, S., Fowlers, S., Gundersen, J., Hooper, L., and Kolbh, R. 2000. Hydrothermal studies in the Aegean Sea. Physics and Chemistry of the Earth, Part B: Hydrology, Oceans and Atmosphere, 25:1-8

Dando, P., Hughes, J., Leahy, Y., Niven, S., Taylor, L. and Smith, C. 1995. Gas venting rates from submarine hydrothermal areas around the island of Milos, Hellenic Volcanic Arc. Continental Shelf Research, 15:913-929

Danovaro, R. 2010. Methods for the Study of Deep-sea Sediments - their Functioning and Biodiversity. Ed. Taylor and Francis

Danovaro, R., Corinaldesi, C., D'Onghia, G., Galil, B., Gambi, C., Gooday, A. J., ... and Tselepides, A. 2010. Deep-sea biodiversity in the Mediterranean Sea: The known, the unknown, and the unknowable. PloS one, 5:e11832

Danovaro, R., Dell'Anno, A., Corinaldesi, C., Magagnini, M., Noble, R., Tamburini, C. and Weinbauer, M., 2008. Major viral impact on the functioning of benthic deep-sea ecosystems. Nature, 454:1084-1087

Danovaro, R., Marrale, D., Della Croce, N., Parodi, P. and Fabiano, M., 1999. Biochemical composition of sedimentary organic matter and bacterial distribution in the Aegean Sea: trophic state and pelagic-benthic coupling. Journal Sea Research, 42:117-129

Danovaro. R., Manini, E. and Dell'Anno, A., 2002. Higher abundance of bacteria than of viruses in deep Mediterranean sediments. Applied Environmental Microbiology, 68:62-68

Davis, P.H., Spies, R.B., 1980. Infaunal benthos of a natural petroleum seep: a study of community structure. Mar. Biol., 59:31-41

De Corte, D., Sintes, E., Yokokawa, T., Reinthaler, T., and Herndl, G. J. 2012. Links between viruses and prokaryotes throughout the water column along a North Atlantic latitudinal transect. The ISME Journal, 6:1566–1577

De Corte, D., Yokokawa, T., Varela, M. M., Agogué, H., and Herndl, G. J. 2008. Spatial distribution of Bacteria and Archaea and amoA gene copy numbers throughout the water column of the Eastern Mediterranean Sea. The ISME journal, 3:147-158

De Santis TZ, Hugenholtz P, Keller K, Brodie EL, Larsen N, Piceno MY, Phan R, Andersen GL. 2006. NAST: a multiple sequence alignment server for comparative analysis of 16S rRNA genes. Nucleic Acids Res, 34:394–399

De Soete, G. 1983. A least squares algorithm for fitting additive

trees to proximity data. Psychometrica, 48:621–626

del Giorgio, P.A. and Duarte, C.M. 2002. Respiration in the open ocean. Nature, 420:379-384

DeLong, E. F. (2006). Archaeal mysteries of the deep revealed. PNAS, 103:6417-6418.

DeLong, E.F. 1992. Archaea in coastal marine environments. PNAS, 89:56-85

DeLong, E.F., Taylor, L.T., Marsh, T.L. and C.M. Preston., 1999. Visualization and Enumeration of Marine Planktonic Archaea and Bacteria by Using Polyribonucleotide Probes and Fluorescent In Situ Hybridization. Applied and Environmental Microbiology, 65:5554-5563

Deming, J.W. and Carpenter, S.D., 2008. Factors influencing benthic bacterial abundance, biomass, and activity on the northern continental margin and deep basin of the Gulf of Mexico. Deep Sea Research II, 55:2597-2606.

Des Marais, D.J. 2000. Evolution: When Did Photosynthesis Emerge on Earth? Science, 289:1703-1705

Des Marais, D.J. 2008. NASA Astrobiology Roadmap 2008. http://astrobiology.arc.nasa.gov/roadmap/retrieved on-line 15 March 2013

Dial, R. and Roughgarden, J. 1998. Theory of marine communities: the intermediate disturbance hypothesis. Ecology, *79:*1412-1424

Dimitrov, L. and Woodside, J., 2003. Deep sea pockmark environments in the eastern Mediterranean. Marine Geology, 195:263-76

Duineveld, G. C. A., Lavaleye, M. S. S., and Berghuis, E.M. 2004. Particle flux and food supply to a seamount cold-water coral community (Galicia Bank, NW Spain). Marine Ecology Progress Series, 277:13-23

Edgar, R.C. 2010. Search and clustering orders of magnitude faster than BLAST. Bioinformatics, 26:2460-2461

Edwards, K.J., Bach, W. and McCollom, T.M. 2005. Geomicrobiology in oceanography: microbe-mineral interactions at and below the seafloor. Trends in Microbiology, 13:449-456

Etiope, G. and Klusman, R.W. 2002. Geologic emissions of methane to the atmosphere. Chemosphere, 49:777-789

Ettwig, K. F., Butler, M. K., Le Paslier, D., Pelletier, E., Mangenot, S., Kuypers, M. M., ... and Strous, M. 2010. Nitrite-driven anaerobic methane oxidation by oxygenic bacteria. Nature, 464:543-548

Fabiano, M., Danovaro, R. and Fraschetti, S., 1995. A three-year time series of elemental and biochemical composition of organic matter in subtidal sandy sediments of the Ligurian Sea (northwestern Mediterranean). Continental Shelf Research, 15:1453-1469

Fitzsimons, M., Dando, P., Hughes, J., Thiermann, F., Akoumianaki, I. and Pratt, S. (1997). Submarine hydrothermal brine seeps off Milos, Greece. Observations and geochemistry. Marine chemistry, 57:325-340

Flach, E., Muthumbi, A. and Heip, C. 2002. Meiofauna and macrofauna community structure in relation to sediment composition at the Iberian margin compared to the Goban Spur (NE Atlantic). Progress in Oceanography, 52:433-457

Fry, J.C. 1990. Direct Methods and Biomass Estimation. Methods in microbiology, 22:41-85

Fuhrman, J.A. 1992. Bacterioplankton roles in cycling of organic matter: the microbial food web. Primary Productivity and Biogeochemical Cycles in the Sea, pp. 361-383, Plenum Press

Fuhrman, J.A., Hewson, I., Schwalbach, M.S., Steele, J.A., Brown, M.V. and Naeem, S. 2006. Annually reoccurring bacterial communities are predictable from ocean conditions. PNAS, 103:13104-13109

Galtier, N., Gouy, M. and Gautier, C. 1996. SEAVIEW and PHYLO_WIN: two graphic tools for sequence alignment and molecular phylogeny. Comput Appl Biosci, 12:543–548

Gasol, J.M., del Giorgio, P.A. and Duarte, C.M. 1997. Biomass distribution in marine planktonic communities. Limnology and Oceanography, 42:1353-1363

Gay A. 2006. Seafloor facies related to upward methane flux within a Giant Pockmark of the Lower Congo Basin. Marine Geology ,226:81-95

Geletti R., Del Ben A., Busetti M., Ramella R. and Volpi V. 2008. Gas seeps linked to salt structures in the Central Adriatic Sea. Basin, 20:1365-2117

Gerchakov, S.M. and Hatcher, P.G. 1972. Improved technique for analysis of carbohydrates in sediments. Limnology and Oceanography, 17:938-943

Giovannelli, D., Grosche, A., Starovoytov, V., Yakimov, M., Manini, E. and Vetriani, C. 2012. *Galenea microaerophila* gen. nov., sp. nov., a mesophilic, microaerophilic, chemosynthetic, thiosulfate-oxidizing bacterium isolated from a shallow water hydrothermal vent. Int J Syst Evol Micr, 62:3060-3066

Giovannoni, S. J., and Stingl, U. (2005). Molecular diversity and ecology of microbial plankton. Nature, 437:343-348.

Glud, R.N., Wenzhöfer, F., Middelboe, M., Oguri, K., Turnewitsch, R., Canfield D.E. and

Kitazato, H. 2013. High rates of microbial carbon turnover in sediments in the deepest oceanic trench on Earth. Nature Geoscience, doi:10.1038/ngeo1773

Gold, T., 1992. The deep, hot Biosphere. PNAS 89:6045e6049.

Gouy, M., Guindon, S. and Gascuel, O. 2010. SeaView version 4: a multiplatform graphical user interface for sequence alignment and phylogenetic tree building. Mol Biol Evol, 27:221-224

Harrington, P.K. 1985. Formation of Pockmarks by Pore-Water Escape. Geo-Marine Letters, 5:193-197

Hartree, E.F. 1972. Determination of proteins: a modification of the Lowry methods that give a linear photometric response. Analitical Biochemestry, 48:422-427

Hedges, J.I. 1992. Global biogeochemical cycles: progress and problems. Marine Chemistry, 39:67-93

Herndl G.J. T. Reinthaler E. Teira H. van Aken C. Veth A. Pernthaler and J. Pernthaler 2005. Contribution of Archaea to total prokaryotic production in the deep Atlantic Ocean. Appl. Environ. Microbiol., 71:2303-2309

Hodges, T.W. and Olson, J.B. 2009. Molecular comparison of bacterial communities within iron-containing flocculent mats associated with submarine volcanoes along the Kermadec Arc. Appl Environ Microbiol, 75:1650-1657

Hoshino, T., Yilmaz, L.S., Noguera, D.R., Daims, H. and Wagner, M. 2008. Quantification of target molecules needed to detect microorganisms by florescence in situ hybridization (FISH) and catalysed reporter deposition-FISH. Applied Environmental Microbiology, 74:5068-5077

Hovland M. and Judd A.G. 1988. Seabed pockmarks and seepages. Graham and Trotman, London

Hovland, M. 1991. Large pockmarks, gas-charged sediments and possible clay diapirs in the Skagerrak. Marine and Petroleum Geology, 8:311-16

Huang, W. and Ferris, J.P. 2006. One-step, regioselective synthesis of up to 50-mers of RNA oligomers by montmorillonite catalysis. J. Am. Chem. Soc., 128:8914–9

Huber, J.A., Cantin, H.V., Huse, S.M., Mark Welch, D.B., Sogin, M.L. and Butterfield, D.A. 2010. Isolated communities of *Epsilonproteobacteria* in hydrothermal vent fluids of the Mariana Arc seamounts. FEMS Microbiol Ecol, 73:538-549

Huber, J.A., Welch, D.B.M., Morrison, H.G., Huse, S.M., Neal, P.R., Butterfield, D.A. and Sogin, M.L. 2007. Microbial population structures in the deep marine biosphere. Science, 318:97-100

Huber, T., Faulkner, G. and Hugenholtz, P. 2004. Bellerophon: a program to detect chimeric sequences in multiple sequence alignments. Bioinformatics, 20:2317-2319

Hügler, M., Gartner, A. and Imhoff, J.F. 2010. Functional genes as markers for sulfur cycling and CO_2 fixation in microbial communities of hydrothermal vents of the Logatchev field. FEMS Microbiol Ecol, 73:526-537

Inagaki, F., Takai, K., Nealson, K.H. and Horikoshi, K. 2004. *Sulfurovum lithotrophicum* gen. nov., sp. nov., a novel sulfur-oxidizing chemolithoautotroph within the *epsilon-Proteobacteria* isolated from Okinawa Trough hydrothermal sediments. Int J Syst Evol Microbiol, 54:1477-1482

Ishii, K., Mussmann, M., MacGregor, B.J. and Amann, R. 2004. An improved fluorescence in situ hybridization protocol for the identification of bacteria and archaea in marine sediments. FEMS Microbial Ecology, 50:203-213

Ivanov, M. V., Lein, A. Yu., Reeburg, W S. and Skyring, G. W 1989. Interaction of sulphur and carbon cycles in marine sediments. In: Brimblecome, P., Lein, A. Yu (ed) evolution of the global biogeochemical sulphur cycles SCOPE 39. John Wilwy and Sons, Chichester, p. 125-179

Iverson, V., Morris, R. M., Frazar, C. D., Berthiaume, C. T., Morales, R. L. and Armbrust, E. V. 2012. Untangling genomes from metagenomes: revealing an uncultured class of marine Euryarchaeota. Science, 335:587-590

Jannasch, H. 1985. Review lecture: The chemosynthetic support of life and the microbial diversity

at deep-sea hydrothermal vents. Proceedings of the Royal Society of London. Series B, Biological Sciences, 225:277-297

Jannasch, H. W., Wirsen, C.O., Nelson, D.C. and Robertson, L. A. 1985. Thiomicrospira crunogena sp. nov., a colorless, sulfur-oxidizing bacterium from a deep-sea hydrothermal vent. Int J Syst Evol Microbiol, 35:422–424

Jørgensen, J.K., Favre, C., Bisschop, S.E., Bourke, T.L., van Dishoeck, E.F. and Schmalzl, M. 2012. Detection of the Simplest Sugar, Glycolaldehyde, in a Solar-type Protostar with ALMA. The Astrophysical Journal Letters, 757:L4

Josenhans, H.W., King, L.H. and Fader, G.B. 1978. A side-scan sonar mosaic of pockmarks on the Scotian Shelf. Canadian Journal of Earth Sciences, 15:831-840

Joyce, G.F. 2002. The antiquity of RNA-based evolution. Nature, 418:214–221

Joye, S.B., Boetius, A., Orcutt, B.N., Montoya, J.P., Schulz, H.N., Erickson, M.J. and Lugo, S.K. 2004. The anaerobic oxidation of methane and sulfate reduction in sediments from Gulf of Mexico cold seeps. Chemical Geology, 205:219-238

Karner, M.B., DeLong, E.F. and Karl, D.M. 2001. Archaeal dominance in the mesopelagic zone of the Pacific Ocean. Nature, 409:507-510

Kelley, J.T., Dickson, S.M., Belknap, D.F., Barnhardt, W.A. and Henderson, M. 1994. Giant sea-bed pockmarks: evidence for gas escape from Belfast Bay, Maine. Geology, 22.59-62

Kelman LM. and Kelman Z. 2003. Archaea: an archetype for replication initiation studies? Mol. Microbiol., 48: 605–15

Kennicutt, M. C., Brooks, J. M., Bidigare, R. R., McDonald, S. J., Adksion, D. L., Macko, S. A. 1989. An upper slope 'cold' seep community: Northern California. Limnol. Oceanogr., 34:635-640

Kennicutt. M C., Brooks, J. M,, Bidigare, R. R., Fay, R. R., Wade, T L., McDonald, S. J. 1985. Vent-type taxa in a hydrocarbon seep region on the Louisiana slope. Nature, 317: 351-352

King, L. H., and MacLEAN, B. 1970. Pockmarks on the Scotian shelf. Geological Society of America Bulletin, 81:3141-3148

Kirchman, D. L., Elifantz, H., Dittel, A. I., Malmstrom, R. R., and Cottrell, M. T. (2007). Standing stocks and activity of Archaea and Bacteria in the western Arctic Ocean. Limnology and oceanography, 495-507.

Knittel, K., Lösekann, T., Boetius, A., Kort, R. and Amann, R. 2005. Diversity and distribution of methanotrophic archaea at cold seeps. Applied and Environmental Microbiology, 71:467-479

Könneke, M., Bernhard, A.E., José, R., Walker, C.B., Waterbury, J.B., and Stahl, D.A. 2005. Isolation of an autotrophic ammonia-oxidizing marine archaeon. Nature, 437:543-546

Koppelmann, R., Weikert, H., Halsband-Lenk, C. and Jennerjahn, T. 2004. Mesozooplankton community respiration and its relation to particle flux in the oligotrophic eastern Mediterranean. Global biogeochemical cycles, 18:GB1039

Kouridaki, I., Polymenakou, P.N., Tselepides, A., Mandalakis, M. and Smith Jr, K.L. 2010. Phylogenetic diversity of sediment bacteria from the deep Northeastern Pacific Ocean: a comparison with the deep Eastern Mediterranean Sea. International Microbiology, 13:143-150

Kuenen, J.G. and Veldkamp, H. 1972. Thiomicrospira pelophila, gen. n., sp. n., a new obligately chemolithotrophic colourless sulfur bacterium. Antonie van Leeuwenhoek, 38:241–256

Kvenvolden, K.A., and Rogers, B.W. 2005. Gaia's breath—global methane exhalations. Marine and Petroleum Geology, 22:579-590

Lane N. and Martin, W.F. 2012. The Origin of Membrane Bioenergetics. Cell, 151:1406-1416

Larkin, M., Blackshields, G., Brown, N., Chenna, R., Mcgettigan, P., Mcwilliam, H., Valentin, F., Wallace, I., Wilm, A. and Lopez, R. 2007. Clustal W and Clustal X version 2.0. Bioinformatics, 23:2947-2948

Levy, M. and Miller, S.L. 1998. The stability of the RNA bases: Implications for the origin of life.

PNAS, 95:7933–8

Lipp, J.S., Morono, Y., Inagaki, F. and Hinrichs, K.U. 2008. Significant contribution of Archaea to extant biomass in marine subsurface sediments. Nature, 454:991-994

Llobet-Brossa, E., Rossello-Mora, R. and Amann, R. 1998. Microbial community composition of Wadden Sea sediments as revealed by fluorescence in situ hybridization. Applied Environmental Microbiology, 64:2691-2696

Loncke, L., Mascle, J., and Parties, F.S. 2004. Mud volcanoes, gas chimneys, pockmarks and mounds in the Nile deep-sea fan (Eastern Mediterranean): geophysical evidences. Marine and Petroleum Geology, 21:669-689

Lonsdale, P. (1977). Clustering of suspension-feeding macrobenthos near abyssal hydrothermal vents at oceanic spreading centers. Deep Sea Research, 24:857-863

Lopez-Garcia, P., Duperron, S., Philippot, P., Foriel, J., Susini, J. and Moreira, D. 2003. Bacterial diversity in hydrothermal sediment and epsilonproteobacterial dominance in experimental microcolonizers at the Mid-Atlantic Ridge. Environ Microbiol, 5:961-976

Luna, G.M., Manini, E. and Danovaro, R. 2002. Large fraction of dead and inactive bacteria in coastal marine sediments: comparison of protocols for determination and ecological significance. Applied Environmental Microbiology, 68:3509-3513

Ma W., Yu C., Zhang W. and Hu J. 2007. Nucleotide synthetase ribozymes may have emerged first in the RNA world. RNA, 13:2012–9

Maher, K.A. and Stevenson, D.J. 1988. Impact frustration of the origin of life. Nature, 331:612–614

Maniatis, T. 1989. Molecular cloning: a laboratory manual. New York: Cold Spring Harbor Laboratory Press

Manini, E. and Danovaro, R. 2006. Synoptic determination of living/dead and active/dormant bacterial fractions in marine sediments. FEMS Microbial Ecology, 55:416-423

Manini, E., Luna, G., Corinaldesi, C., Zeppilli, D., Bortoluzzi, G., Caramanna, G., Raffa, F. and Danovaro, R. 2008. Prokaryote diversity and virus abundance in shallow hydrothermal vents of the Mediterranean Sea (Panarea Island) and the Pacific Ocean (North Sulawesi-Indonesia). Microb Ecol, 55:626-639

Martin, W., Baross, J., Kelley, D., and Russell, M.J. 2008. Hydrothermal vents and the origin of life. Nature Reviews Microbiology, 6:805-814

Martínez-García, M., Stief, P., Díaz-Valdés, M., Wanner, G., Ramos-Esplá, A., Dubilier, N. and Antón, J. 2008. Ammonia-oxidizing Crenarchaeota and nitrification inside the tissue of a colonial ascidian. Environmental microbiology, 10:2991-3001

Mason, O.U., Di Meo-Savoie, C.A., Van Nostrand, J.D., Zhou, J., Fisk, M.R. and Giovannoni, S.J. 2008. Prokaryotic diversity, distribution, and insights into their role in biogeochemical cycling in marine basalts. The ISME journal, 3:231-242

Massana R., DeLong E. F., Pedrós-Alio, C. 2002. A few cosmopolitan phylotypes dominate planktonic archaeal assemblages in widely different oceanic provinces. Appl. Environ. Microbiol., 66:1777-1787

Massana, R., Murray, A.E., Preston, C.M. and DeLong, E.F. 1997. Vertical distribution and phylogenetic characterization of marine planktonic Archaea in the Santa Barbara Channel. Applied Environmental Microbiology, 63:50-56

Mauclaire, L., Zepp, K., Meister, P., McKenzie, J. 2004. Direct in situ detection of cell in deep-sea sediment cores from the Peru Margin (ODP Leg 201, Site 1229). Geobiology, 2:217-223

Maugeri, T.L., Lentini, V., Gugliandolo, C., Cousin, S. and Stackebrandt, E. 2010. Microbial Diversity at a Hot, Shallow-Sea Hydrothermal Vent in the Southern Tyrrhenian Sea (Italy). Geomicrobiology Journal, 27:380-390

Maugeri, T.L., Lentini, V., Gugliandolo, C., Italiano, F., Cousin, S, and Stackebrandt, E. 2009. Bacterial and archaeal populations at two shallow hydrothermal vents off Panarea Island (Eolian Islands, Italy). Extremophiles, 13:199-212

Mei, M.L. and Danovaro, R. 2004. Virus production and life strategies in aquatic sediments. Limnology and Oceanography, 49:459-470

Mesbah, M., Premachandran, U. and Whitman, W. 1989. Precise measurement of the G + C content of deoxyribonucleic acid by high performance liquid chromatography. Int J Syst Bacteriol, 39:159–167

Michaelian, K. 2011. Biological Catalysis of the Hydrological Cycle: Life's Thermodynamic Function. Hydrol. Earth Syst. Sci. Discuss., 8:1093–1123

Middelboe M., Glud R.N., Filippini M. 2011. Viral abundance and activity in the deep sub-seafloor biosphere. Aquatic Microbial Ecology, 63:1–8

Middelboe, M. and Jøgensen, N.O.G. 2006. Viral lysis of bacteria: an important source of dissolved amino acids and cell wall compounds. Journal of Marine Biology Association UK, 86:605-612

Miller, S.L. 1953. A Production of Amino Acids Under Possible Primitive Earth Conditions. Science, 117: 528–9

Mills, H.J., Hodges, C., Wilson, K., Macdonald, I.R. and Sobecky, P. 2003. Microbial diversity in sediments associated with surface-breaching gas hydrate mounds in the Gulf of Mexico. FEMS microbiology ecology, 46:39–52

Mojzsis, SJ, Arrhenius, G, McKeegan, KD, Harrison, TM, Nutman, AP, Friend, CRL. 1996. Evidence for life on Earth before 3,800 million years ago. Nature, 384:55-59

Molari M. Giovannelli D., d'Errico G. and Manini E., 2012. Factor influencing prokaryotic community structure composition in sub-surface coastal sediments. ECSS, 97:141–148

Molari, M. and Manini, E. 2012. Reliability of CARD-FISH Procedure for Enumeration of Archaea in Deep-Sea Surficial Sediments. Current microbiology, 64:1-9

Molari, M., Manini, E. and Dell'Anno, A. 2013. Dark inorganic carbon fixation sustains the functioning of benthic deep-sea ecosystems. Global Biogeochemical Cycles, doi: 10.1002/jgrd.50265

Morbidelli, A.J. Chambers, J.I. Lunine, J.M. Petit, F. Robert, G.B. Valsecchi, K.E. 2010. Source regions and timescales for the delivery of water to the Earth. Meteoritics and Planetary Science, 35:1309–1320

Moyer, C.L., Dobbs, F.C. and Karl, D.M. 1995. Phylogenetic diversity of the bacterial community from a microbial mat at an active, hydrothermal vent system, Loihi Seamount, Hawaii. Appl Environ Microbiol, 61:1555-1562

Murray A.E., Preston C.M., Massana R., Taylor L.T., Blakis A., Wu K. and DeLong E.F. 1998. Seasonal and spatial variability of bacterial and archaeal assemblages in the coastal waters near Anvers Island, Antarctica. Applied Environmental Microbiology, 64:2585-2595

Musata, N., Wernera, U., Knittela, K, Kolba, S., Dodenhofa, T., van Beusekomb, J.E.E., de Beera, D., Dubiliera, N. and Amann, R., 2006. Microbial community structure of sandy intertidal sediments in the North Sea, Sylt-Rømø Basin, Wadden Sea. Systematic and Applied Microbiology, 29:333-348

Muyzer, G., Teske, A., Wirsen, C.O. and Jannasch, H.W. 1995. Phylogenetic relationships of Thiomicrospira species and their identification in deep-sea hydrothermal vent samples by denaturing gradient gel electrophoresis of 16S rDNA fragments. Arch Microbiol, 164:165–172

Myers, N., Mittermeier, R.A., Mittermeier, C.G., da Fonseca Gustavo, A.B., Kent, J. 2000. Biodiversity hotspots for conservation priorities. Nature, 403:853–858

Nakagawa, S. and Takai, K. 2008. Deep-sea vent chemoautotrophs: diversity, biochemistry and ecological significance. FEMS Microbiol Ecol, 65:1-14

Nakagawa, S., Takai, K., Inagaki, F., Hirayama, H., Nunoura, T., Horikoshi, K., and Sako, Y. 2005. Distribution, phylogenetic diversity and physiological characteristics of *epsilon-Proteobacteria* in a deep-sea hydrothermal field. Environ Microbiol, 7:1619-1632

Nealson, K. H., Conrad, P. G., Nealson, K. H., and Conrad, P. G. 1999. Life: past, present and future. Philosophical Transactions of the Royal Society of London. Series B: Biological Sciences, 354:1923-1939

Nisbet, E. and Fowler, C. 1996. The hydrothermal imprint on life: did heat-shock proteins, metalloproteins and photosynthesis begin around hydrothermal vents? Geological Society, London, Special Publications, 118:239-251

Nisbet, E. and Sleep, N. 2001. The habitat and nature of early life. Nature, 409:1083-1091

Oksanen, J., Blanchet, F.G., Kindt, R., Legendre, P., Minchin, P.R., O'Hara, R.B., ... and Suggests, M.A. 2012. Package 'vegan'.

Orphan, V.J., House, C.H., Hinrichs, K.U., McKeegan, K.D. and DeLong, E.F. 2002. Multiple archaeal groups mediate methane oxidation in anoxic cold seep sediments. PNAS, 99:7663-7668

Parkes, R.J., Cragg, B.A., Bale, S.J., Getliff, J. M., Goodman, K., Rochelle, P. A., Fry, J.C., Weightman, A. J., Harvey, S.M. 1994. Deep bacterial biosphere in Pacific Ocean sediments. Nature, 371:410 – 413

Parkes, R.J., Cragg, B.A., Wellsbury, P. 2000. Recent studies on bacterial populations and process in subseafloor sediments: a review. Hydrogeology Journal, 8:11-28

Paull C.K. Ussler W.III. Borowski W.S. 1999. Freshwater ice rafting: an additional mechanism for the formation of some high-latitude submarine pockmarks. Geo-Marine Letters, 19:164-168

Payne, J. L., Boyer, A. G., Brown, J. H., Finnegan, S., Kowalewski, M., Krause Jr, R. A., ... and Wang, S. C. 2009. Two-phase increase in the maximum size of life over 3.5 billion years reflects biological innovation and environmental opportunity. PNAS, 106:24-27

Pearson, A. 2008. Biogeochemistry: who lives in the sea floor? Nature, 454:952-953

Pernthaler, A., Pernthaler, J., Amann, R. 2002. Fluorescence in situ hybridization and catalysed reporter deposition for the identification of marine bacteria. Applied Environmental Microbiology, 68:3094-3101

Pernthaler, J. 2005. Predation on prokaryotes in the water column and its ecological implication. Nature Review Microbiology, 3:537-546

Perriere, G. and Gouy, M. 1996. WWW-query: an on-line retrieval system for biological sequence banks. Biochimie, 78:364-369

Pfannkuche, O. (1992). Organic carbon flux through the benthic community in the temperate abyssal Northeast Atlantic. Deep-sea food chains and the global carbon cycle, 183-198.

Pfannkuche, O. and Soltwedel, T. 1998. Small benthic size classes along the NW European Continental Margin: spatial and temporal variability in activity and biomass. Progress in oceanography, 42:189-207

Pflug, H.D. 2001. Earliest organic evolution. Essay to the memory of Batholomew Nagy. Precambrian Research, 106:79–91

Pickrill R.A. 1993. Shallow seismic stratigraphy and pockmarks of a hydrothermally influenced lake, Lake Rotoiti, New Zealand. Sedimentology, 40:813-828

Plante-Cuny, M.R. 1974. Evaluation par spectrophotometrie des teneurs en chlorophylle a fonctionnelle et en pheopigments des substrats meubles marins. Doc. Sci. Mission ORSTOM Nosy-B, 45:1-76

Pommier, T., Canbäck, B., Riemann, L., Boström, K. H., Simu, K., Lundberg, P., ... and Hagström, Å. (2006). Global patterns of diversity and community structure in marine bacterioplankton. Molecular ecology, 16:867-880.

Pratscher, J., Dumont, M. G. and Conrad, R. 2011. Ammonia oxidation coupled to CO2 fixation by

archaea and bacteria in an agricultural soil. PNAS, 108:4170-4175

Preston C.M., K.Y. Wu, T.F. Molinski and E.F. DeLong. 1996. A psychrophilic crenarchaeon inhabits a marine sponge: Cenarchaeum symbiosum gen. nov., sp. nov.. Proceedings of the National Academy of Sciences of the United States of America. 93:6241-6246

Pusceddu A. Bianchelli S. Canals M. Sanchez-Vidal A. Durrieu De Madron X. 2010 Heussner S. Lykousis V. de Stigter H. Trincardi, F. and Danovaro R. Organic matter in sediments of canyons and open slopes of the Portuguese, Catalan, Southern Adriatic and Cretan Sea margins, Deep-Sea Res. I., 57:441-457

Quèric, N.V., Soltwedel, T. and Arntz, W.E. 2004. Application of a rapid direct viable count method to deep-sea sediment bacteria. Journal Microbiology Methods, 57:351-367

R development Core Team, 2010. R: A Language and Environment for Statistical Computing. R Foundation for Statistical computing. Vienna, Austria. ISBN: 3-900051-07-0. http://www.R-project.org

Ravenschlag, K., Sahm, K. and Amann, R. 2001. Quantitative molecular analysis of the microbial community in marine Arctic sediments (Svalbard). Applied Environmental Microbiology, 67:387-395

Reinthaler, T., Van Aken, H., Veth, C., Arístegui, J., Robinson, C., Williams, P.J.L.B., ... and Herndl, G.J. 2006. Prokaryotic respiration and production in the meso-and bathypelagic realm of the eastern and western North Atlantic basin. Limnology and Oceanography, 1262-1273

Rogers, J.N., Kelley, J.T., Belknap, D.F., Gontz, A. and Barnhardt, W.A. 2006. Shallow-water pockmark formation in temperate estuaries: A consideration of origins in the western gulf of Maine with special focus on Belfast Bay. Marine Geology, 225:45-62

Rossello-Mora, R. and Amann, R. 2001. The species concept for prokaryotes. FEMS Microbiol Rev, 25:39-67

Ruby, E.G. and Jannasch, H.W. 1982. Physiological characteristics of Thiomicrospira sp. strain L-12 isolated from deep-sea hydrothermal vents. J Bacteriol, 149:161–165

Russell, M. J., and Hall, A. J. (1997). The emergence of life from iron monosulphide bubbles at a submarine hydrothermal redox and pH front. Journal of the Geological Society, 154:377-402.

Sahm, K. and Berninger, U.R. 1998. Abundance, vertical distribution, and community structure of benthic prokaryotes from permanently cold marine sediments (Svalbard, Arctic Ocean). Marine Ecology Progress Series, 165:71-80

Saladino, R., Botta, G., Pino, S., Costanzo, S. and Di Mauro, E. 2012. Genetics first or metabolism first? The formamide clue. Chem. Soc. Rev., 41:5526–5565

Sandman K. and Reeve JN. 2006. Archaeal histones and the origin of the histone fold. Curr. Opin. Microbiol. 9:520–525

Santinelli, C., Nannicini, L. and Seritti, A. 2010. DOC dynamics in the meso and bathypelagic layers of the Mediterranean Sea. Deep Sea Research Part II: Topical Studies in Oceanography, 57:1446-1459

Schauer, R., Bienhold, C., Ramette, A., and Harder, J. 2009. Bacterial diversity and biogeography in deep-sea surface sediments of the South Atlantic Ocean. The ISME Journal, 4:159-170

Schippers, A., Neretin, L.N., Kallmeyer, J., Ferdelman, T.G., Cragg, B.A., Parkes, R.J. and Jørgensen, B.B. 2005. Prokaryotic cells of the deep subseafloor biosphere identified as living bacteria. Nature, 433:861-864

Schmalijohann, R., Flugel, H. 1987. Methane oxidizing bacteria in Pogonophora. Sarsia, 72:91-98

Schmidt, J.L., Deming, J.W., Jumars, P.A. and Keil, R.G. 1998. Constancy of bacterial abundance in surficial marine sediments. Limnology Oceanography, 43:976-982

Schneider, C.A., Rasband, W.S., and Eliceiri, K.W. 2012. NIH Image to ImageJ: 25 years of image analysis. Nature Methods, 9:671-675

Schopf, J.W. 1993. Microfossils of the early Archean Apex chert: new evidence of the antiquity of life. Science, 260:640-646

Schrenk, M.O., Huber, J.A. and Edwards, K. 2010. Microbial Provinces in the Subseafloor. Annual Review Marine Science, 2:279-304

Schulz, H. N., Brinkhoff, T., Ferdelman, T. G., Marine, M. H., Teske, A. and Jørgensen, B. B. 1999. Dense populations of a giant sulfur bacterium in Namibian shelf sediments. Science, 284:493–495

Schwartzman D.W. and Lineweaver C.H. 2004. The hyperthermophilic origin of life revisited. Biochem. Soc. Trans., 32:168-71

Sievert, S.M. and Vetriani, C. 2012. Chemoautotrophy at deep-sea vents: Past, present, and future. Oceanography, 25:218–233

Sievert, S.M., Brinkhoff, T., Muyzer, G., Ziebis, W, and Kuever, J. 1999. Spatial heterogeneity of bacterial populations along an environmental gradient at a shallow submarine hydrothermal vent near Milos Island (Greece). Appl Environ Microbiol, 65:3834-3842

Sievert, S.M., Kuever, J. and Muyzer, G. 2000a. Identification of 16S ribosomal DNA-defined bacterial populations at a shallow submarine hydrothermal vent near Milos Island (Greece). Appl Environ Microbiol, 66:3102-3109

Sievert, S.M., Ziebis, W., Kuever, J. and Sahm, K. 2000b. Relative abundance of Archaea and Bacteria along a thermal gradient of a shallow-water hydrothermal vent quantified by rRNA slot-blot hybridization. Microbiology, 146:1287-1293

Smith Jr, K. L., Ruhl, H. A., Bett, B. J., Billett, D. S. M., Lampitt, R. S., and Kaufmann, R. S. (2009). Climate, carbon cycling, and deep-ocean ecosystems. PNAS, 106:19211-19218.

Smith, E. and Morowitz, H. 2004. Universality in Intermediary Metabolism. PNAS, 101:13168-73

Sorokin, D.Y., Lysenko, A.M., Mityushina, L.L., Tourova, T.P., Jones, B.E., Rainey, F.A., Robertson, L.A. and Kuenen, G.J. 2001. Thioalkalimicrobium aerophilum gen. nov., sp. nov. and Thioalkalimicrobium sibericum sp. nov., and Thioalkalivibrio versutus gen. nov., sp. nov., Thioalkalivibrio nitratis sp. nov., novel and Thioalkalivibrio denitrificancs sp. nov., novel obligately alkaliphilic and obligately chemolithoautotrophic sulfur-oxidizing bacteria from soda lakes. Int J Syst Evol Microbiol, 51:565–580

Stahl, D. A., and Amann, R. I. (1991). Sequencing and Hybridization Techniques in Bacterial Systematics. Edition Wiley, Chichester

Staley, J.T. and Reysenbach, A.L. 2002. Biodiversity of microbial life: Foundation of earth's biosphere. Vol. 25. Wiley-Liss New York

Stockdale, A., Davison, W. and Zhang, H. 2009. Micro-scale biogeochemical heterogeneity in sediments: a review of available technology and observed evidence. Earth Sci Rev, 92:81–97.

Stoica, E. and Herndl, G. J. 2007. Contribution of Crenarchaeota and Euryarchaeota to the prokaryotic plankton in the coastal northwestern Black Sea. Journal of plankton research, 29:699-706

Takai, K., and Horikoshi, K. (1999). Genetic diversity of archaea in deep-sea hydrothermal vent environments. Genetics, 152:1285-1297.

Takai, K., Hirayama, H., Nakagawa, T., Suzuki, Y., Nealson, K.H. and Horikoshi, K. 2004. Thiomicrospira thermophila sp. nov., a novel microaerobic, thermotolerant, sulfur-oxidizing chemolithomixotroph isolated from a deep-sea hydrothermal fumarole in the TOTO caldera, Mariana Arc, Western Pacific. Int J Syst Evol Microbiol, 54:2325–2333

Takai, K., Miyazaki, M., Nunoura, T., Hirayama, H., Oida, H., Furushima, Y., ... and Horikoshi, K. 2006. Sulfurivirga caldicuralii gen. nov., sp. nov., a novel microaerobic, thermophilic, thiosulfate-oxidizing chemolithoautotroph, isolated from a shallow marine hydrothermal system occurring in a coral reef, Japan. International journal of systematic and evolutionary microbiology, 56:1921-1929

Talbert, P.B. and Henikoff, S. 2010. Histone variants – ancient wrap artists of the epigenome.

Nature Reviews Molecular Cell Biology, 11: 264-275

Tamburini, C., Garel, M., Al Ali, B., Mérigot, B., Kriwy, P., Charrière, B., and Budillon, G. 2009. Distribution and activity of Bacteria and Archaea in the different water masses of the Tyrrhenian Sea. Deep Sea Research Part II: Topical Studies in Oceanography, 56:700-712

Tarasov, V., Gebruk, A., Mironov, A. and Moskalev, L. 2005. Deep-sea and shallow-water hydrothermal vent communities: two different phenomena? Chemical Geology, 224:5-39

Taviani, M. 2011. The deep-sea chemoautotroph microbial world as experienced by the Mediterranean metazoans through time. Advances in Stromatolite Geobiology, 277-295

Teira, E., Reinthaler, T., Pernthaler, A., Pernthaler, J. and Herndl, G.J. 2004. Combining catalyzed reporter deposition-fluorescence in situ hybridization and microautoradiography to detect substrate utilization by bacteria and archaea in the deep ocean. Applied Environmental Microbiology, 70:4411-4414

Teske, A., Brinkhoff, T., Muyzer, G., Moser, D.P., Rethmeier, J. and Jannasch, H. W. 2000. Diversity of thiosulfate-oxidizing bacteria from marine sediments and hydrothermal vents. Appl Environ Microbiol, 66:3125–3133

Thiel, H., Peannkuche, O., Schriever, G., Lochte, K., Gooday, A.J., Hemleben, C., Mantoura, R.F., Turley, C.M., Patching, J.W. and Riemann, F. 1988. Phytodetritus on the deep-sea floor in a central oceanic region of the Northeast Atlantic. Biological Oceanography, 6:203-239

Thingstad, T.F. and Lignell, R. 1997. Theoretical models for the control of bacterial growth rate, abundance, diversity and carbon demand. Aquatic Microbial Ecology, 13:19-27

Thompson, J.D., Gibson, T.J., Plewniak, F., Jeanmougin, F. and Higgins, D.G. 1997. The CLUSTAL_X windows interface: flexible strategies for multiple sequence alignment aided by quality analysis tools. Nucleic Acids Res, 25:4876–4882

Tindall, B. J., Rossello-Mora, R., Busse, H.J., Ludwig, W. and Kampfer, P. 2010. Notes on the characterization of prokaryote strains for taxonomic purposes. Int J Syst Evol Microbiol, 60:249–266

Tindall, B.J. 1990a. A comparative-study of the lipid composition of Halobacterium saccharovorum from various sources. Syst Appl Microbiol, 13:128–130

Tindall, B.J. 1990b. Lipid composition of Halobacterium lacusprofundi. FEMS Microbiol Lett, 66:199–202

Tokuda, G., Yamada, A., Nakano, K., Arita, N.O. and Yamasaki, H. 2007. Colonization of Sulfurovum sp. on the gill surfaces of Alvinocaris longirostris, a deep-sea hydrothermal vent shrimp. Marine Ecology, 29:106-114

Torsvik, V., Ovreas, L. and Thingstad, T.F. 2002. Prokaryotic diversity--magnitude, dynamics, and controlling factors. Science Signalling, 296:1064

Trincardi, F., Cattaneo, A., Correggiari, A., and Ridente, D. 2004. Evidence of soft sediment deformation, fluid escape, sediment failure and regional weak layers within the late Quaternary mud deposits of the Adriatic Sea. Marine Geology, 213:91-119

Turley, C. M. and Dixon, J. L. 2002. Bacterial numbers and growth in surficial deep-sea sediments and phytodetritus in the NE Atlantic: Relationships with particulate organic carbon and total nitrogen. Deep Sea Research Part I: Oceanographic Research Papers, 49:815-826

Turley, C.M. and Stutt, E.D. 2000. Depth-related cell-specific bacterial leucine incorporation rates on particles and its biogeochemic

Underwood, A. 1991. Beyond BACI: experimental designs for detecting human environmental impacts on temporal variations in natural populations. Marine and Freshwater Research, 42:569-587

Valentine, D. L. and Reeburgh, W.S. 2008. New perspectives on anaerobic methane oxidation. Environmental Microbiology, 2:477-484

Valentine, D.L. 2007. Adaptations to energy stress dictate the ecology and evolution of the Archaea. Nature Review Microbiology, 5:316-323

Valsami-Jones, E., Baltatzis, E., Bailey, E., Boyce, A., Alexander, J., Magganas, A., Anderson, L., Waldron, S. and Ragnarsdottir, K. 2005. The geochemistry of fluids from an active shallow submarine hydrothermal system: Milos island, Hellenic Volcanic Arc. Journal of volcanology and geothermal research, 148:130-151

Van Kranendonk, M.J. 2006. Volcanic degassing, hydrothermal circulation and the flourishing of early life on Earth: a review of the evidence from c. 3490–3240 Ma rocks of the Pilbara Supergroup, Pilbara Craton, Western Australia. Earth-Science Reviews, 74:197–240

Vanney, J.R. and Gennesseaux, M. 1985. Mediterranean seafloor features: Overview and assessment. In: Stanley D.J., Wezel F-C., editors. Geological evolution of the Mediterranean Basin. New York: Springer. pp. 3–32

Varela, M.M., van Aken, H.M., Sintes, E. Herndl, G.J. 2008. Latitudinal trends of Crenarchaeota and Bacteria in the meso- and bathypelagic water masses of the eastern North Atlantic. Environ Microbiol., 10:110−124

Vetriani, C., Jannasch, H.W., MacGregor, B.J., Stahl, D.A. and Reysenbach, A.L. 1999. Population structure and phylogenetic characterization of marine benthic archaea in deep-sea sediments. Applied Environmental Microbiology, 65:4375-4384

Vetriani, C., Speck, M. D., Ellor, S. V., Lutz, R. A., and Starovoytov, V. (2004). Thermovibrio ammonificans sp. nov., a thermophilic, chemolithotrophic, nitrate-ammonifying bacterium from deep-sea hydrothermal vents. International journal of systematic and evolutionary microbiology, 54:175-181.

Voordeckers, J. W., Starovoytov, V. and Vetriani, C. 2005. Caminibacter mediatlanticus sp. nov., a thermophilic, chemolithoautotrophic, nitrate-ammonifying bacterium isolated from a deep-sea hydrothermal vent on the Mid-Atlantic Ridge. Int J Syst Evol Microbiol, 55:773–779.

Wächtershäuser, G. 1990. Evolution of the First Metabolic Cycles. PNAS, 87: 200-204

Wächtershäuser, G. 2000. Origin of Life: Life as We Don't Know It. Science, 289:1307-1308

Wegener, G., Niemann, H., Elvert, M., Hinrichs, K.U. and Boetius, A. 2008. Assimilation of methane and inorganic carbon by microbial communities mediating the anaerobic oxidation of methane. Environ Microbiol, 10:2287-2298

Weinbauer, M.G. 2004. Ecology of prokaryotic viruses. FEMS Microbiology Review, 28:127-181

Weisburg, W.G., Barns, S.M., Pelletier, D.A. and Lane, D.J. 1991. 16S ribosomal DNA amplification for phylogenetic study. J. Bacteriol, 173:697-703

Wenzhöfer, F., Holby, O., Glud, R.N., Nielsen, H.K., and Gundersen, J.K. 2000. In situ microsensor studies of a shallow water hydrothermal vent at Milos, Greece. Marine chemistry, 69:43-54

Whelan, J., Eglinton, L., Cathles, L., Losh, S. and Roberts, H. 2005. Surface and subsurface manifestations of gas movement through a N–S transect of the Gulf of Mexico. Marine and Petroleum Geology, 22:479-497

Whitman, W.B., Coleman, D.C. and Wiebe, W.J. 1998. Prokaryotes: the unseen majority. PNAS, 95:6578-6583

Willey JM, Sherwood LM. and Woolverton CJ. Microbiology 7th ed. 2008. Ch. 19 pp. 474–475

Williamson, S.J., Cary, S.C., Williamson, K.E., Helton, R.R., Bench, S.R., Winget, D. and Wommack, K.E. 2008. Lysogenic virus-host interactions predominate at deep-sea diffuse-flow hydrothermal vents. The ISME Journal, 2:1112-1121

Wilms, R., Köpke, B., Sass, H., Chang,T.S., Cypionka, H., Engelenet, B. 2006a. Deep biosphere-related bacteria within the subsurface of tidal flat sediments. Environmental Microbioliology, 8:709-719

Wilms, R., Sass, H., Köpke, B., Köster, J., Cypionka, H. and Engelen, B. 2006b. Specific Bacterial, Archaeal, and Eukaryotic Communities in Tidal-Flat Sediments along a Vertical Profile of Several Meters. Applied and Environmental Microbiology, 72:2756-2764

Winter, C., Smit, A., Herndl, G.J. and Weinbauer, M.G. 2005. Linking bacterial richness with viral abundance and prokaryotic activity. Limnology and Oceanography, 50:968-977

Wirsen, C. O., Brinkhoff, T., Kuever, J., Muyzer, G., Molyneaux, S. and Jannasch, H.W. 1998. Comparison of a new Thiomicrospira strain 3066 from the mid-Atlantic ridge with known hydrothermal vent isolates. Appl Environ Microbiol, 64:4057–4059

Woese *C. and Fox G. 1977. Phylogenetic structure of the prokaryotic domain: the primary kingdoms. PNAS, 74:5088-90*

Wood, S.N. 2006. Generalized Additive Models: An Introduction with R. Chapman and Hall/CRC

Wuchter, C., Abbas, B., Coolen, M. J., Herfort, L., Van Bleijswijk, J., Timmers, P., ... and Damsté, J. S. S. (2006). Archaeal nitrification in the ocean. PNAS, 103:12317-12322.

Yakimov, M. M., La Cono, V., Denaro, R., D'Auria, G., Decembrini, F., Timmis, K. N. ... and Giuliano, L. 2007. Primary producing prokaryotic communities of brine, interface and seawater above the halocline of deep anoxic lake L'Atalante, Eastern Mediterranean Sea. The ISME journal, 1:743-755

Zar, J. H. 1999. Biostatistical Analysis, 4th edn. (Prentice Hall: Upper Saddle River, NJ.)

Zillig W. 1991. Comparative biochemistry of Archaea and Bacteria. Curr. Opin. Gen. Dev., 1:544–551